Suspended Particulate Matter in Douglas Channel from MODIS and MERIS Ocean Colour Data

G. Lazin, E. Devred, and C. G. Hannah

Fisheries and Oceans Canada
Bedford Institute of Oceanography
1 Challanger Drive,
Dartmouth, NS, Canada
B2Y 4A2

Fisheries and Oceans Canada
Institute of Ocean Sciences
9860 West Saanich Road
Sidney, BC, Canada
V8L 4B2

2017

Canadian Technical Report of Fisheries and Aquatic Sciences 3241

Fisheries and Oceans Canada | Pêches et Océans Canada

Canada

Canadian Technical Report of Fisheries and Aquatic Sciences

Technical reports contain scientific and technical information that contributes to existing knowledge but which is not normally appropriate for primary literature. Technical reports are directed primarily toward a worldwide audience and have an international distribution. No restriction is placed on subject matter and the series reflects the broad interests and policies of Fisheries and Oceans Canada, namely, fisheries and aquatic sciences.

Technical reports may be cited as full publications. The correct citation appears above the abstract of each report. Each report is abstracted in the data base *Aquatic Sciences and Fisheries Abstracts*.

Technical reports are produced regionally but are numbered nationally. Requests for individual reports will be filled by the issuing establishment listed on the front cover and title page.

Numbers 1-456 in this series were issued as Technical Reports of the Fisheries Research Board of Canada. Numbers 457-714 were issued as Department of the Environment, Fisheries and Marine Service, Research and Development Directorate Technical Reports. Numbers 715-924 were issued as Department of Fisheries and Environment, Fisheries and Marine Service Technical Reports. The current series name was changed with report number 925.

Rapport technique canadien des sciences halieutiques et aquatiques

Les rapports techniques contiennent des renseignements scientifiques et techniques qui constituent une contribution aux connaissances actuelles, mais qui ne sont pas normalement appropriés pour la publication dans un journal scientifique. Les rapports techniques sont destinés essentiellement à un public international et ils sont distribués à cet échelon. II n'y a aucune restriction quant au sujet; de fait, la série reflète la vaste gamme des intérêts et des politiques de Pêches et Océans Canada, c'est-à-dire les sciences halieutiques et aquatiques.

Les rapports techniques peuvent être cités comme des publications à part entière. Le titre exact figure au-dessus du résumé de chaque rapport. Les rapports techniques sont résumés dans la base de données *Résumés des sciences aquatiques et halieutiques.*

Les rapports techniques sont produits à l'échelon régional, mais numérotés à l'échelon national. Les demandes de rapports seront satisfaites par l'établissement auteur dont le nom figure sur la couverture et la page du titre.

Les numéros 1 à 456 de cette série ont été publiés à titre de Rapports techniques de l'Office des recherches sur les pêcheries du Canada. Les numéros 457 à 714 sont parus à titre de Rapports techniques de la Direction générale de la recherche et du développement, Service des pêches et de la mer, ministère de l'Environnement. Les numéros 715 à 924 ont été publiés à titre de Rapports techniques du Service des pêches et de la mer, ministère des Pêches et de l'Environnement. Le nom actuel de la série a été établi lors de la parution du numéro 925.

Canadian Technical Report of
Fisheries and Aquatic Sciences 3241

2017

SUSPENDED PARTICULATE MATTER IN DOUGLAS CHANNEL FROM MODIS AND MERIS OCEAN COLOUR DATA

G. Lazin[1], E. Devred[1] and C.G. Hannah[2]

[1]Fisheries and Oceans Canada
Bedford Institute of Oceanography
1 Challenger Drive,
Dartmouth, NS, Canada
B2Y 4A2

[2]Fisheries and Oceans Canada
Institute of Ocean Sciences
9860 West Saanich Road,
Sidney, B.C.,
V8L 4B2

© Her Majesty the Queen in Right of Canada, 2017
Cat. No. Fs97-6/3241E ISBN 978-0-660-23862-3 ISSN 0706-6457 (print version)
Cat. No. Fs97-6/3241E-PDF ISBN 978-0-660-23861-6 ISSN 1488-5379 (electronic version)

Correct citation for this publication:

Lazin, G., Devred, E., and Hannah, C.G. 2017. Suspended Particulate Matter in Douglas Channel from MODIS and MERIS Ocean Colour Data. Can. Tech. Rep. Fish. Aquat. Sci. 3241: vi + 68 p.

CONTENTS

ABSTRACT

Lazin, G., Devred, E., and Hannah, C.G. 2017. Suspended Particulate Matter in Douglas Channel from MODIS and MERIS Ocean Colour Data. Can. Tech. Rep. Fish. Aquat. Sci. 3241: vi + 68 p.

Spatial and temporal patterns of suspended particulate matter concentration (SPM) in the surface waters of Douglas Channel were assessed using MODIS and MERIS high resolution ocean colour satellite data for the period 2002-2014. Both sensors show similar SPM patterns in the region, but large absolute discrepancies were observed for areas with high SPM loads, which are attributed to the different SPM algorithms. MODIS seems to be affected by the proximity of the coast (i.e., adjacency effects) and appeared to be less suitable for narrow parts of the channel. Monthly climatology for both sensors shows average SPM value of about 1-2 g/m^3 and very high standard deviation, indicating significant variation in SPM concentration in the region. The time series extracted from daily MERIS images at several stations located along the channel revealed low background median SPM of 0.5 g/m^3 with periodic pulses of high SPM, up to 60 g/m^3, in the upper channel. In the absence of ground truth measurements we attempted to validate variation in observed SPM using rain and river discharge data. It was found that SPM pulses corresponded to the spatially well-defined SPM plumes which coincide with periods of heavy rain, suggesting that sediments are transported to the Channel by runoff. In addition, seasonal SPM variability at the stations close to Kitimat and Kemano estuaries are consistent with the seasonal rainfall and river discharge patterns. At those locations SPM is peaking in June when the river discharge reaches its maximum flow as a result of snowmelt, and again in October and April concurrent with annual precipitation maxima. Large SPM pulses are also observed in January and can be attributed to the rain-on-snow events that result in amplified runoff. The relationship between SPM and river discharge (C-Q relationship) was investigated at the Kitimat River estuary and indicates counter-clockwise hysteresis loop. This study demonstrated value of ocean colour data in environmental investigations as well as its potential for hydrological studies.

RÉSUMÉ

Lazin, G., Devred, E., et Hannah, C.G. 2017. Matières particulaires en suspension dans le Chenal Douglas d'après les données de MERIS et MODIS sur la couleur de l'océan. Rapp. Tech. Can. Sci. Halieut. Aquat. 3241: vi + 68 p.

Les profils spatiotemporels de la concentration de matières particulaires en suspension dans les eaux superficielles du chenal Douglas ont été évalués à l'aide des données satellitaires à haute résolution sur la couleur de l'océan fournies par MODIS et MERIS pour la période 2002-2014. Les deux spectroradiomètres montrent des profils semblables de matières particulaires en suspension (MPES), mais également de grands écarts absolus pour les zones sur lesquelles les données sont nombreuses. Ces écarts ont été attribués aux différents algorithmes utilisés pour mesurer les matières particulaires en suspension. Les données de MODIS semblent affectées par la proximité de la côte (effets de la contiguïté) et moins bien adaptées aux parties étroites du chenal. Les climatologies mensuelles des deux capteurs indiquent une valeur moyenne d'environ 1-2 g/m^3 pour les matières particulaires en suspension et un écart-type très élevé, révélateur des variations importantes de leur concentration dans la région. La série temporelle issue des images quotidiennes de MERIS aux stations situées le long du chenal donne une valeur médiane faible de 0,5 g/m^3 de la concentration en MPES, avec des pics périodiques pouvant atteindre 60 g/m^3 dans la partie supérieure du chenal. En l'absence de mesures vérifiées sur le terrain, nous avons tenté de valider l'écart entre les valeurs observées de matières particulaires en suspension à l'aide des données pluviométriques et sur l'écoulement fluvial. Nous avons constaté que les pics de matières particulaires en suspension correspondent à des panaches bien définis et coïncident avec les périodes de fortes pluies, ce qui permet de penser que les sédiments sont acheminés dans le chenal sous l'effet du ruissellement. De plus, la variabilité saisonnière des matières particulaires en suspension aux stations proches des estuaires des rivières Kitimat et Kemano est conforme aux modèles saisonniers de précipitations et d'écoulement fluvial. À ces stations, les pics des matières particulaires en suspension se produisent en juin, lorsque l'écoulement fluvial est maximal en raison de la fonte des neiges, ainsi qu'en octobre et en avril, au moment des maxima annuels des précipitations. Des pics élevés de matières particulaires en suspension sont également observés en janvier à la suite de fortes chutes de pluie ou de neige qui entraînent un accroissement de l'écoulement des rivières. La relation entre les matières particulaires en suspension et l'écoulement fluvial (relation C-Q) a été étudiée dans l'estuaire de la rivière Kitimat et s'exprime sous la forme d'une boucle d'hystérésis dans le sens antihoraire. Cette étude montre la valeur des données couleur de l'océan dans les études environnementales, ainsi que le potentiel qu'elles représentent pour les études hydrologiques.

INTRODUCTION

This report documents remote sensing activities related to the oceanography component of the World Class Tanker Safety Program with the aim of investigating spatial and temporal patterns of suspended particulate matter concentration (SPM, g/m^3) in the surface waters of Douglas Channel using ocean colour satellite images.

Douglas Channel is one of the principal inlets on the north-west coast of British Colombia that is part of the Kitimat fjord system (McDonald, 1983). It is about 140 km-long and is used as a shipping route that extends from the ocean (Hecate Strait) to the Kitimat international port located at its head. Further plans for development include a proposed oil pipeline with a terminal at Kitimat, from where the oil would be shipped along the channel by marine tankers, which has raised environmental concerns regarding oil spills. Our study of the SPM distribution complements scientific investigations addressing oil spills in the region, since suspended particles under certain conditions can interact with oil droplets by forming sinking oil-particle aggregates that can transport oil from the surface to the bottom (Wu et al 2016).

During the first phase of the project, monthly climatology of SPM was derived using the Moderate Resolution Imaging Spectroradiometer (MODIS) ocean colour sensor from the National Aeronautics and Space Administration (NASA), which was operational at the time of this investigation. In the second phase, we used an archive of ocean colour images from the Medium Resolution Imaging Spectrometer (MERIS) sensor from the European Space Agency (ESA), which collected data between 2003 and 2012. MERIS and MODIS sensors were chosen because of their relative high spatial resolution at nadir of 250 m and 300 m respectively, which made them appropriate candidates to resolve relatively narrow areas such as the 3 to 5 km wide Douglas Channel. In addition, both sensors have a high revisiting frequency of one to two passes per day. Each sensor has a unique set of wavebands and employs a specific atmospheric correction and substantially different SPM algorithms. Both data sets were explored in attempt to establish the most accurate SPM estimates in Douglas Channel from ocean colour satellite data.

In the third phase of the project a time series of MERIS-derived SPM was extracted at 25 stations along the Douglas Channel and Gardener Canal and was investigated in relation to the daily rainfall records and discharge data for Kitimat and Kemano rivers (Figure 1).

DATA AND METHODS

MODIS

MODIS top of the atmosphere Level 1A data were downloaded from NASA ocean colour website (https://oceancolor.gsfc.nasa.gov) for the time period 2003 to 2014 and included 8000 files or about 1.6 TB of compressed data. Level 1A images were geo-located using SeaDAS 7.0 and calibration coefficients were applied to derive top-of-atmosphere calibrated radiances (Level 1B data). Subsequently, an atmospheric correction scheme was applied to the Level 1B data to derive remote sensing reflectance at 645 nm (Level 2 data) at sea level. Due to the storage limitation, Level 1A data were deleted immediately after being downloaded and processed to the Level 1B while Level 1B, Level 2, and geolocation files were archived. Further processing was done using in-house code in Python to derive the SPM concentration from the remote sensing reflectance. The final SPM images were stored in the NetCDF format (GRD files) at a nominal spatial resolution of 250 m. The storage requirements for each level are listed in Table 1.

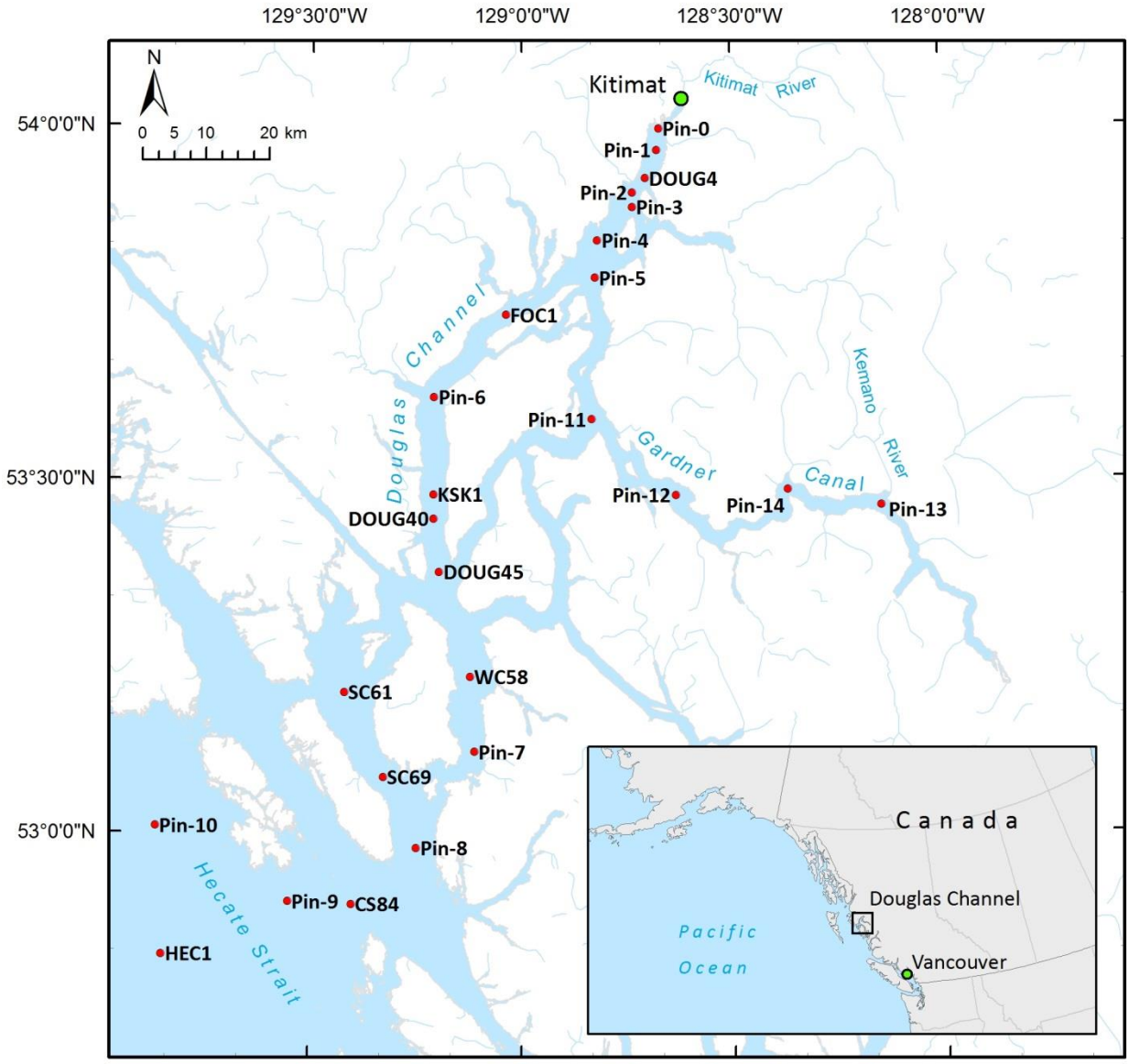

Figure 1: Douglas Channel with station locations.

SPM concentration was derived from MODIS data using a polynomial expression applied to the remote sensing reflectance in the 645 nm spectral band (Nechad et al., 2010). The atmospheric correction scheme used in this study (Wang and Shi, 2007) was modified to avoid flagging of very turbid waters as sea-ice or clouds (Doxaran et al., 2015). This step required a visual inspection of every individual image to discard abnormal patterns in the SPM concentration based on our experience (e.g. speckles or high SPM values in open waters).

Due to the frequent cloud coverage in the region large proportion of the images did not contain any valid pixels or were contaminated with broken clouds, thus decreasing the number of usable pixels in the images. After extensive quality control of more than 4000 images that contained data we selected two groups of images for further analysis: the cloud free scenes of the whole region (174 images) and cloud free images of the Douglas Channel (361 images).

Composite images for a desired time period were computed as the arithmetic average on a pixel-per-pixel basis of all available individual images. Because of missing data in any single image, the number of observations contributing to each pixel in the composite image can vary. To derive composite images we used custom made R scripts applied to the gridded daily SPM products to compute statistics for each pixel (i.e., average and standard deviation). Since MODIS SPM product did not include quality flags to identify contaminations such as cloud edges, we used only cloud free images that were identified as part of the quality control described in the previous paragraph.

Table 1: Storage requirements for MODIS dataset 2003-2014

File Type	Storage requirement per year of data	Total
BZ2	151 GB	1.6 TB
L1B	145 GB	1.5 TB
GEO	35 GB	0.4 TB
L2	2.7 GB	29 GB
GRD	56 MB	616 MB
Total	**334 GB**	**3.53 TB**

MERIS

MERIS Level 1B top of the atmosphere calibrated radiance data were downloaded from NASA ocean colour website for the time period January 2003 to April 2012 and included 2774 files (3TB of data). For MERIS only full swaths were offered for download so approximate size of each image containing the region of interest was about 1GB. There were around 20-30 files available for each month with the exception of 2008 where only two files were available for April and there were no files for May and June of that year.

All the processing of MERIS data was done using the BEAM processing software (VISAT 4.11) and custom made bash scripts for data handling and manipulation. In order to decrease data volume and to increase processing speed, the region of interest was extracted from full swaths by creating Level 1B subsets and the original files were subsequently deleted. Each 1GB full swath file was replaced by 45MB Level 1B subset in dim format, decreasing the amount of Level 1B data from 3TB to 78GB. RGB true colour images were created to allow for visual examination of each original file.

Level 2 products, containing SPM concentrations, were created from the Level 1 subsets using the Case-2 Regional Processor (C2R) included in the BEAM processing software. C2R is a two-step algorithm, which first performs atmospheric correction (Doerffer and Schiller, 2008) and then retrieves the water constituents from 8 visible spectral bands using a neural network (Doerffer and Schiller, 2007). The C2R processor has been developed as a joint effort between GKSS Research Centre (Germany), the Institute for Coastal Research (Germany), and Brockmann Consult (Germany) under contract of the European Space Agency. It is the standard algorithm for MERIS 3rd reprocessing in coastal waters. The only adjustment we have made to the standard C2R processing is the modification of the threshold for cloud/ice detection from 0.2 to 0.02, to enable proper flagging of ice and clouds in the region.

Visual inspection and quality control was performed on SPM daily images that were created as part of the Level-2 processing. The final Level 2 MERIS dataset (19.33 GB) included 1573 daily scenes with valid pixels and 733 completely overcast images that were consequently discarded. All the data are stored as ESA-MERIS dim files, which are based on the NetCDF format.

MERIS composite images were computed using BEAM Level 3 binning processor and custom made scripts in XML. All available images were aggregated by month and Level 3 processor was used to compute monthly statistics for each pixel in the image (mean SPM value, standard deviation, and number of pixels averaged). Pixels flagged as invalid were excluded from the computations. The final images were re-projected using a Mercator projection and a land mask was added with 50 m spatial resolution. The land mask was provided as a plug-in for the BEAM processing software, and is based on the NASA's Shuttle Radar Topography Mission (SRTM) shape files.

MODIS AND MERIS COMPARISON

Comparisons between MODIS- and MERIS-derived SPM were conducted in order to assess differences and potential biases in the SPM estimates by each sensor and associated algorithms. It is important to point out that each sensor employs different atmospheric correction and substantially different approaches for SPM computation. For MODIS, SPM product is computed using a polynomial equation applied to the remote sensing reflectance at 645 nm, whereas MERIS SPM product is derived using a Neural Network approach that uses remote sensing reflectance at 8 spectral bands to simultaneously derive SPM concentration, chlorophyll-a concentration, and absorption of yellow substances. In addition, MERIS SPM is readily available in the standard Level 2 products from ESA while SPM is not provided in MODIS data stream from NASA and it must be derived from Level 1 images by coding the desired algorithm. The comparison of MODIS and MERIS are summarized in Table 2.

The comparison of the SPM products was performed using a composite image created for the week of April 22, 2005, which included several clear sky days. The comparison reveals that, despite very different approaches between the two sensors, MERIS and MODIS are showing similar spatial patterns in SPM distribution with the highest SPM concentration at the Skeena River estuary and in the Kitimat Arm, with MERIS seemingly resolving finer spatial variability (Figure 2, top panel). The range of SPM concentration is similar in both images except for the areas with sediment concentrations greater than about 10 g/m^3 where disagreement between sensors becomes substantial (Figure 2, bottom panel). Largest sediment loadings in the area of

interest are seen only at the Skeena River estuary, where disagreement between MODIS and MERIS is the highest. In Douglas Channel, the SPM concentration derived from both sensors are lower and lie within a similar range.

The comparison of the SPM algorithms was assessed on a daily image acquired by MERIS under clear sky conditions on April 23rd of 2005. Direct comparison of the MERIS and MODIS SPM computational approaches was possible since MERIS has the 645 nm band that is used as an input into MODIS algorithm. For this particular MERIS image SPM concentration was computed using both, neural network and the one-band algorithm, and was plotted versus remote sensing reflectance in the 645 nm spectral band, Rrs (645). For the one-band algorithm, SPM is directly related to Rrs (645) via a polynomial regression, while SPM derived using the neural network (i.e., 8 spectral bands) seem to be related to the red band only for moderate SPM concentrations (from about 2-10 g/m^3). In that range, the neural network performs in a similar fashion to the polynomial relationship (Figure 3). For high and low SPM (i.e. < 2 g/m^3 and >10 g/m^3), neural network outputs do not correlate with the reflectance in the red spectral band, and those SPM values are associated with a wide range of Rrs (645).

From this analysis it appears that the difference between MODIS and MERIS SPM estimates for the regions with very low and very high SPM loads may be largely attributed to the different approaches for SPM computation. Potential issues related to the atmospheric correction or instrumentation were not investigated in this study.

Table 2: Summary of MODIS and MERIS specifications.

Property	**MODIS**	**MERIS**
Spatial Resolution	250 m	300 m
Data Availability	2002-present	2002-2012
Data Frequency	~2 images per day ~ 57 images per month	~1 image per day ~22 images per month
SPM Products	Not available for download	Available from ESA in Level 2 files
Atmospheric Correction	Wang and Shi, 2007	Doerffer and Schiller, 2008
SPM Algorithm	One-band polynomial equation	Neural Network
SPM Algorithm Input	Rrs in 645 nm band	Rrs in 8 spectral bands
SPM Algorithm Output	SPM Concentration	-SPM Concentration -Chlorophyll-a concentration -Absorption of yellow substances

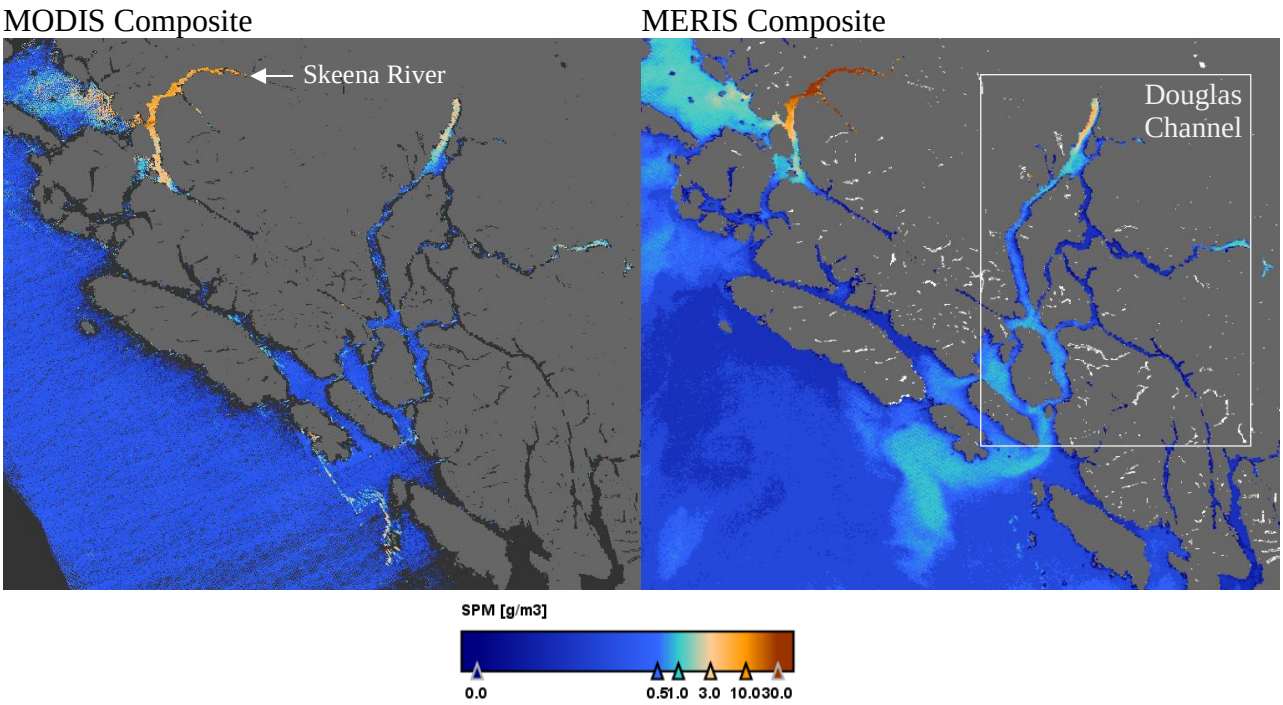

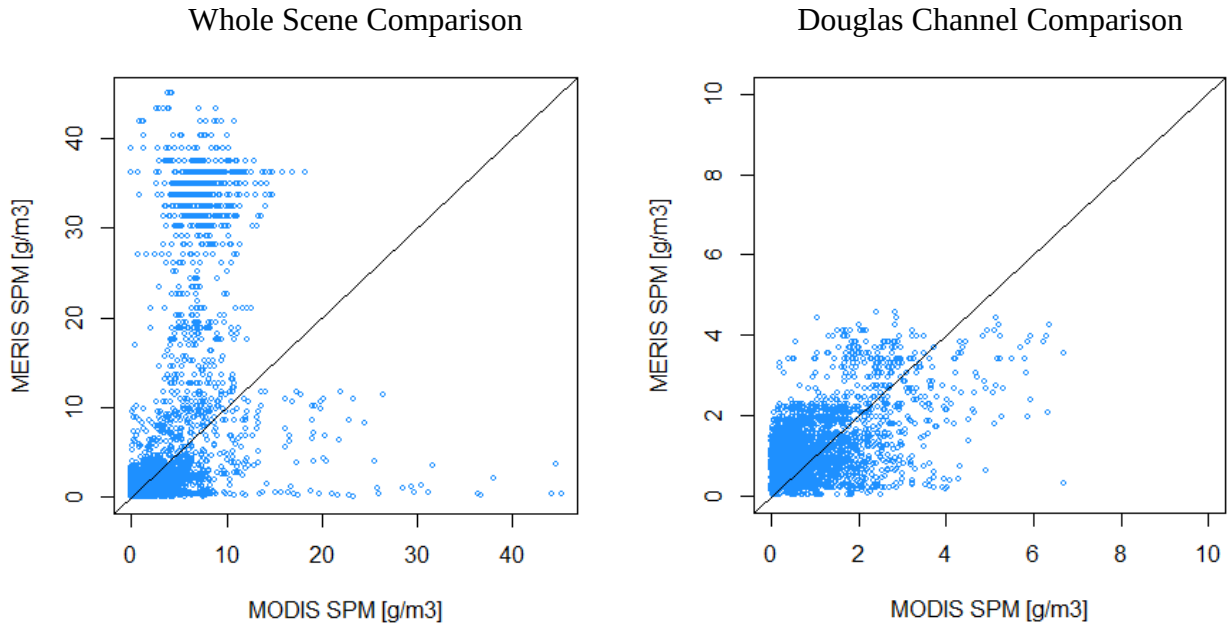

Figure 2: MODIS and MERIS composite images for the week of April 22, 2005 (top). Scatter plots comparing pixels for the whole scene and Douglas Channel are shown on the bottom left and bottom right respectively. Note that MERIS-derived SPM is substantially higher for areas with high SPM loads which is located at the Skeena River estuary. Both sensors show similar SPM distribution pattern in Kitimat region and similar range of values for SPM concentrations in the Douglas Channel.

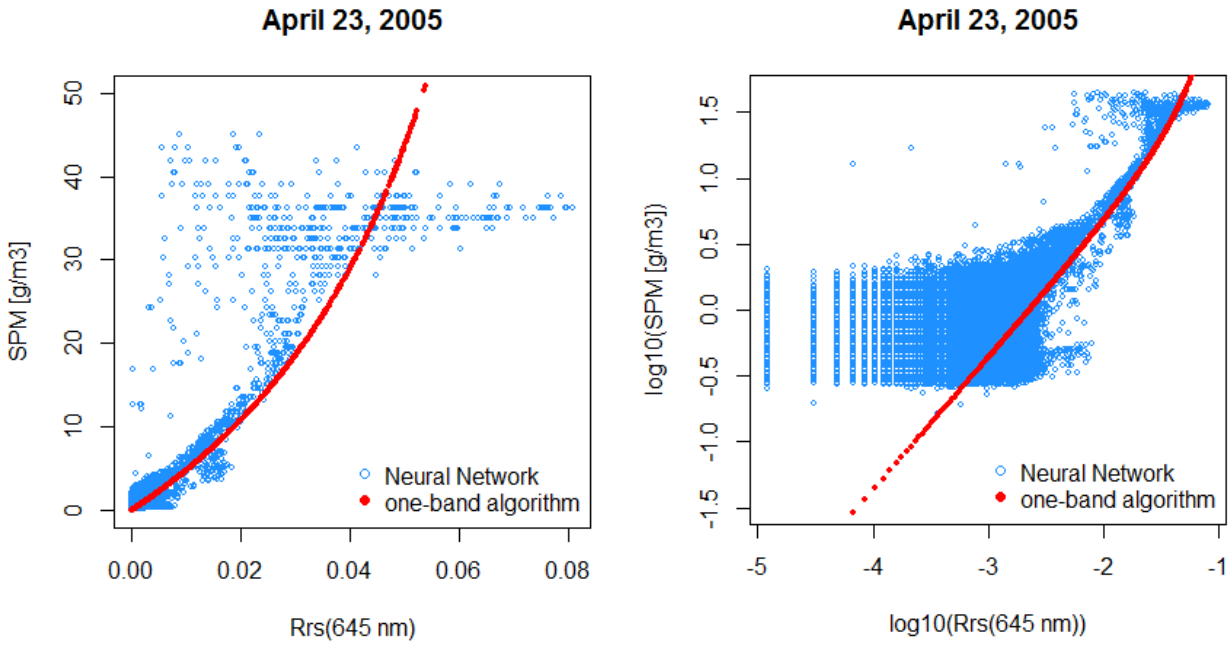

Figure 3: Relationship between Remote Sensing Reflectance at 645 nm and SPM computed by two different algorithms (neural network and polynomial one-band algorithm) applied to the same MERIS clear sky image, on linear scale (left) and logarithmic scale (right).

MONTHLY CLIMATOLGY

Monthly SPM climatology refers to a long-term average of SPM computed using all available data for each month. In the case of the remote sensing products, the averages are computed by creating so called monthly composite images, where each pixel is associated with an average monthly SPM value, monthly standard deviation, and a number of valid pixels. MERIS and MODIS monthly composite images are included in the Appendix A and B respectively.

To assess annual SPM patterns in the region, monthly SPM concentration for MODIS were extracted from climatology images for two sub-regions, one region encompassing the whole Douglas Channel and the other one encompassing the area around Kitimat (Figure 4). The SPM monthly average and standard deviation were computed for each box. The monthly data indicate that the mean SPM concentrations vary between 0.91 and 2.8 g/m^3 in the Douglas Channel and between 0.77 and 3.24 g/m^3 in the Kitimat region throughout the year. However, both areas exhibit large variations in the winter and spring months with standard deviation up to 6.22 g/m^3 for the Kitimat region in January and 6.13 g/m^3 for the Douglas Channel in December indicating large variability of SPM concentrations observed for those months (Table 3).

A comparison between climatology derived from MERIS and MODIS was performed only for the smaller box surrounding Kitimat region (Figure 4 and Figure 5). Both sensors show similar range of SPM values throughout the year but different seasonal patterns, with the largest absolute differences in January and February and the best agreement during summer months. It also appears that the differences are large for the months associated with large standard deviation.

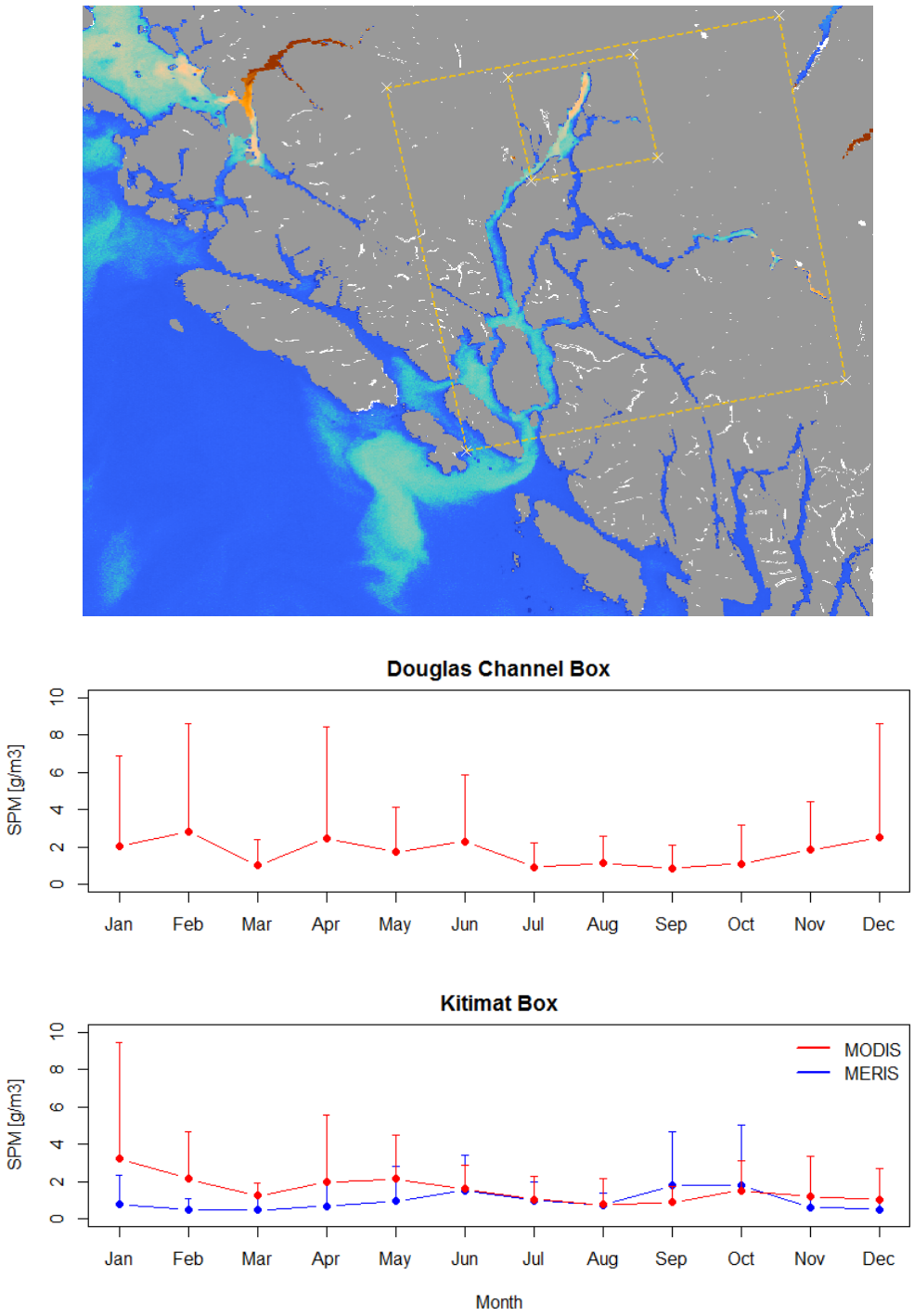

Figure 4: Climatology of SPM concentration for the period 2003-2014 for two sub-regions shown on the top map: Douglas Channel (large box) for which the climatology is shown only for MODIS, and region around Kitimat (small box) for which climatology is shown for both MERIS and MODIS. Error bars represent standard deviation of the climatology.

Table 3: Climatological concentrations of SPM in g/m^3 for Douglas Channel and Kitimat region derived from MODIS.

	Kitimat Region			Douglas Channel		
Month	Mean SPM	SD	Median SPM	Mean SPM	*SD*	Median SPM
January	3.24	6.22	1.02	2.05	4.81	0.44
February	2.14	2.52	1.43	2.80	5.81	1.01
March	1.23	0.68	1.06	0.99	1.39	0.69
April	1.96	3.62	0.98	2.46	5.93	0.56
May	2.13	2.37	1.70	1.72	2.41	1.02
June	1.59	1.30	1.12	2.28	3.57	1.28
July	1.03	1.22	0.63	0.91	1.31	0.41
August	0.77	1.36	0.47	1.13	1.46	0.52
September	0.89	0.86	0.58	0.83	1.28	0.38
October	1.52	1.61	0.99	1.11	2.09	0.40
November	1.18	2.18	0.57	1.85	2.55	0.93
December	1.05	1.64	0.64	2.48	6.13	0.55

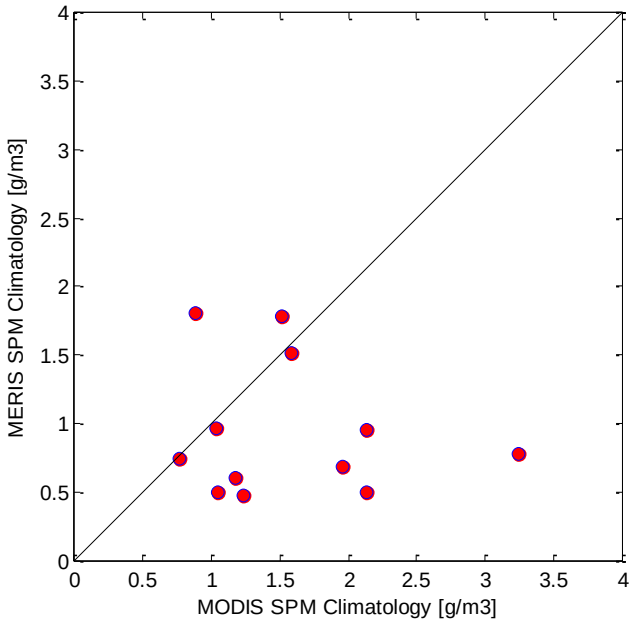

Figure 5: Comparison of the climatological SPM values derived from MODIS and MERIS for the box surrounding Kitimat region.

To explore the difference between MODIS and MERIS, monthly images were collocated and the difference |(i.e., $SPM_{MERIS} - SPM_{MODIS}$) was computed for each pixel (Figure 6). This exercise revealed following pattern: (1) MERIS estimates of SPM are much larger at the Skeena River estuary; (2) MODIS appears to estimate higher SPM in the Douglas Channel; (3) both sensors yield similar SPM concentrations in the open ocean, with MERIS SPM slightly higher than MODIS.

Close inspection of the pixels in the channel showed that MODIS pixels with high SPM estimates are frequently located along the coast indicating the so-called adjacency effects (Figure 7). Adjacency effects always occur in the presence of a scattering atmosphere over a non-uniform reflecting surface, which causes the radiance from high reflectivity areas to spill over neighboring low reflectivity regions, and modify their apparent brightness (Frouin et al. 2009). In the red spectral bands the contrast between land and water is high, indicating strong adjacency effects which substantially increase brightness of the water pixels in the red bands, leading to large overestimation of SPM using the MODIS red-band algorithm. Water land contrast is less pronounced in the visible part of the spectrum which could explain absence of such a strong adjacency effect in the MERIS SPM estimates, as MERIS employs multi-spectral SPM algorithm. The differences between MERIS and MODIS SPM close to the coast are often between 5-20 g/m^3 and can range up to 90 g/m^3. Adjacency effect is also expected to be higher in the winter as snow on the ground further increases contrast between land and water, which is consistent with the higher MODIS estimates observed in the winter months (Figure 4).

Further comparison was conducted by extracting 3x3 pixel boxes centered at four stations: two stations in the narrow part of the channel (Doug4 and Pin-2), one station in the wide part of the channel (SC61) and one station outside the channel (Pin-10). The location of the stations is shown on Figure 1. The comparison shows that the differences are greater for the stations in the narrow part of the channel, particularly for months showing large standard deviation within the MODIS box, which indicates presence of the adjacency-affected pixels with high SPM values. In the open ocean and in the wider parts of the channel both sensor show low standard deviation within 3x3 pixel box and fairly constant difference, with MERIS SPM about 0.2 g/m^3 to 0.5 g/m^3 higher than MODIS estimates (on average 0.46 g/m^3 at Pin-10, and 0.42 g/m^3 at SC61).

In conclusion, the differences between MODIS and MERIS SPM climatology and larger variations in MODIS-derived SPM within the channel are mostly due to the noise introduced by the strong adjacency effects observed in MODIS data, which substantially increases SPM values of the affected pixels close to the coast. Further analysis of MODIS-derived SPM in the channel would not be meaningful before affected pixels are addressed or filtered out. This was out of scope for this project so further analysis was performed using MERIS data only.

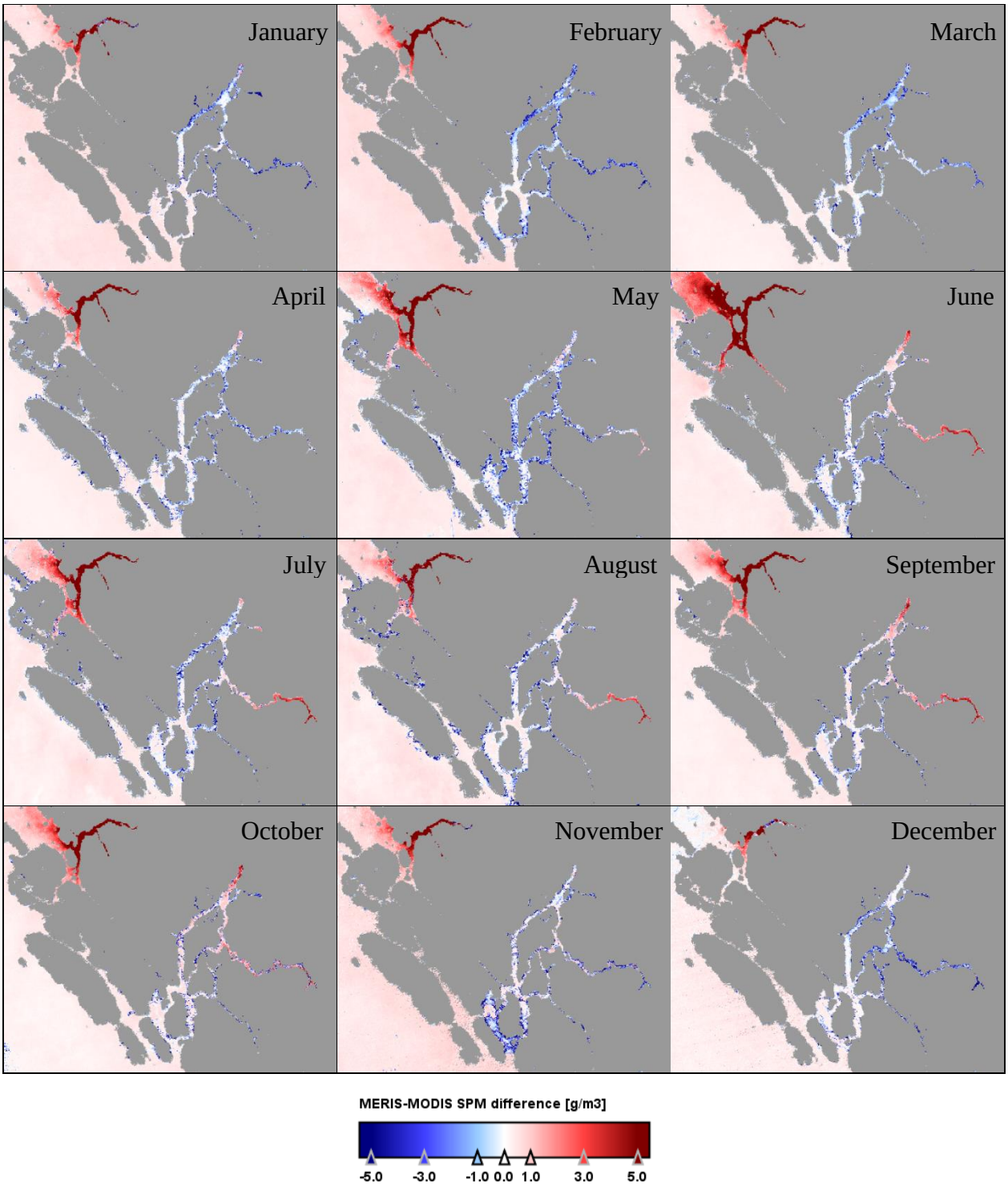

Figure 6: Difference between SPM monthly climatology derived from MERIS and MODIS ocean colour sensors.

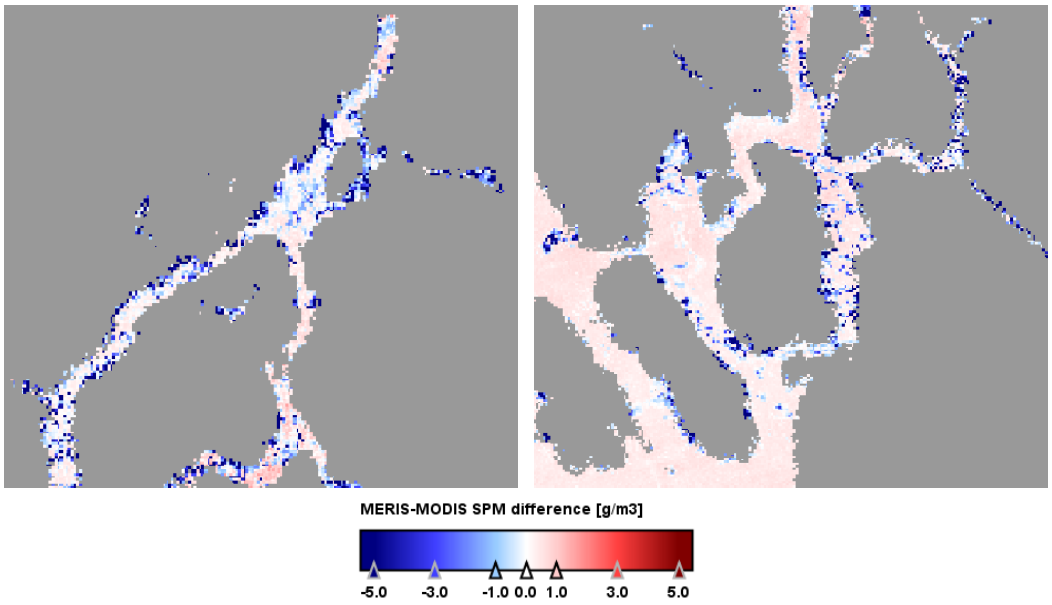

Figure 7: Difference between MERIS and MODIS SPM: Example of MODIS pixels along the coast that are affected by adjacency effect (blue pixels). Close to the coast MODIS SPM can be extremely overestimated and can range up to 90 g/m^3.

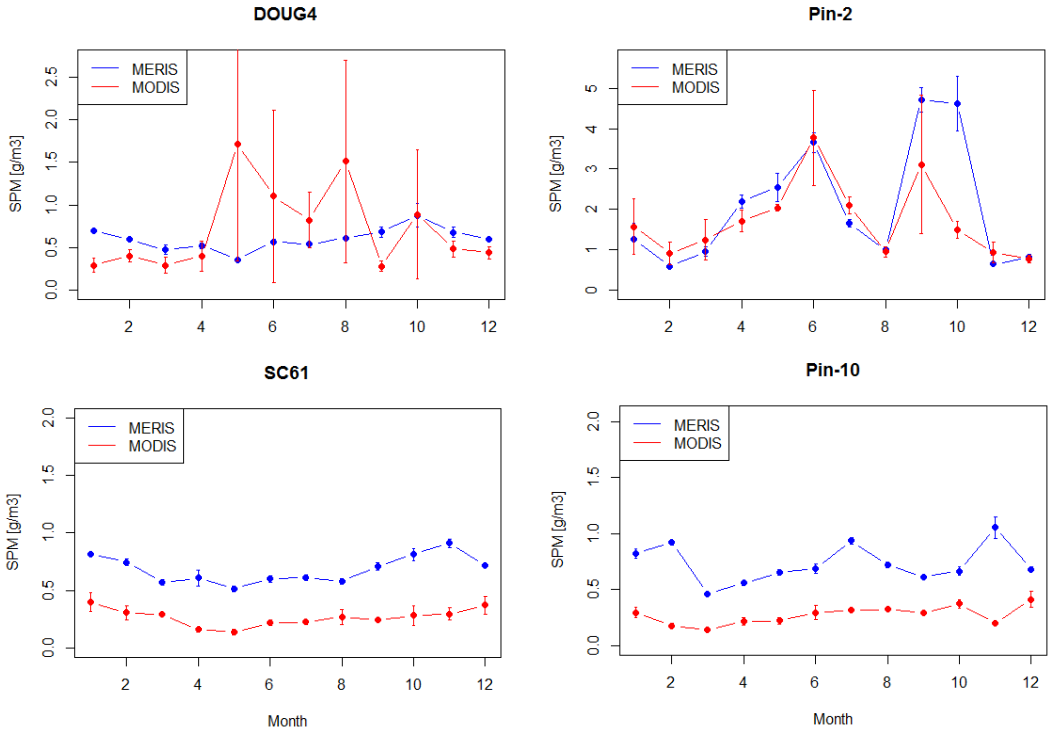

Figure 8: Example of monthly SPM values derived from MERIS and MODIS climatology images for two stations in the narrow part of the channel (Doug4 and Pin-2), one station in the wide part of the channel (SC61) and one station outside the channel (Pin-10). The error bars represent standard deviation of the pixels within 3x3 box centered at the station location.

MERIS TIME SERIES

To further assess spatial and temporal patterns and to explore the causes of large standard deviations in SPM associated with monthly averages, a time series of SPM concentrations derived from MERIS daily images was investigated for the 25 stations distributed along the Douglas Channel (Figure 1). Ten of those locations correspond to the IOS sampling sites, where SPM concentration is measured in situ. The other 15 locations were added along the Douglas Channel and Gardner Canal to obtain additional information on the SPM spatial variability in the Channel and in the Kitimat River plume. Station locations are listed in Table 4.

Table 4 : List of DFO stations and additional locations in the Douglas Channel for which SPM data was extracted from MERIS images.

DFO Stations		
Station	Longitude	Latitude
HEC1	-129.84402	52.82829
KSK1	-129.20822	53.48002
SC61	-129.41792	53.19967
SC69	-129.32596	53.07984
WC58	-129.12073	53.22202
CS84	-129.39941	52.89975
DOUG4	-128.7041	53.92676
DOUG40	-129.20866	53.44552
DOUG45	-129.1951	53.37022
FOC1	-129.03683	53.73405

Additional Locations		
Station	Longitude	Latitude
Pin 0	-128.67105	53.9973
Pin 1	-128.67708	53.96676
Pin 2	-128.73462	53.90665
Pin 3	-128.73573	53.88612
Pin 4	-128.81865	53.83901
Pin 5	-128.82504	53.78618
Pin 6	-129.20782	53.61777
Pin 7	-129.1109	53.11571
Pin 8	-129.24765	52.97957
Pin 9	-129.54854	52.90351
Pin 10	-129.8606	53.00983
Pin 11	-128.83267	53.58611
Pin 12	-128.6334	53.47863
Pin 13	-128.14629	53.46415
Pin 14	-128.36705	53.48669

EXTRACTION BOXES

The extraction was conducted for two boxes of different sizes to assess the performance of the algorithm and to obtain information on fine scale structure. The size of the small box was 3x3 pixels corresponding to a spatial resolution of about 900 x 900 m at nadir (i.e., foot print under the satellite) and the size of the large box is 9x9 pixels corresponding to a size of about 2.7 x 2.7 km at nadir. Each box was centered at the station location. The data were extracted for all the pixels in the box but only valid pixels were retained for further analysis. Data extraction from MERIS scenes was performed in batch mode using BEAM pixel extraction operators.

The small 3x3 pixel box is more suitable to assess SPM concentration at a particular location and is less likely to include large SPM variations within the box. Space agencies recommend this

size when performing is situ validation of satellite geophysical products such as SPM. On the other hand, the 9x9 pixel boxes can yield a better representation of the wide sections of Douglas Channel and can exhibit a larger range of SPM variation than the small 3x3 boxes, particularly when the large box includes edge of a sediment plume.

The average SPM values for the large 9x9 pixel boxes and the small 3x3 pixel boxes centered at the same station are compared in Figure 9 and Figure 10. The comparison reveals that the size of the box results in differences of up to about 3 g/m^3 for the locations that are characterized by a large spatial variability and large SPM gradients, such as the Pin 0 at the mouth of the Kitimat River and two other stations in the Gardner Canal. For all other stations located along the channel the difference between average SPM value within 3x3 and 9x9 pixel boxes is small, no more than 0.5 g/m^3 (Figure 10).

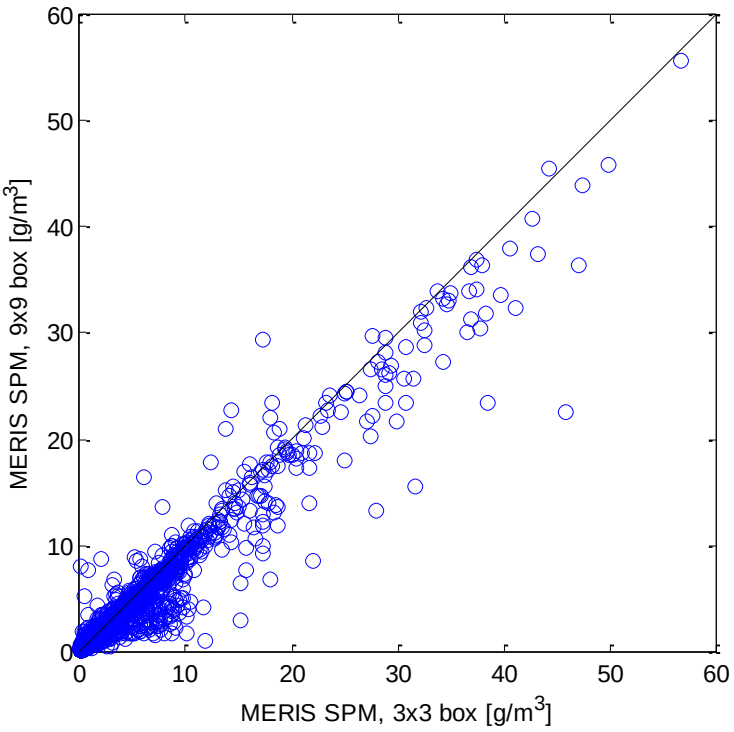

Figure 9: Average SPM of all valid pixels in 3x3 pixel boxes compared to the values derived from 9x9 pixel boxes for all 25 stations. Note that in many cases where SPM spatial distribution is fairly uniform the box size did not influence average SPM value in the box. In some cases, where the spatial variability and SPM gradients within the box are larger, the average SPM in the box varies with box size.

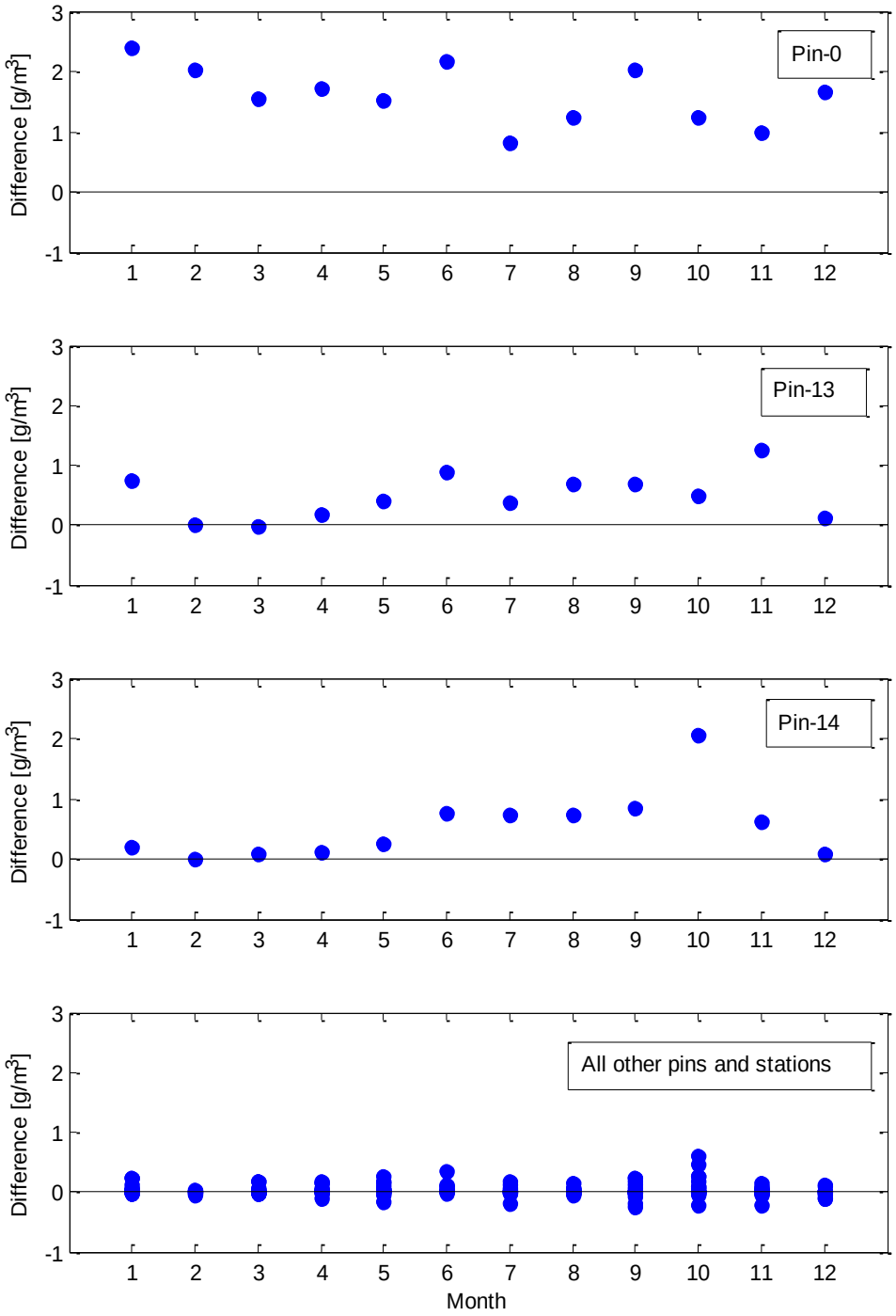

Figure 10: Difference between average SPM in 3x3 pixel box and average SPM in 9x9 pixel box extracted from MERIS climatology images. Note that for only three locations (Pin-0, Pin-13 and Pin-14) the average SPM value in 3x3 box was mostly higher than the average SPM in 9x9 box, indicating greater spatial variability and SPM gradients around those stations. For all other stations the size of the box yielded to no more than 0.5 g/m^3 difference in average SPM concentration.

SPM TIME SERIES

The time series for all 25 stations was created using data extracted from 3x3 pixel boxes centered at the station locations. All data were first aggregated by month to establish the range of SPM in the region (Figure 11). Note that all the months exhibit large variations in SPM concentration with the most extreme values above 50 g/m^3 in January, February, and October.

The time series was further plotted for each station and the plots were grouped based on the station locations in the channel (Figure 12 to Figure 16).

The plots show that the stations located in the Kitimat region are characterized by a background of sediment concentration superimposed by intense events with high SPM concentrations. These events seem to occur during the period January-March and in the fall (October). They are most likely related to periods of snowmelt or heavy rain which increases the river flow and therefore the transport of sediment to the Douglas Channel. These events appear to be short lived with the SPM concentration dropping quickly to the background level in a few days, which indicates that sediment is rapidly removed from the surface layer either by export to the mouth or rapid sinking. The highest concentrations are observed for the locations closest to the mouth of the Kitimat River. The stations located further from the Kitimat river mouth and in the middle part of the channel show low sediment concentrations, usually below 2 g/m^3 and occasional high concentration that do not exceed 9 g/m^3. The stations in the lower part of the channel and outside of the channel show low SPM concentrations, not exceeding 4 g/m^3 and do not seem to be greatly influenced by the events occurring in the Kitimat region. The stations in the Gardner Canal however show events with larger SPM concentration and a seasonal pattern, with the highest concentrations in the summer.

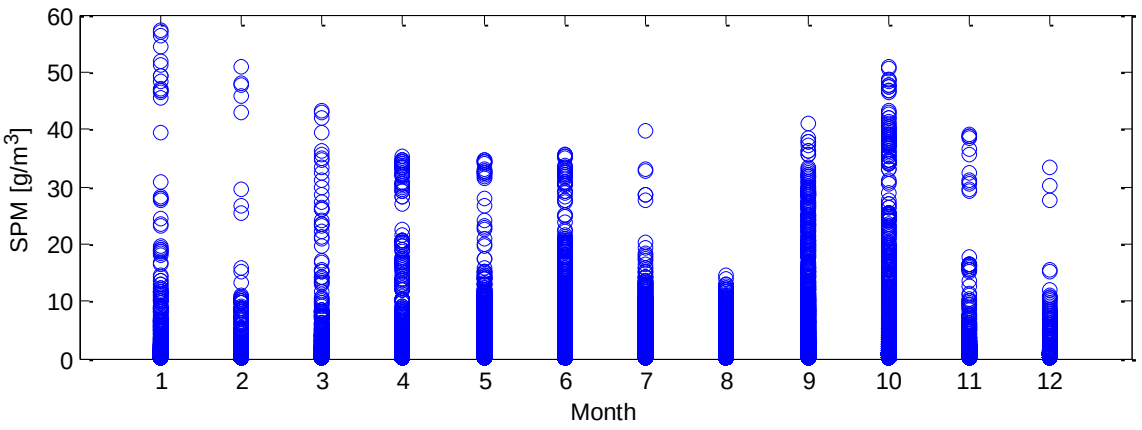

Figure 11 : SPM concentration extracted from 10 years of MERIS images (3x3 boxes) for all the stations in the Douglas Channel aggregated by month. Note that the events with the highest sediment concentration in the region occur in January and October.

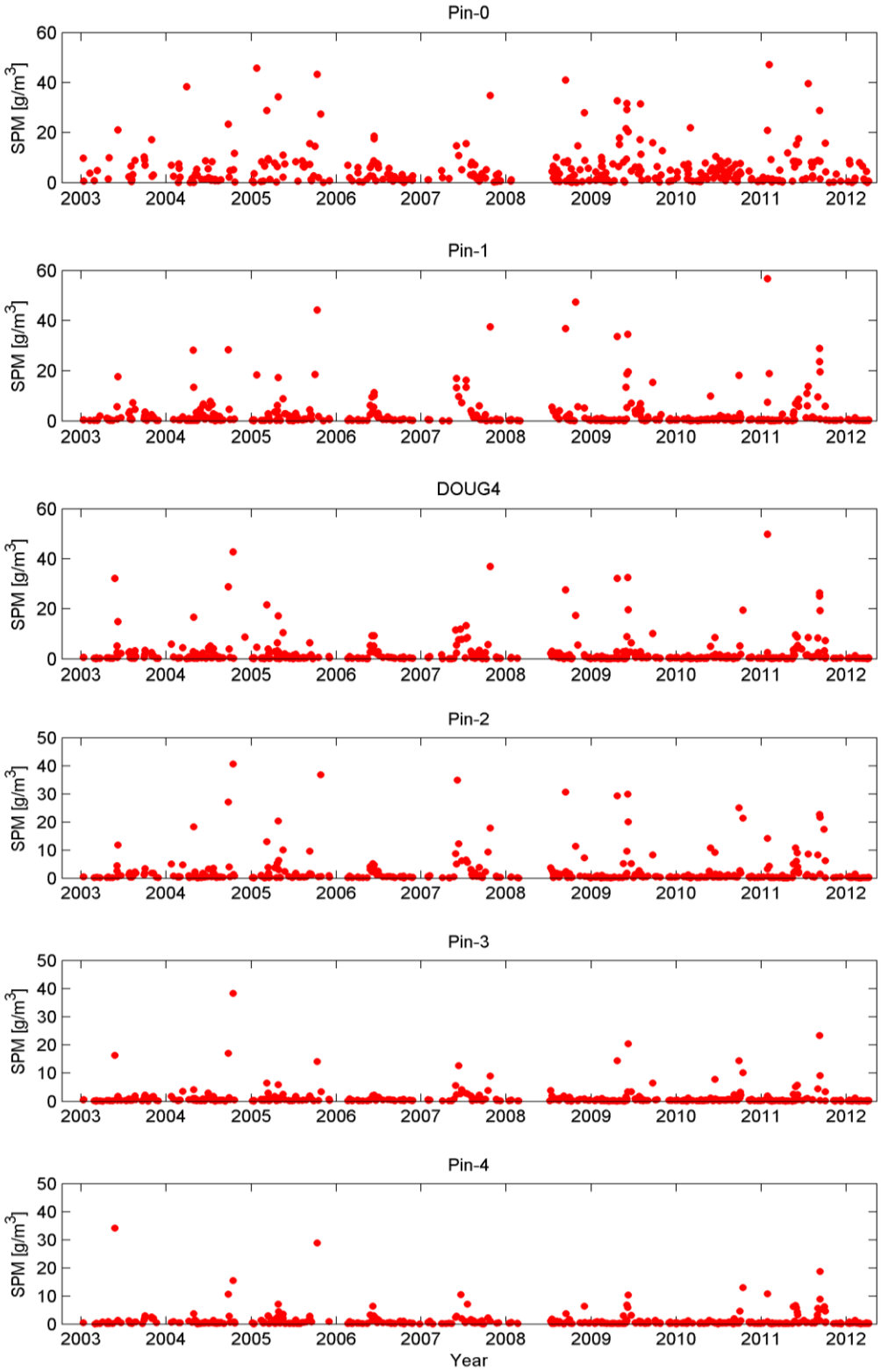

Figure 12 : Time series of SPM concentration extracted from MERIS daily images for the stations in the Kitimat region. Station names are shown in the title of each plot. The SPM concentration is an average value of 3x3 pixel box centered at the station location (900x900m). Note that the top three and bottom three plots are plotted on different scale.

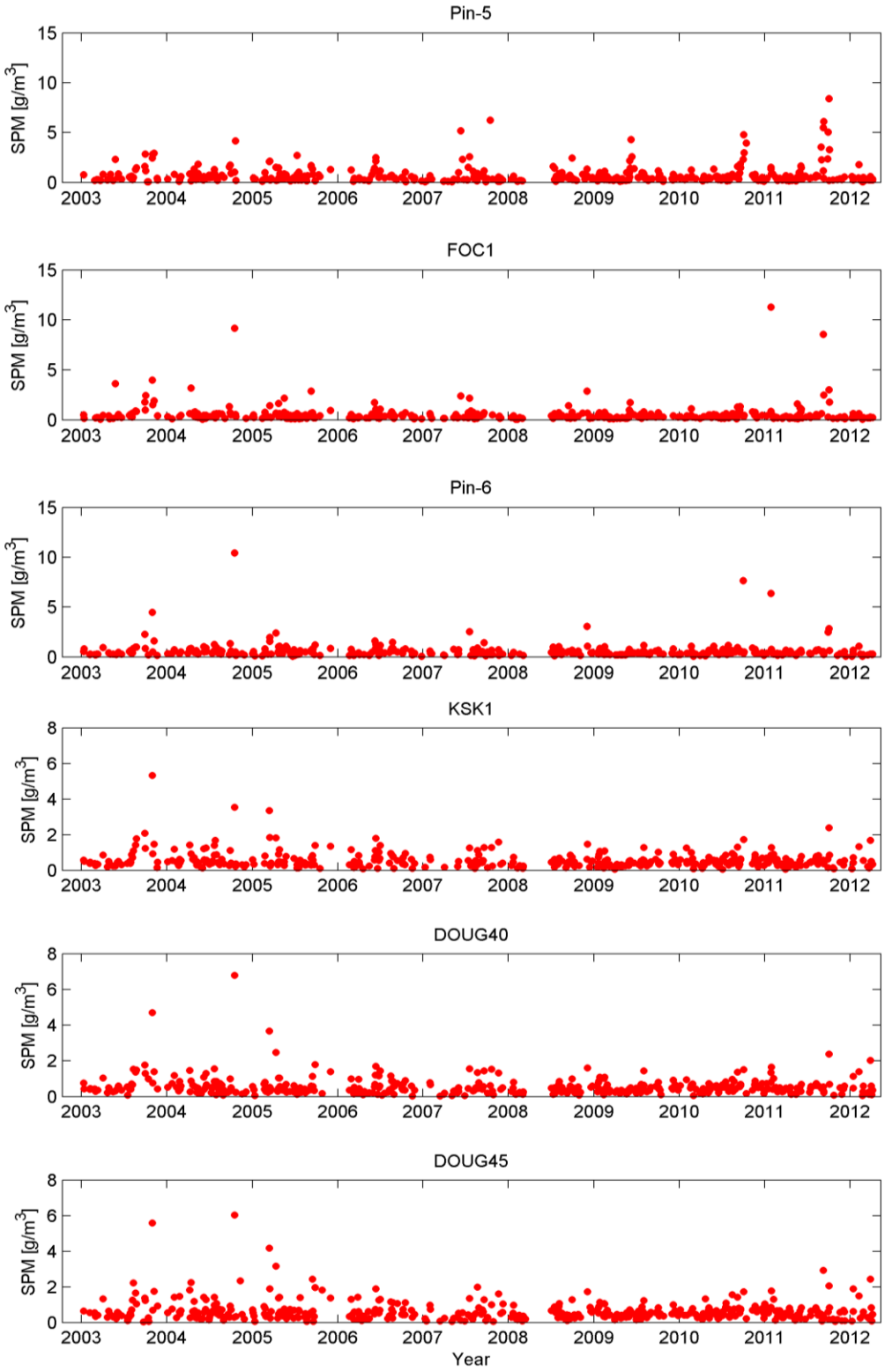

Figure 13 : Time series of SPM concentration extracted from MERIS daily images for the stations in the upper and middle Douglas Channel. Station names are shown in the title of each plot. SPM concentration is an average value of 3x3 pixel box centered at the station location (900x900m). Note that the top three and bottom three plots are plotted on different scale.

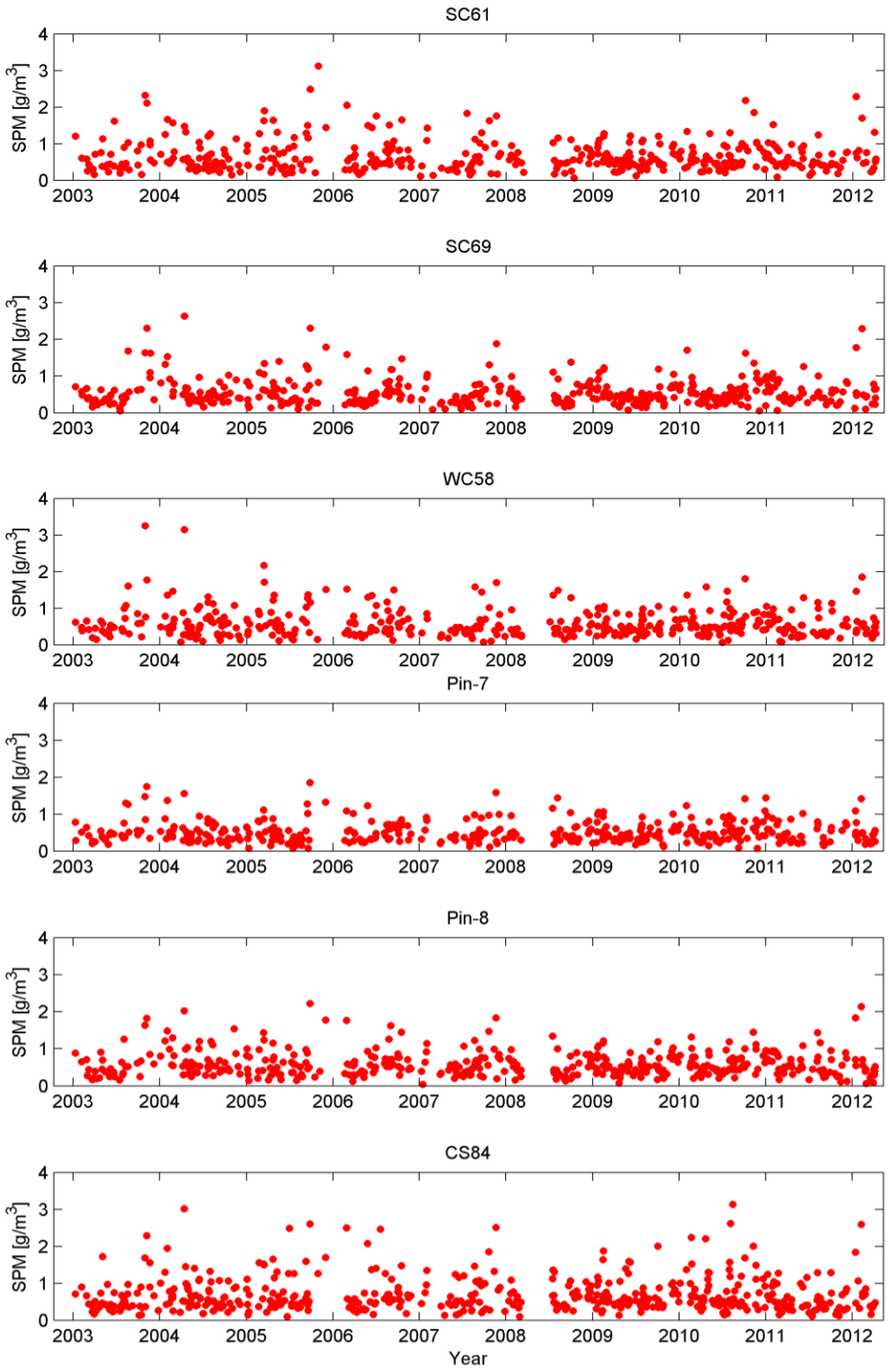

Figure 14 : Time series of SPM concentration extracted from MERIS daily images for the stations in the lower part of Douglas Channel. Station names are shown in the title of each plot. SPM concentration is an average value of 3x3 pixel box centered at the station location (900x900m).

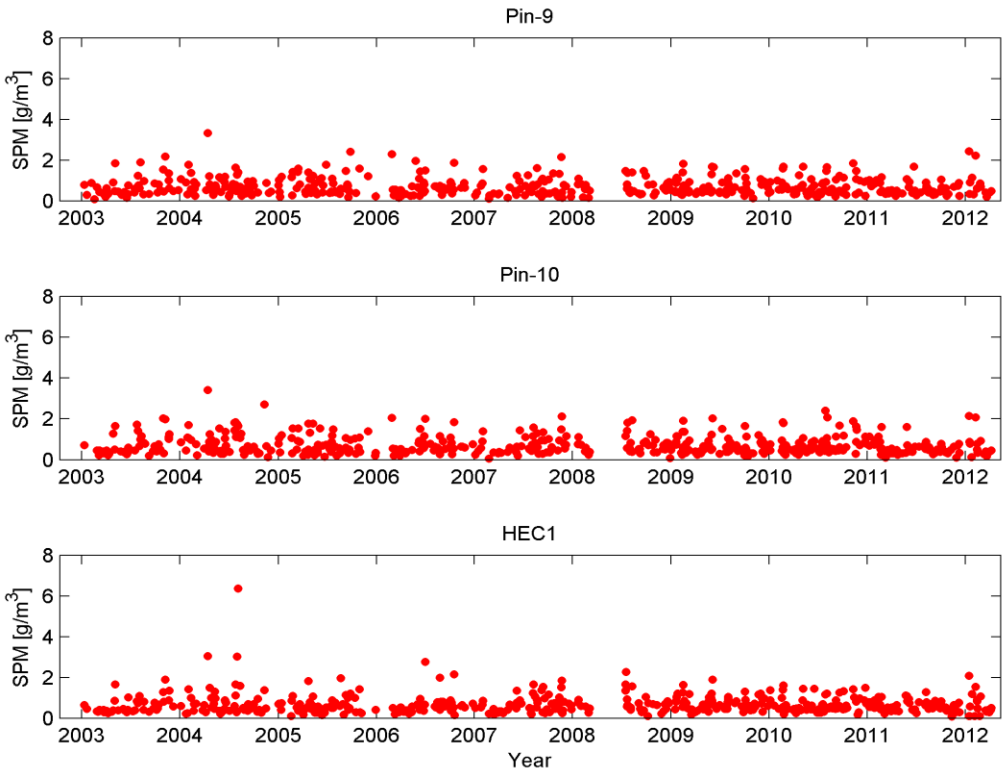

Figure 15: Time series of SPM concentration extracted from MERIS daily images for the stations outside of the Douglas Channel. Station names are shown in the title of each plot. SPM concentration is an average value of 3x3 pixel box centered at the station location (900x900m).

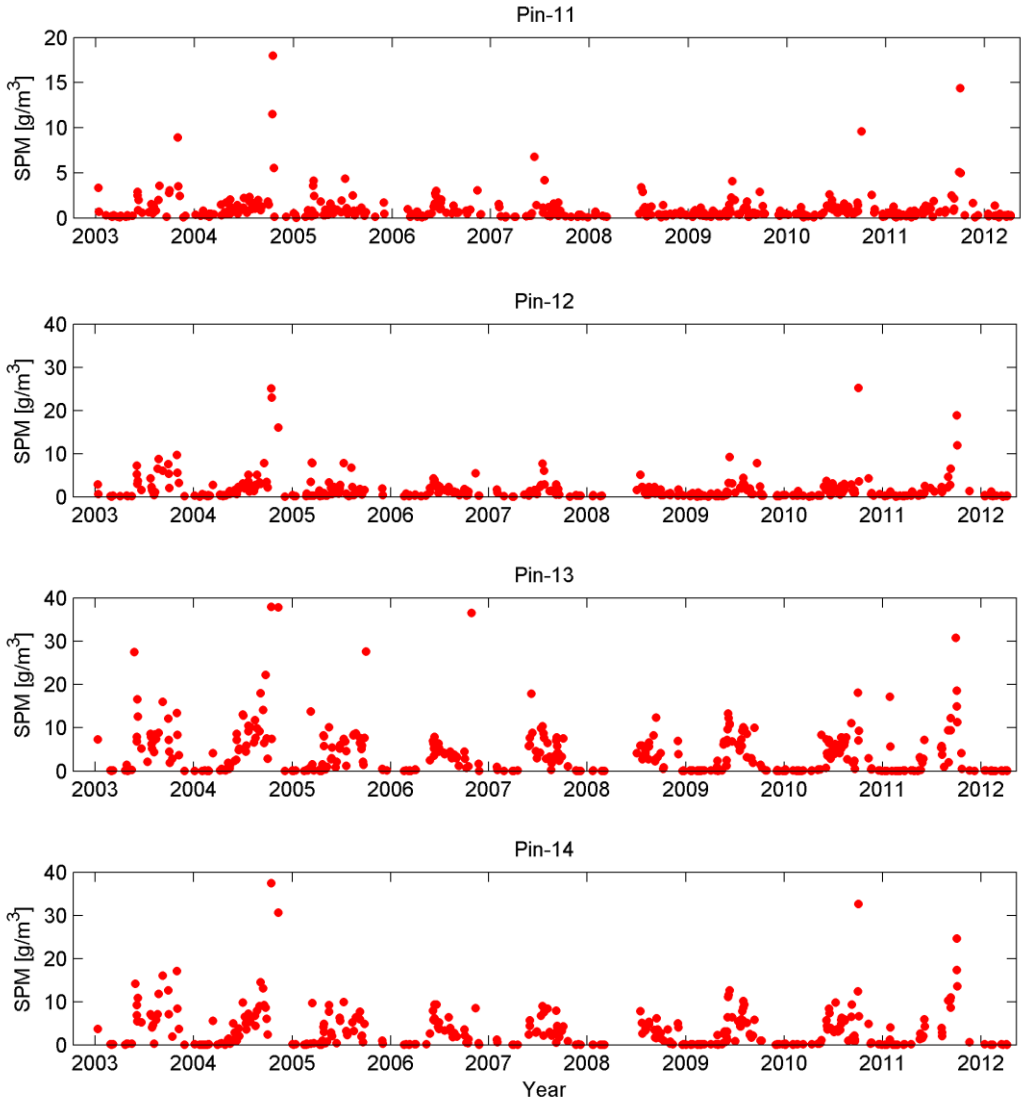

Figure 16 : Time series of SPM concentration extracted from MERIS daily images for the stations in the Gardner Canal. Station names are shown in the title of each plot. SPM concentration is an average value of 3x3 pixel box centered at the station location (900x900m). Note that the top plot and bottom three plots are plotted on different scale.

BOX PLOTS AND SPM FREQUENCY DISTRIBUTIONS

Given the nature of MERIS SPM time series data we decided to use box plots as convenient visual display of the simple sample statistic, which is particularly useful for identifying outliers and for assessing and comparing data distributions.

The box plot is a rectangle which encloses the middle half of the sample with an end at each quartile. Median value is shown as a line across the box and indicates the centrality of the distribution. The length of the box represents interquartile range (IQR) that measures the spread of the centre of the data distribution. The whiskers spread to the ±1.5*IQR from the end of the box or to the closest data value falling within that region and indicate the length of the tail of the

distribution. The outliers are defined as values outside the region bound by ±1.5*IQR from the end of the box, and the extreme outliers as values falling outside the region bound by ±3*IQR from the end of the box (Figure 17).

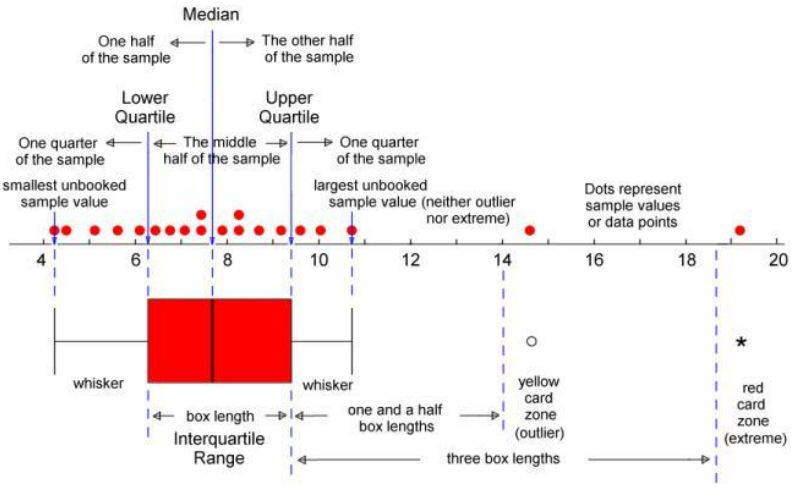

Figure 17: Diagram showing elements of a boxplot. Adopted from http://web.pdx.edu/~stipakb/download/PA551/boxplot.html

Examples of SPM frequency distribution histograms for three stations located at the different parts of the Douglas Channel (top, middle, and lower part) and associated box plots are shown on Figure 18.

In general, all three stations exhibit positively skewed asymmetrical distribution with the low median SPM values, relatively small IQR (spread in the middle half of the sample), large positive tail (indicated by the length of the whisker in the boxplot) and many outliers and extreme outliers. The stations closer to the mouth of the Kitimat Rriver exhibit larger asymmetry, longer tail, and larger number of outliers and extreme outliers extending to very high SPM values.

The frequency distributions for all stations summarized on the box plot (Figure 19) are showing similar pattern along the Douglas Channel. Low median SPM values of about 0.5 g/m^3 seem to persist along the channel except at the station Pin-0 located at the Kitimat River mouth where median SPM concentration increases to about 3 g/m^3.

The range of variability associated with the median (IQR and whisker range) remains low along the channel and increases only at the last few stations close to the river mouth (Figure 21). The outliers and extreme outliers increase in number and magnitude toward the mouth of the Kitimat River indicating more frequent intense sediment plumes with the number of the extreme outliers and their magnitude increasing considerably for the stations Pin-5 to Pin-0 (Figure 20 and Figure 21).

The maximum in the number of extreme outliers at the station DOUG4 (Figure 20) indicates more frequent intense plumes that could be due to the additional runoff from the surrounding creeks. The smaller peak in a number of extreme outliers at station DOUG45 could be due to the additional SPM plumes arriving from Gardner Canal through Verney Passage, as it was observed on several MERIS images.

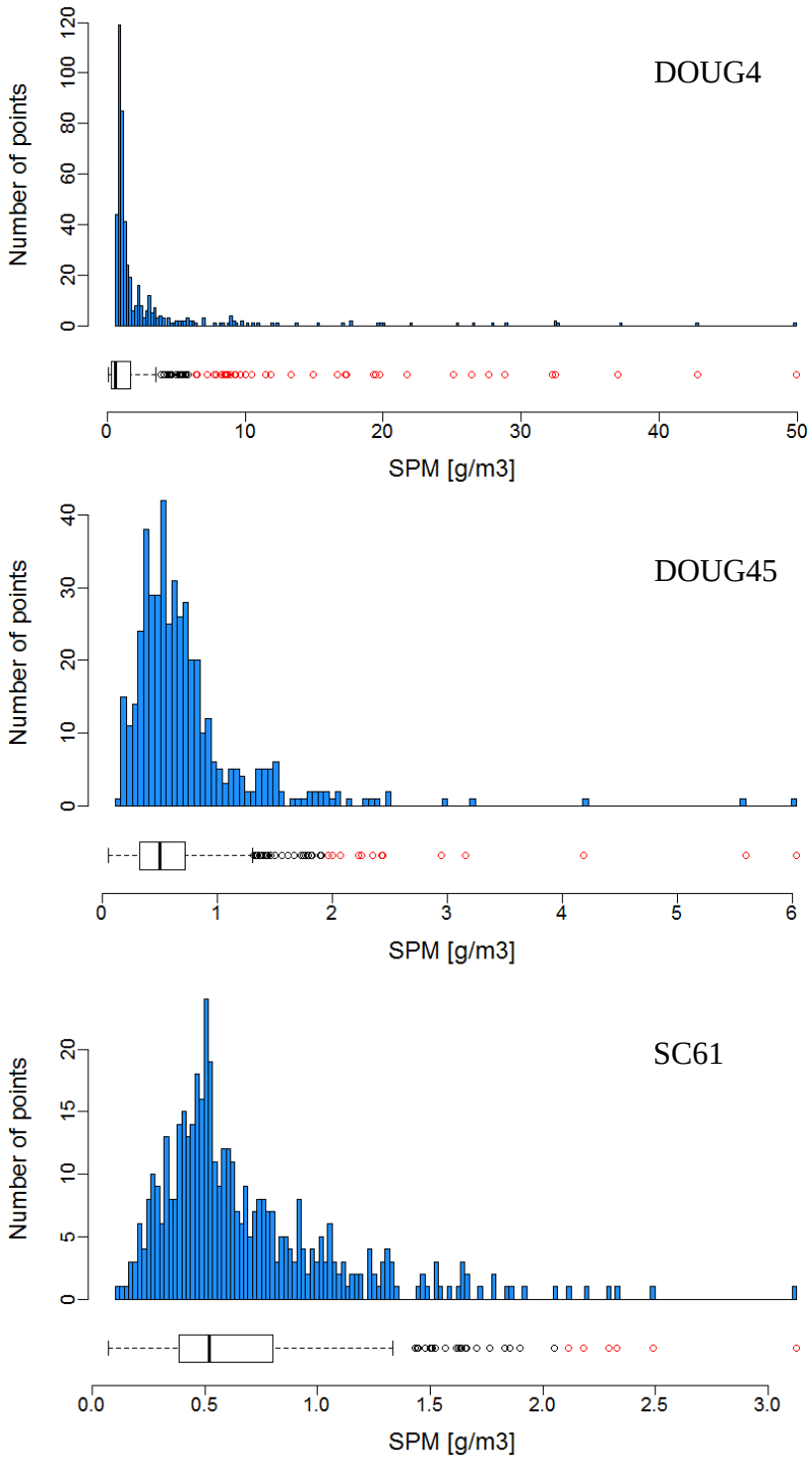

Figure 18: Frequency distribution of SPM concentration extracted from MERIS data for years 2002-2012 and the associated box plots. The outliers in the box plot that are outside 1.5*IQR are shown in black and the extreme outliers exceeding 3*IQR are shown in red. The three panels show a station in the upper part of the channel (DOUG4), in the middle part (DOUG45), and in the lower part of the channel (SC61).

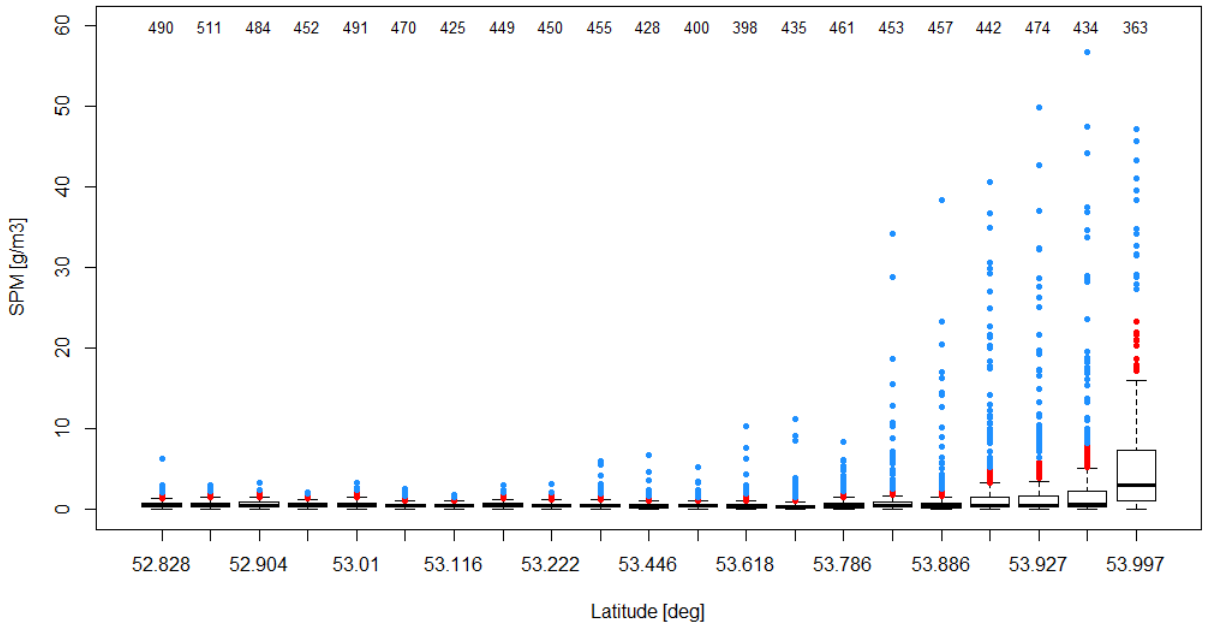

Figure 19: Box plots for each station along the Douglas Channel shown as a function of latitude. The first station on the right hand side corresponds to Pin-0 at the mouth of the Kitimat River and the last station on the left to HEC1 outside the Douglas Channel. The red symbols represent outliers exceeding 1.5*IQR and the blue symbols represent extreme outliers exceeding 3*IQR. The number of points for each station is indicated at the top of the plot and includes all seasons.

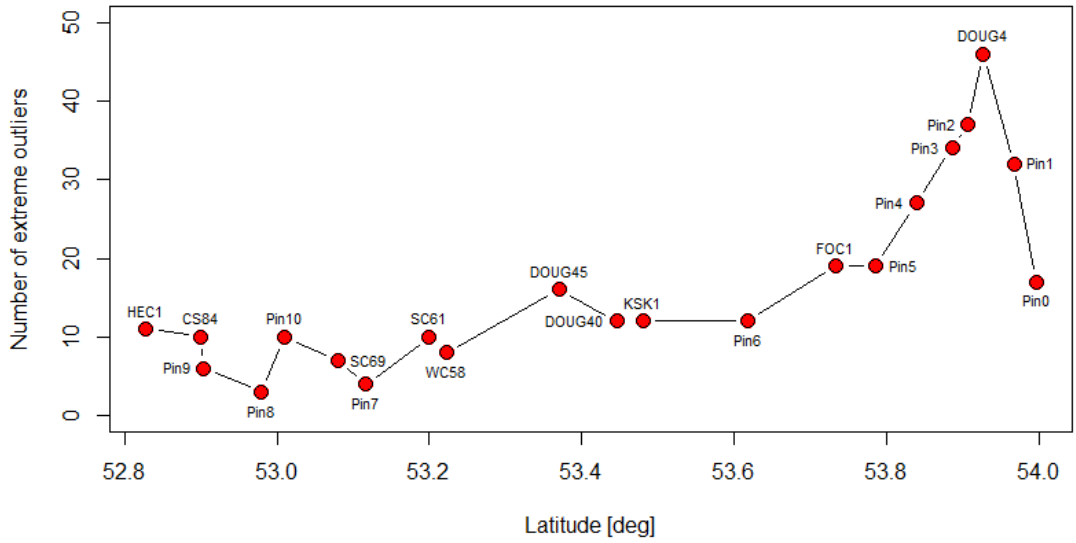

Figure 20: Number of extreme SPM outliers in dataset extracted from MERIS images (2002-2012) for each station along the Douglas Channel plotted as a function of latitude.

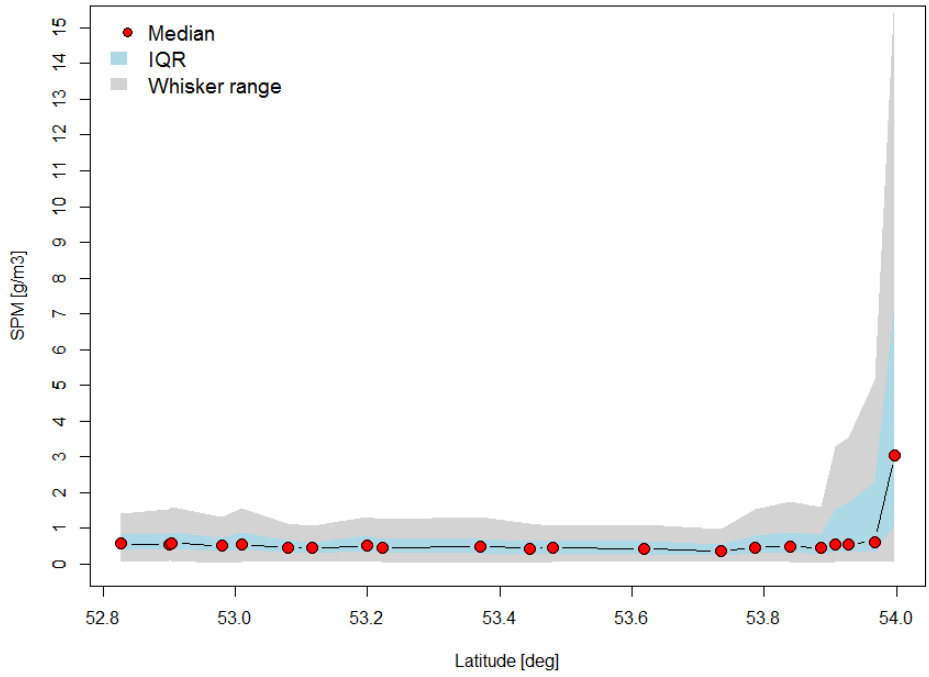

Figure 21: Summary statistics for all MERIS SPM data along Douglas Channel. Red symbols represent median SPM at each station, the light blue area is IQR (range containing 50% of the data), and the gray area is the range of the data that are not considered outliers (whisker range).

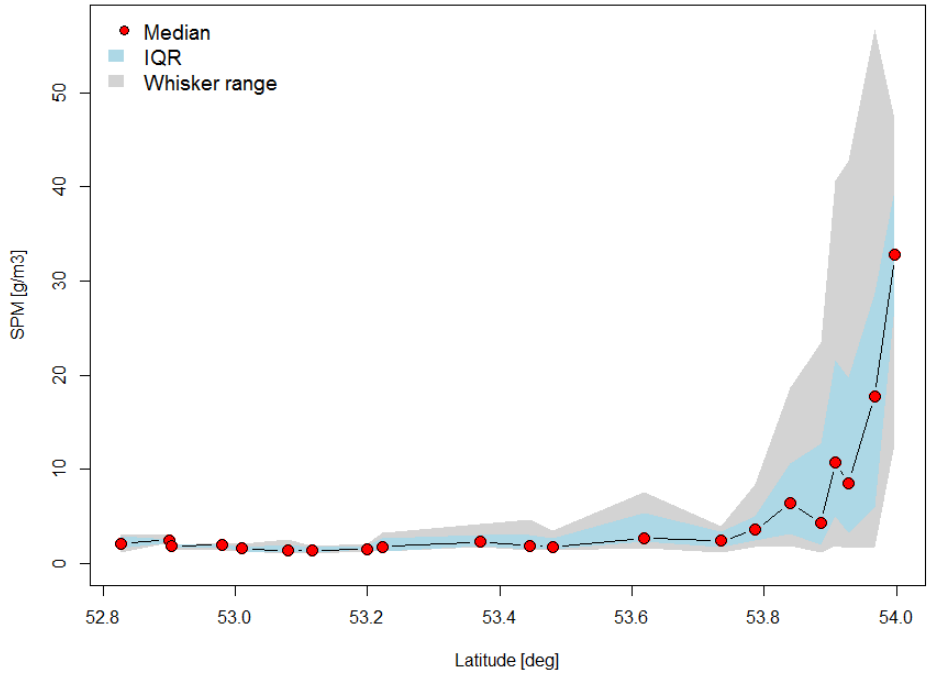

Figure 22: Summary statistics for extreme SPM outliers. Red symbols represent median value of extreme outliers at each station, the light blue area is IQR (range containing 50% of the extreme outliers), and the gray area is the range of the extreme outliers.

SPATIAL AND TEMPORAL SPM PATTERNS

To assess SPM spatial and temporal patterns in Douglas Channel, MERIS SPM time series was grouped by month and box plots were created for each station location (Figure 23 to Figure 26). Outliers and extreme outliers were identified for each month and station as described in the previous section. This monthly dataset was then divided in two sets:

(1) background SPM dataset that does not include outliers and
(2) extreme outliers dataset containing values exceeding 3*IQR.

The statistics (mean, median, standard deviation, and number of points) was computed for all SPM data, for background SPM (1), and for extreme outliers only (2) and are presented on the Hovmöller diagrams on Figure 27 to Figure 30.This exercise revealed the following spatial and temporal SPM patterns in the Douglas Channel:

The number of MERIS SPM data points for all stations is highest in August, followed by July and June with about 45-60 points collected over 10-year period leading to average 4-6 valid monthly observations during summer months (Figure 27). The lowest number of observation, 1 or 2 per month, is associated with November and December in the upper part of the Douglas Channel and Gardner Canal due to the frequent cloud coverage. The lower part of the Douglas Channel and Hecate Strait seem to be less cloudy in the winter with the average number of observation of about 3 per month. In the spring there seem to be more observations in the upper part of the Douglas Channel than in the middle part of the channel. The month of February is also showing more data points indicating less frequent cloud coverage. The number of data points in each month does not correlate with the SPM values.

Average SPM values that include all data (Figure 27) are strongly influenced by outliers and show high values in the Kitimat Arm from April to July and again in September and October. The stations in Gardner Canal show high average values from June to November. Those periods correspond with the high summer river discharge and spring/fall rain seasons. The standard deviation computed from all data shows the highest variability in the upper part of the Douglas Channel particularly in October when the variability is extending to the DOUG45 station in the middle of the Channel. For Gardner Canal stations the variability is also highest in the fall.

The background SPM in the Doulas Channel, represented by the median SPM diagrams (Figure 27 and Figure 28), is mostly low throughout the entire year, except for the stations in the Kitimat Arm and Gardner Canal which show seasonal variability. The highest median SPM value is observed at the mouth of Kitimat River (Pin-0) in June, which corresponds to the highest river discharge due to the summer snow melt indicating that the background SPM patterns are driven mostly by the river discharge. Somewhat higher SPM values are also observed as far as Pin-5 in the Kitimat Arm in the summer with slight increase again in the fall indicating that frequent rain events might slightly elevate background SPM. The variability of background values, represented by the standard deviation, is clearly highest in June for the Kitimat Arm up to Pin-4, and again in September and October. The stations in Gardner Canal show elevated median values for the period from June to November with highest average values and variability in October.

The number of extreme outliers (Figure 29) is low at the river mouth (Pin-0) indicating that the outliers are not strongly driven by the Kitimat river discharge, except in March and October. The highest number of extreme outliers is seen in the Kitimat Arm, particularly at DOUG4 and Pin-02 locations extending to Pin-5 and DOUG45 in the fall, which suggests that strong runoffs from creeks and mountain sides are happening in this region after frequent spring and fall rainstorms. The intensity of extreme outliers seems to be higher in September and October. The variability of extreme outliers, described by standard deviation, is the highest in January, followed by the period March to June and again in September and October.

Maximum SPM values in Douglas Channel for the whole 10-year period (Figure 30) are observed interestingly in January in the Kitimat Arm. This can be explained with rain-on-snow events where high snow melt rates due to the rain and mild temperature amplify the runoff caused by a rain storm (Karanka 1993). The other pronounced peak in maximum values for Douglas Channel is in October while maximum values in Gardner Canal are observed in November.

Maximum background SPM values (Figure 30) exhibit peaks in June and September/October for the stations in Kitimat Arm. In Gardner Canal higher maximums are seen from May to November with the peak in October.

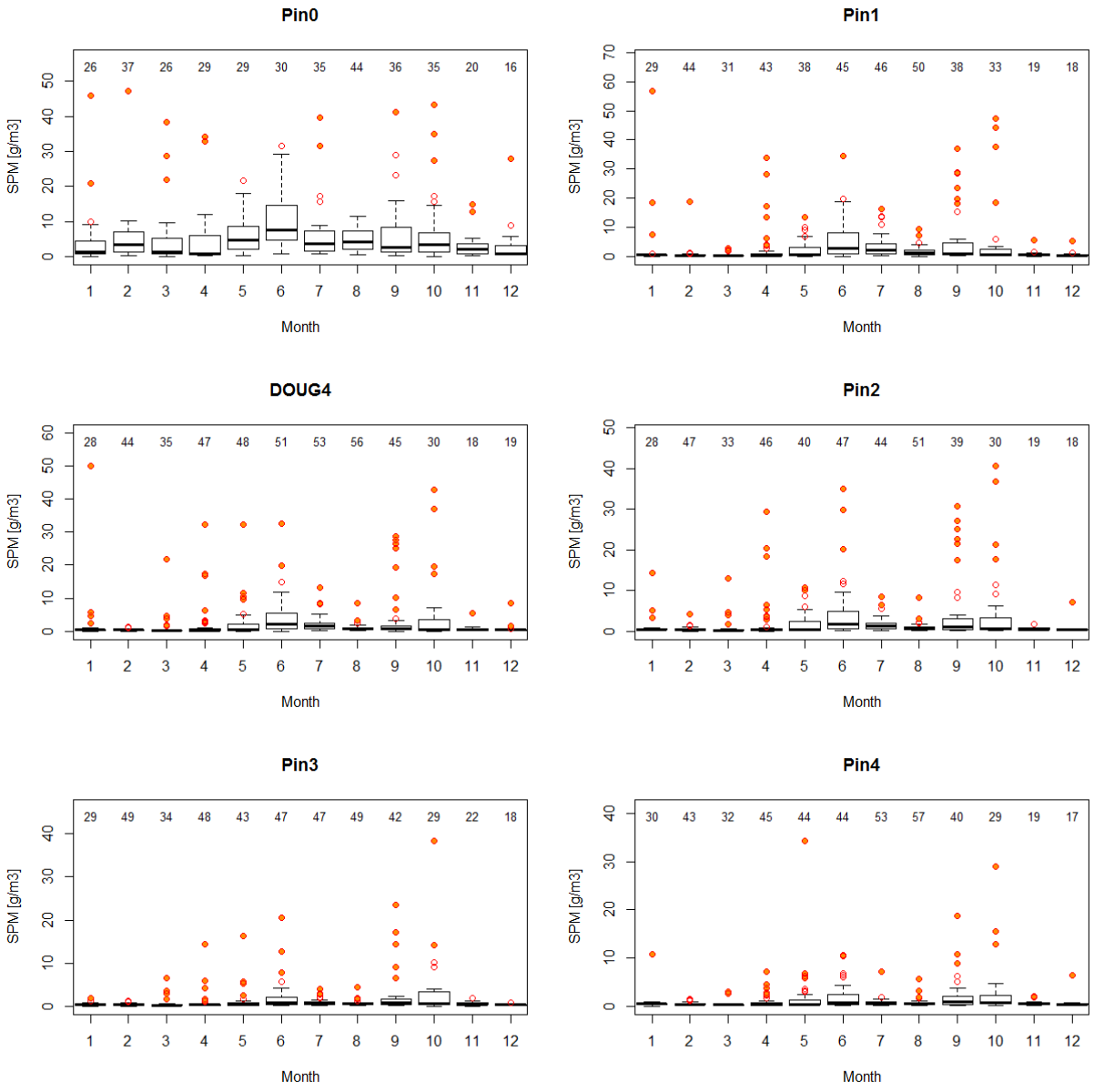

Figure 23: Box plots for the monthly SPM concentration extracted from MERIS images (2002-2012) for the stations in the upper part of the Douglas Cannel, close to the mouth of the Kitimat River. The outliers exceeding 1.5* IQR are shown as hollow circles and the extreme outliers exceeding 3*IQR as solid circles. The number of data points available for each month is shown at the top of the plot. Note the different scale for each plot.

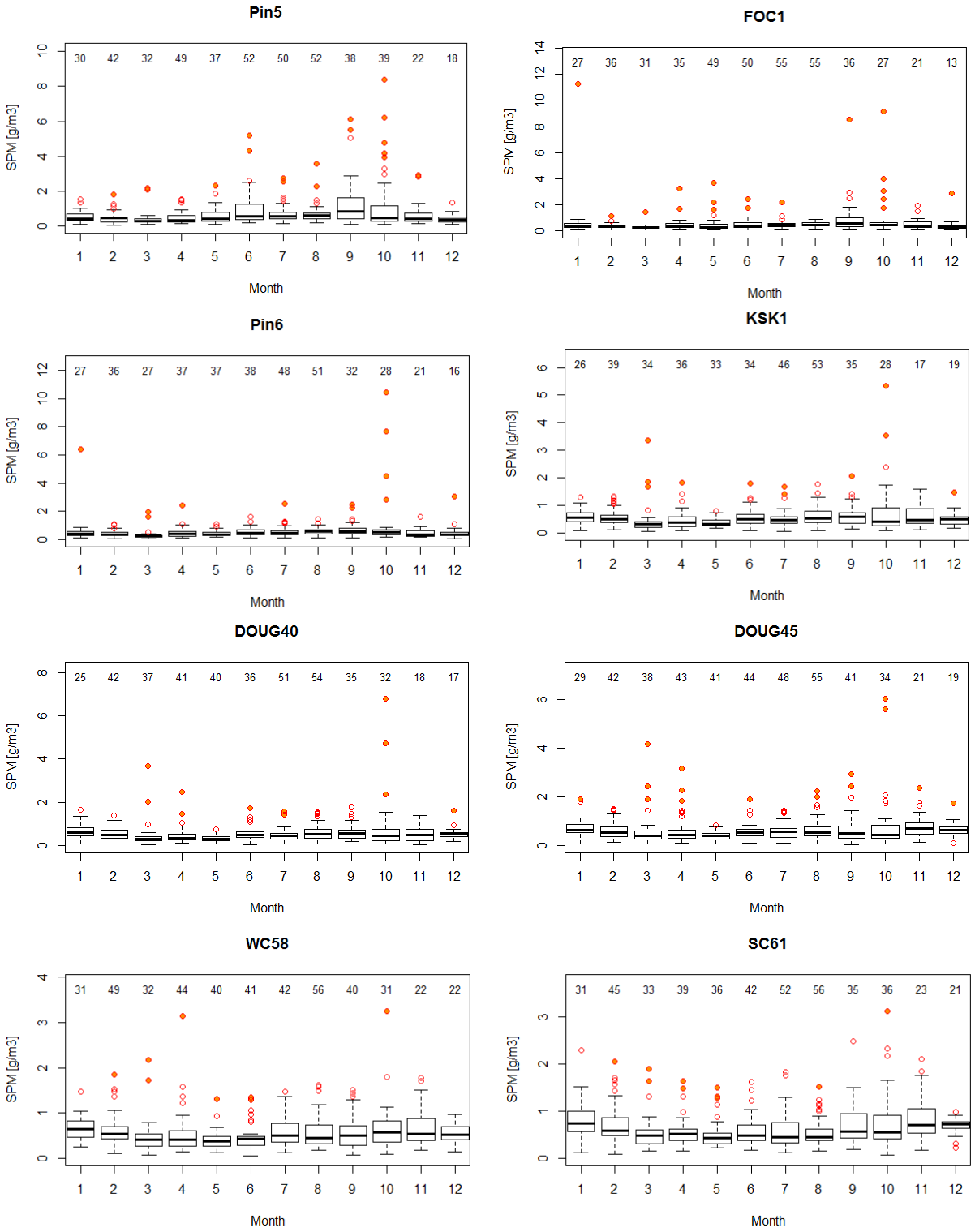

Figure 24: Box plots for the monthly SPM concentration extracted from MERIS images (2002-2012) for the stations in the middle part of the Douglas Cannel. The outliers exceeding 1.5* IQR are shown as hollow circles and the extreme outliers exceeding 3*IQR as solid circles. The number of data points available for each month is shown at the top of the plot. Note the different scale for each plot.

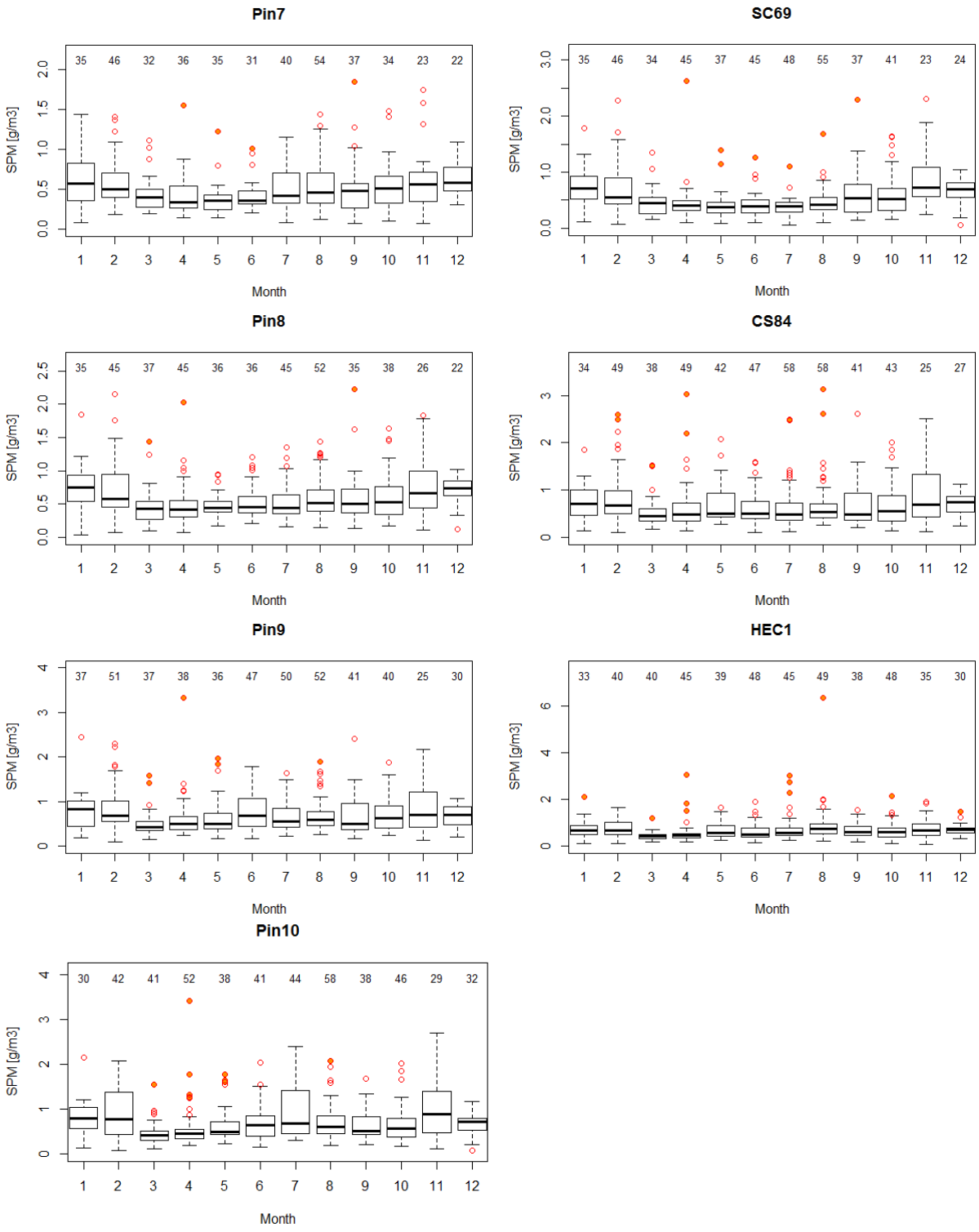

Figure 25: Box plots for the monthly SPM concentration extracted from MERIS images (2002-2012) for the stations in the lower part of the Douglas Cannel and in Hecate Strait. The outliers exceeding 1.5* IQR are shown as hollow circles and the extreme outliers exceeding 3*IQR as solid circles. The number of data points available for each month is shown at the top of the plot. Note the different scale for each plot.

Gardner Canal

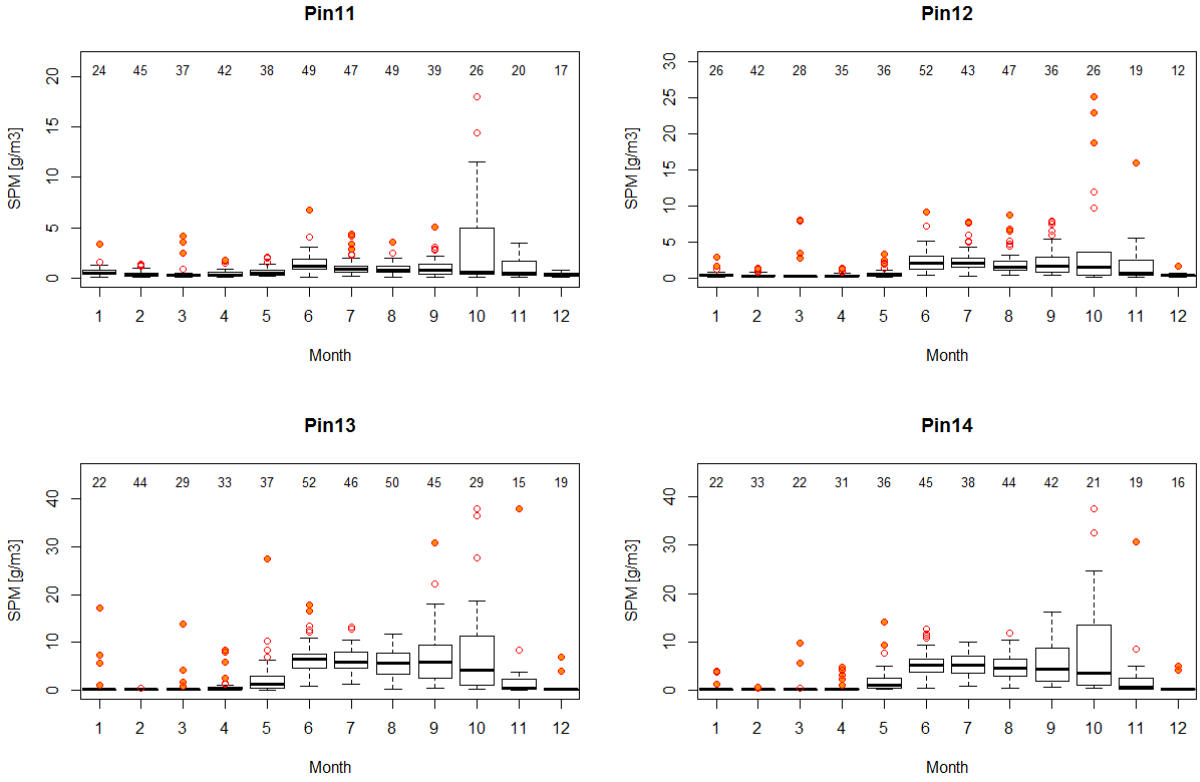

Figure 26: Box plots for the monthly SPM concentration extracted from MERIS images (2002-2012) for the stations in the Gardner Canal. The outliers exceeding 1.5* IQR are shown as hollow circles and the extreme outliers exceeding 3*IQR as solid circles. Note the different scale for each plot.

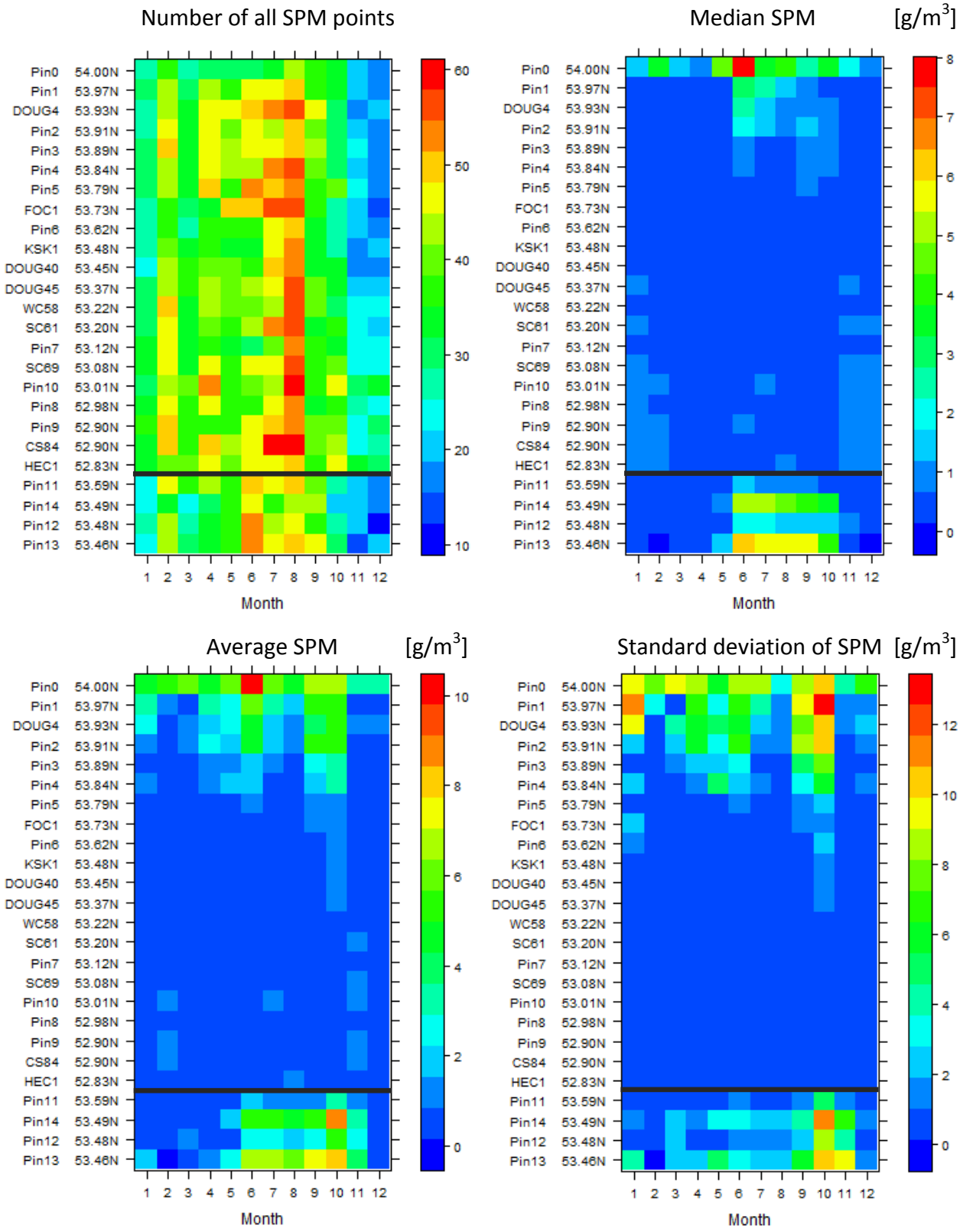

Figure 27: Spatial and temporal distribution of the statistical parameters for all MERIS SPM data. Four stations in the bottom of the plot (Pin-11 to Pin-14) are located in the Gardner Canal.

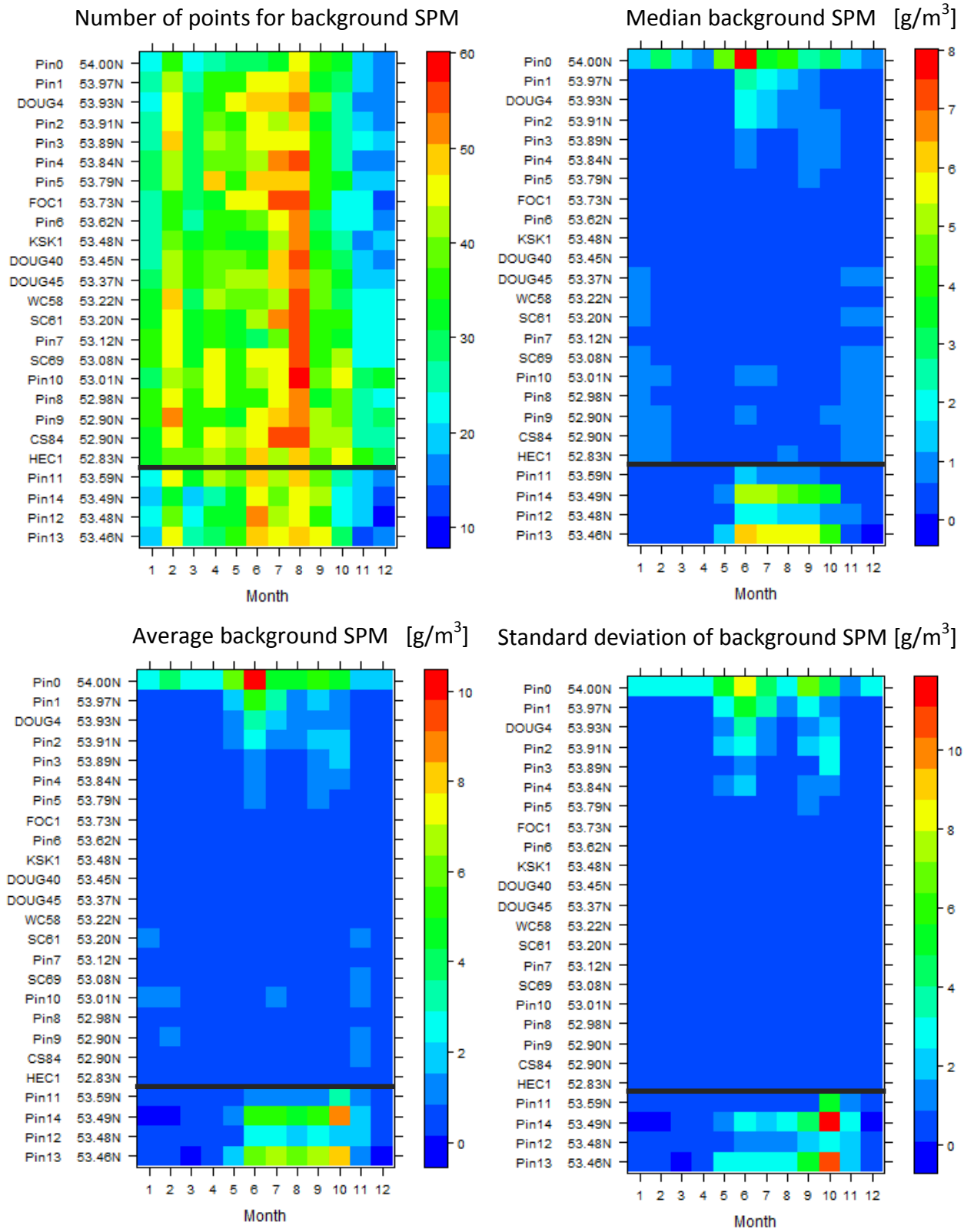

Figure 28: Spatial and temporal distribution of the statistical parameters for background SPM (without outliers). Stations below the black line are located in the Gardner Canal (Pin 11-14)

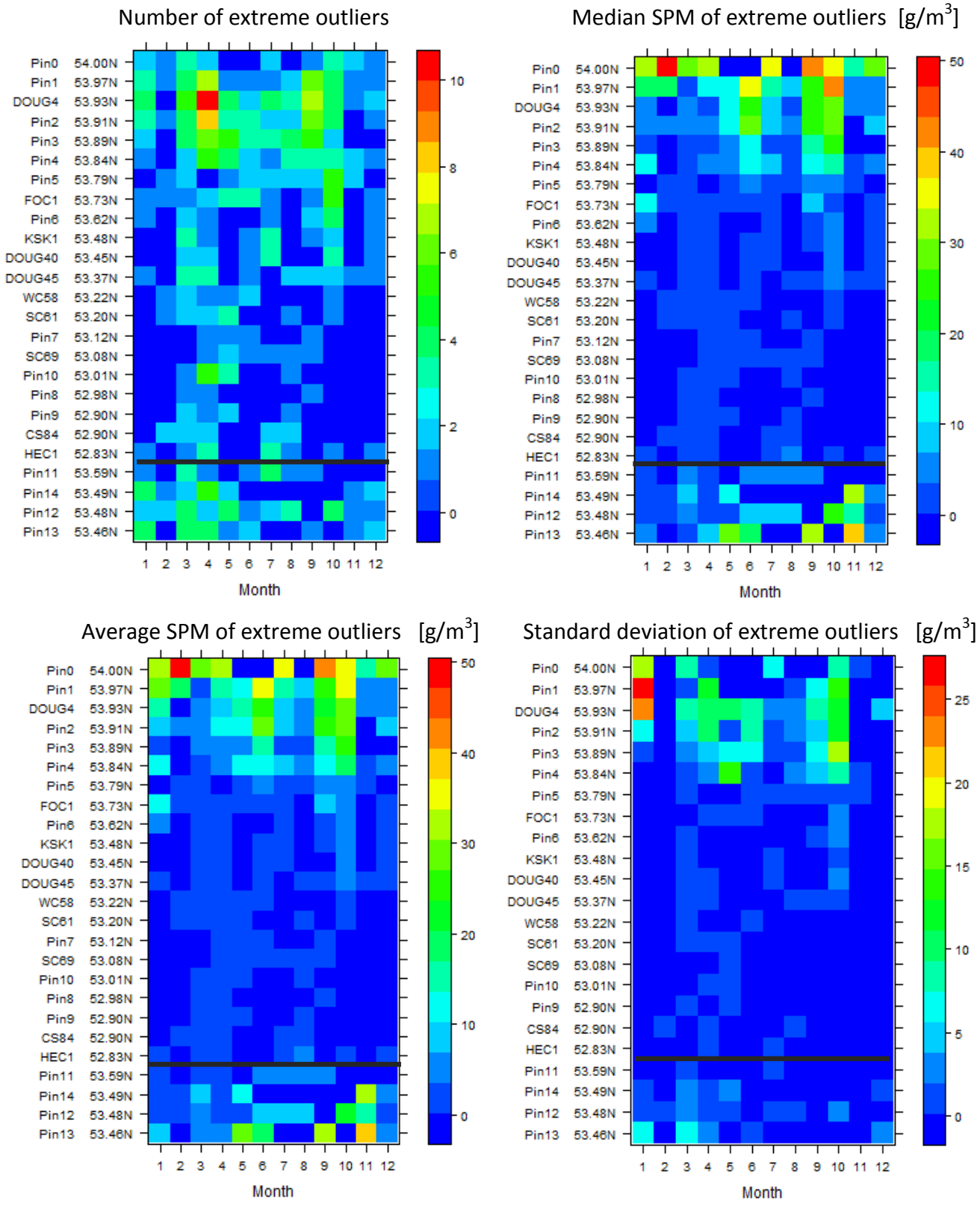

Figure 29: Spatial and temporal distribution of the statistical parameters for extreme SPM outliers (>3*IQR). Stations below the black line are located in the Gardner Canal (Pin 11-14)

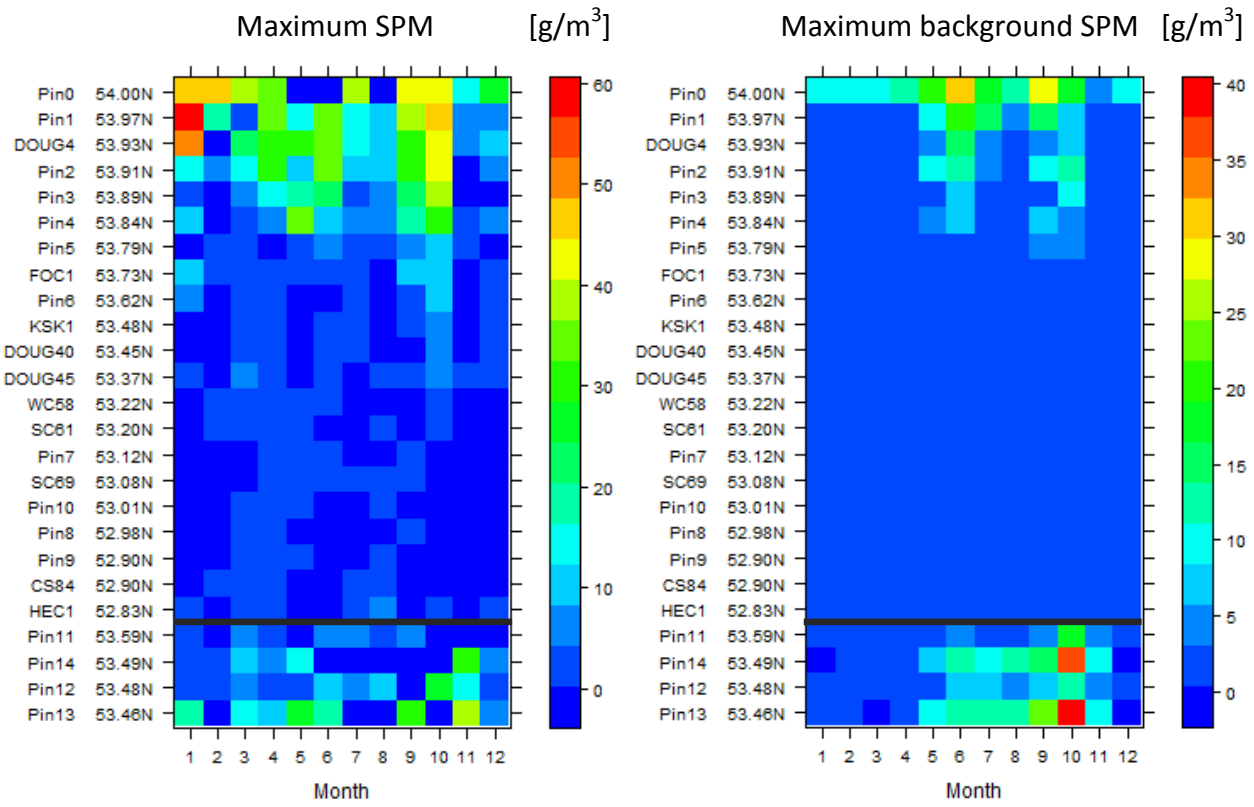

Figure 30: Spatial and temporal distribution of the maximum SPM for all data (left) and for the background SPM (without outliers). Stations below the black line are located in the Gardner Canal (Pin 11-14)

MERIS SPM AND HYDROLOGY

RIVER DISCHARGE AND RAINFALL DATA

Due to the lack of ground truth data for MERIS SPM product validation, we attempted to qualitatively validate SPM patterns in Douglas Channel and Gardner Canal using hydrological data for the rainfall and river discharge.

River discharge data was downloaded from the Wateroffice website maintained by Water Survey of Canada (WSC), Environment Canada (https://wateroffice.ec.gc.ca), and rainfall data from the Environment Canada climate archive (http://climate.weather.gc.ca). Daily river discharge for Kitimat River (station FF001) and Kemano River (station FE001) and rainfall data for Kitimat Townsite and Kemano for years 2002-2013 are shown on Figure 32 and 33.

Kitimat River and Kemano River are the only metered fresh water inputs to the Douglas Channel (Macdonald 1983). They are both characterized by the increased discharge during summer

months due to the seasonal snow melt and by sporadic pulses of high discharge in the spring and fall due to the heavy rain events (Figure 33).

In addition to the river input, Douglas Channel receives runoff from the numerous smaller rushing streams and waterfalls (Figure 32) that drain into it from the steep sides of the fjord (Conway et al., 2013). The majority of the fresh water inputs to the channel is attributed to the runoff, with Kitimat River discharge contributing 1/3 of the total fresh water flux into Douglas Channel, and Kemano River discharge representing only 1/17 of the total water flux into Gardener Canal (Webster 1980b). It was also noted by scientists during a field campaign in the area that the water seems to leap off the mountains when it rains (Wan et al. 2017).

The annual average rainfall at Kitimat Townsite station is 1.9 m per year and 1.8 m at Kemano site. The seasonal rain pattern is showing the very high precipitation levels in the fall with frequent heavy rain events that can reach more than100 mm per day. Low levels of total rain are received during the summer months, and medium amounts in the spring with occasional heavy rain events of lower intensity than the fall rainstorms, with daily rainfall reaching up to 60 mm (Figure 34).

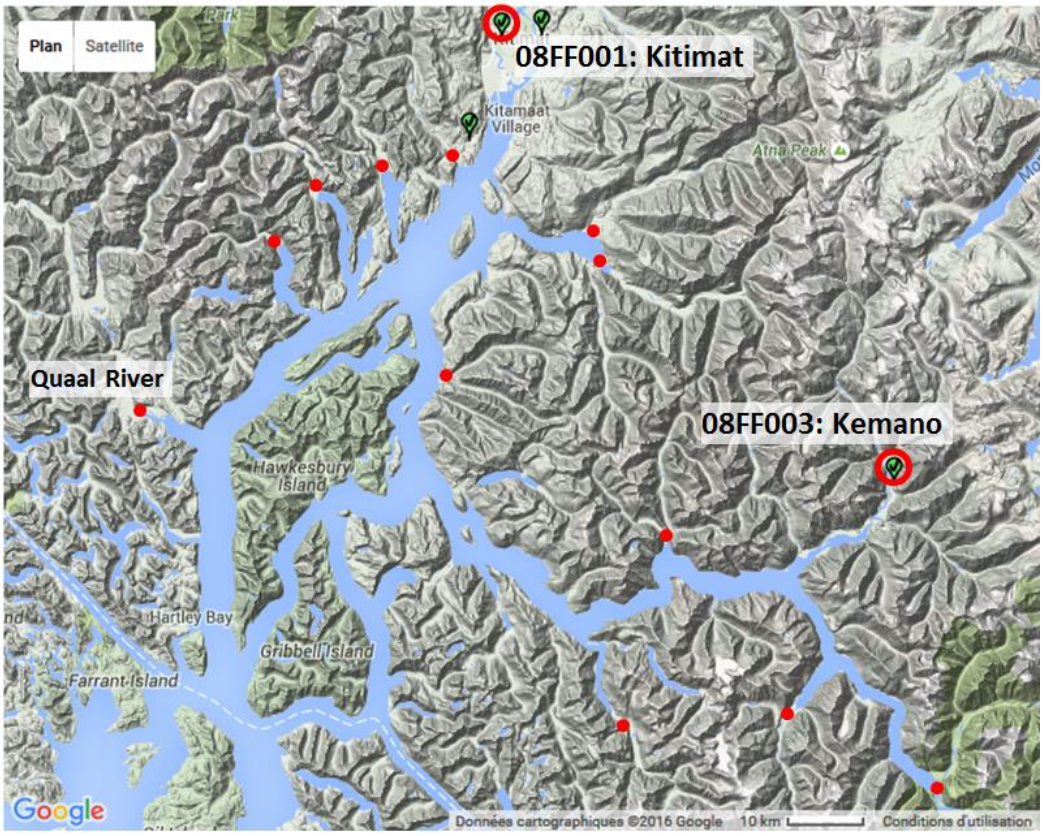

Figure 31: Locations of Kitimat and Kemano metered river discharge stations and several larger streams (red bullets).

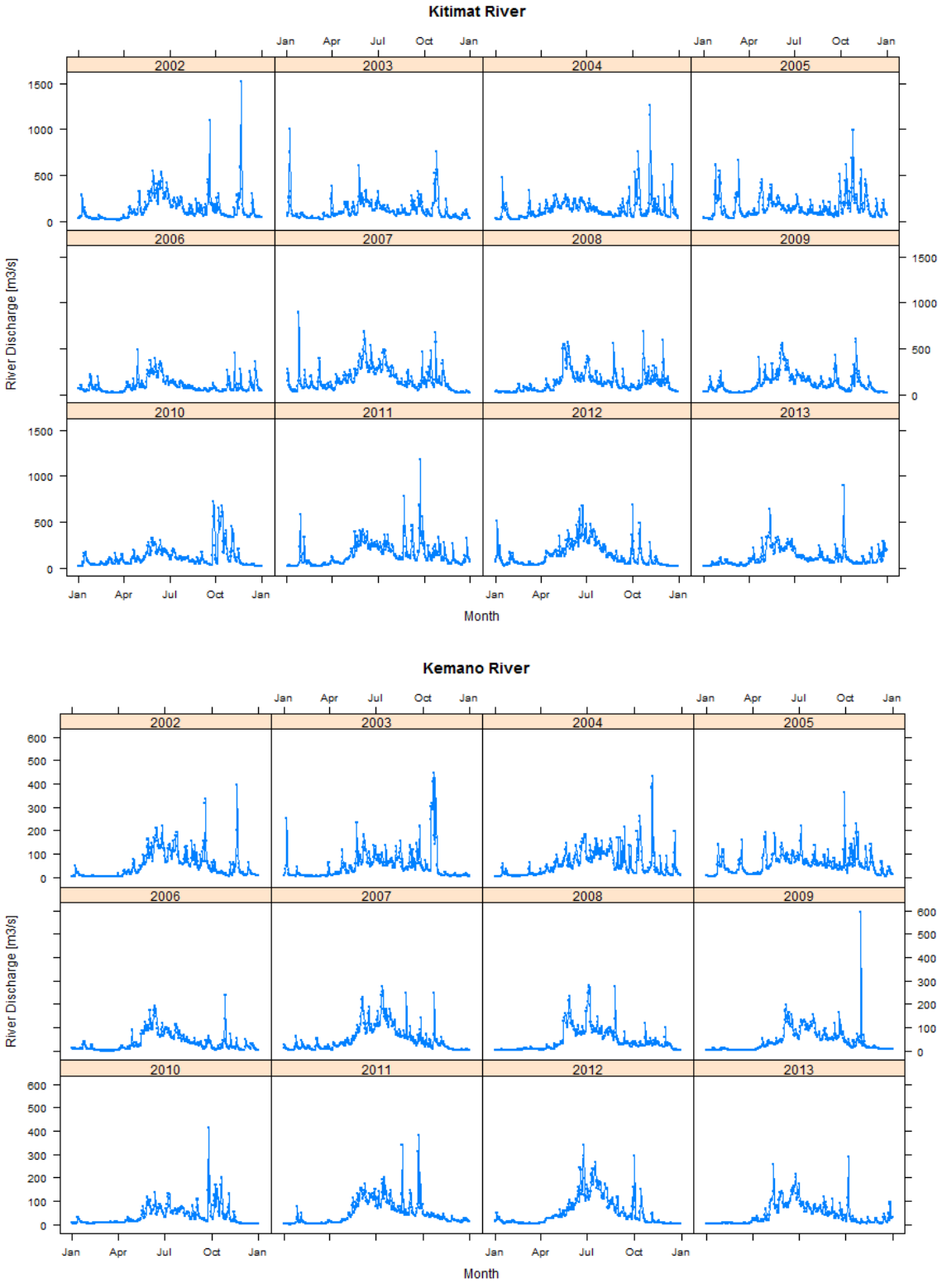

Figure 32: Kitimat River discharge (top panel) and Kemano River discharge (bottom panel).

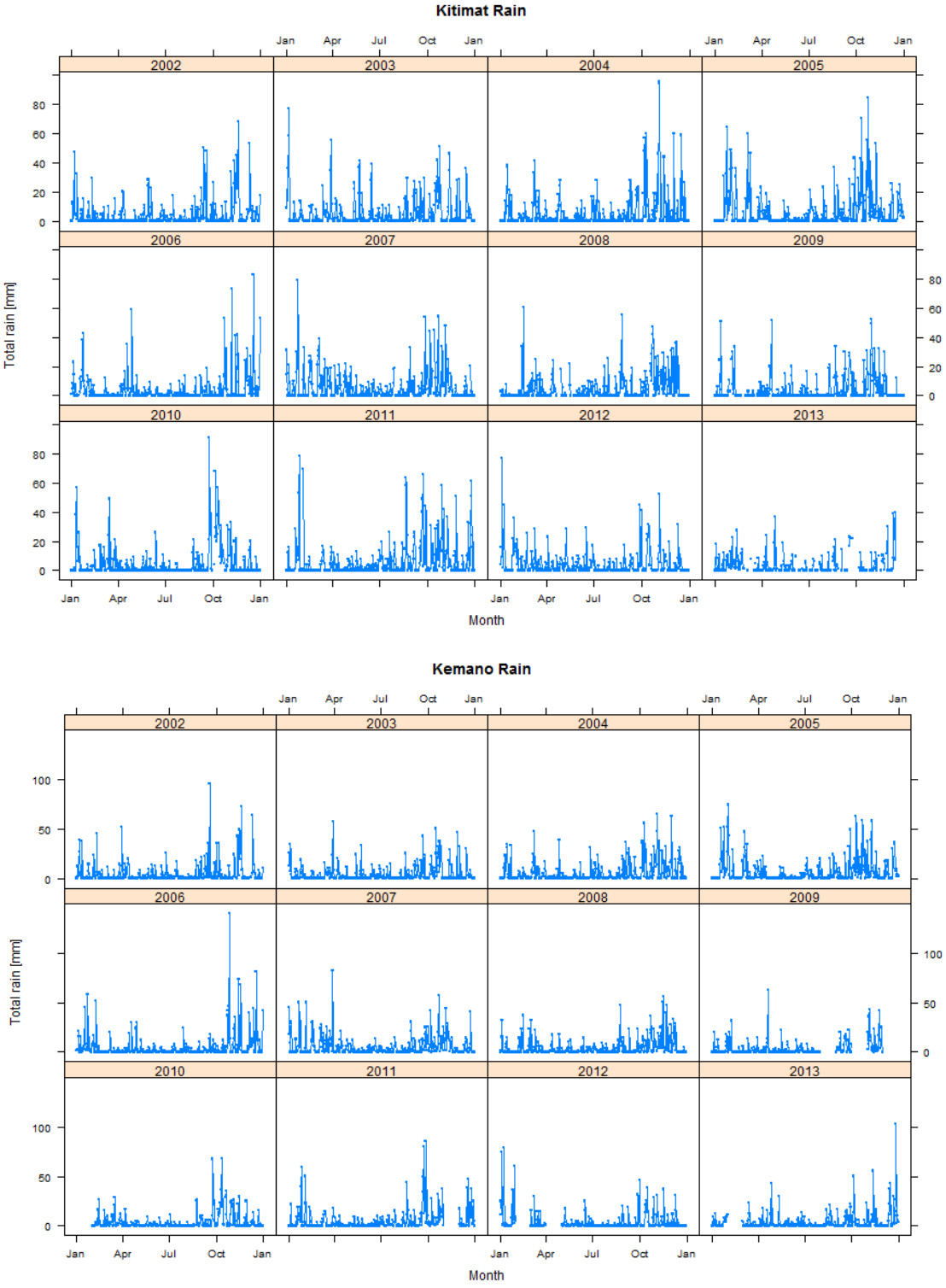

Figure 33: Total daily rain for Kitimat Townsite (top panel) and Kemano (bottom panel) for years 2002-2013, In both cases the rain distribution is characterized by intense rain events in spring and fall and less precipitation in the summer.

SEASONAL PATTERNS

Seasonal patterns in SPM derived from MERIS seem very consistent with the seasonal patterns in rain and river discharge (Figure 34). Average monthly SPM concentration observed at Pin-0 located close to the Kitimat River mouth matches closely to the seasonal pattern of the river discharge with both peaking in June, when the discharge is the largest due to the snow melt. Two smaller SPM peaks in October and April are consistent with the peaks observed in the rainfall. It is interesting to note that the discharge is showing rain related peak only in October indicating that the spring rain does not on average increase the discharge but it does affect average SPM concentrations.

SPM peaks in June and October are also observed at the stations along the upper and middle channel (Figure 35), with June "snow-melt" peak slowly disappearing with distance from the river mouth and October "rain" peak dominating the annual pattern up to the station DOUG45 located in the middle part of the Douglas Channel. This indicates that high intensity plumes from Kitimat River and the creeks along the channel caused by the heavy rainstorms are increasing SPM concentrations in the larger portion of the channel then the plumes caused by a constant increased discharge in the summer due to snow melt.

For the Kemano site at Pin-13 located close to the mouth of Kemano River, elevated SPM concentration persist from June to October which is consistent with the relatively high Kemano river discharge during summer and early fall. The maximum in SPM concentration however is reached in October and coincides with the timing of the most intense rainfall, while smaller SPM peak in June coincides with the maximum in the river discharge (Figure 34). The other stations in the Gardner Canal exhibit similar seasonal SPM patters with October "rain" peak dominating the peak related to the summer snow-melt runoff (Figure 36).

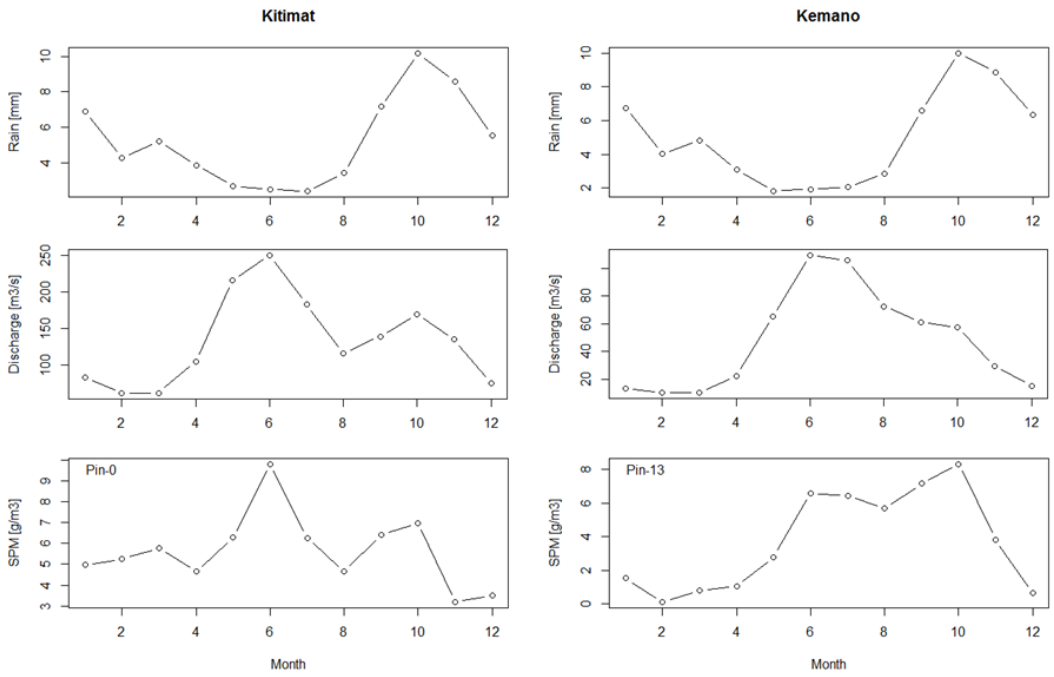

Figure 34: Average monthly rain (top row), river discharge (middle row) and SPM concentration (bottom row) extracted from MERIS images at the locations close to the river mouth for Kitimat River (left) and Kemano River (right) .

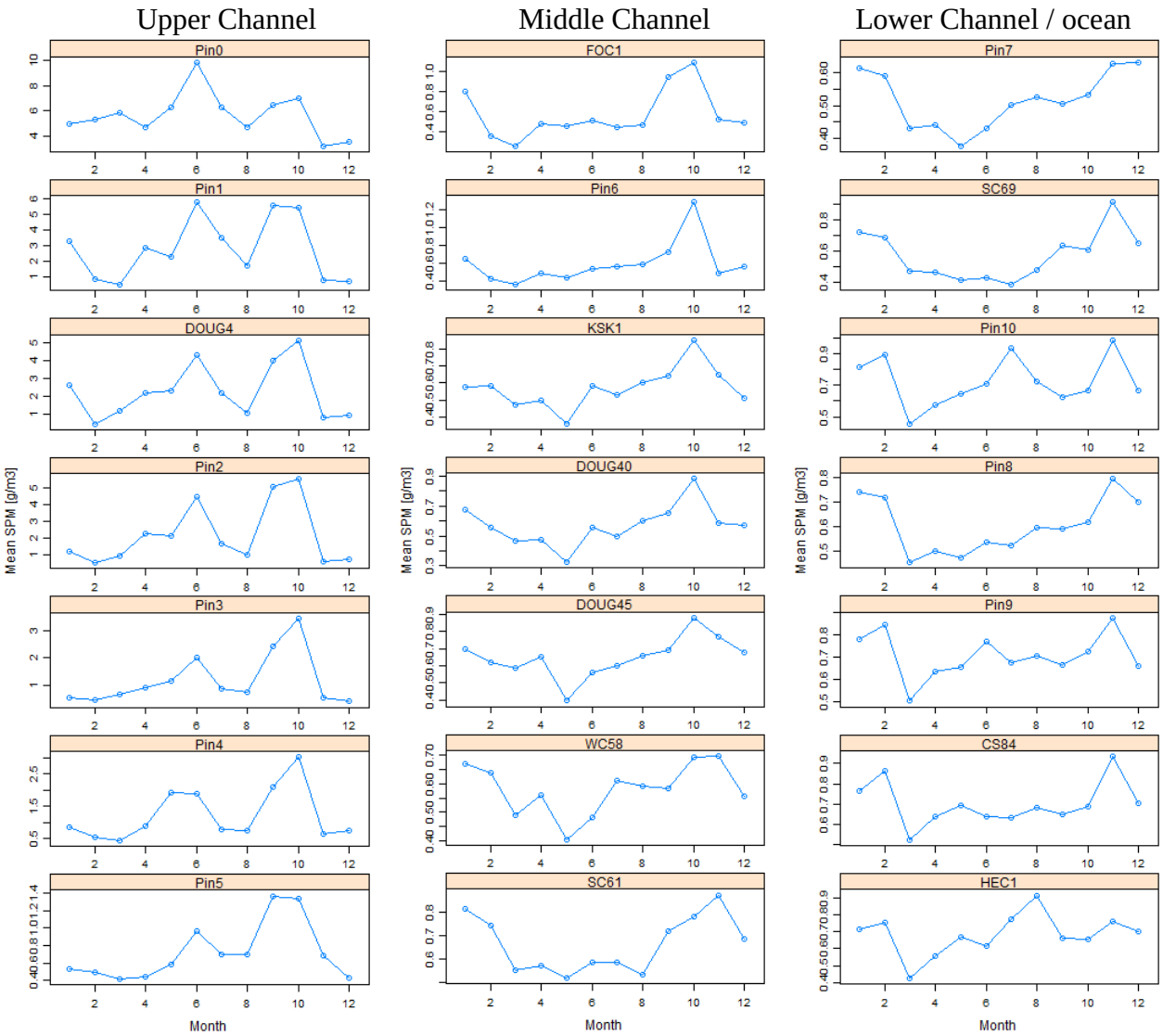

Figure 35: Average monthly SPM concentration at the stations along the Douglas Channel. The stations grouped by location and ordered by the distance from the mouth of the Kitimat River. To emphasize the seasonal patterns, y axis range is determined by the SPM range at each station.

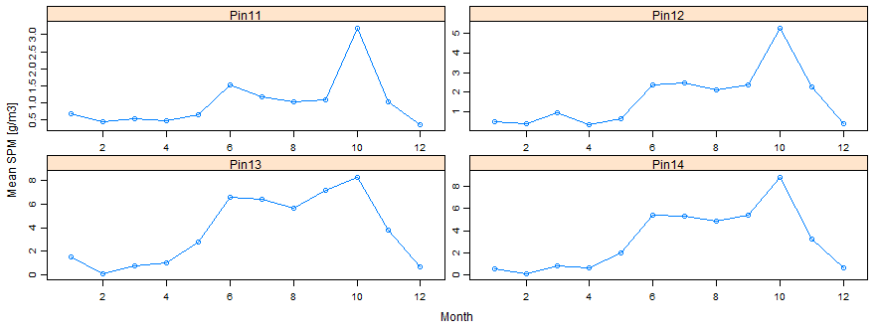

Figure 36: Average monthly SPM concentration at the stations in Gardner Canal. To emphasize the seasonal patterns, y axis range is determined by the SPM range at each station. Pin-13 is located at the mouth of the Kemano River.

DAILY SPM-DISCHARGE RELATIONSHIP

SPM data was further assessed in terms of a relationship between sediment concentration (C) and water discharge (Q) that are commonly studied by hydrologists to evaluate sediment transport in the rivers. The C-Q relations often involve hysteresis loops as sediment concentration may be different on the rising and falling limbs of the discharge. Williams (1989) classified C-Q relations in five common classes that arise from different shapes and relationships between temporal graphs of discharge and concentration. An example of Class III relation from his publication is shown on Figure 37.

SPM concentration from MERIS was plotted versus Kitimat River discharge for several stations located at various distances from the river mouth, distinguishing the points for increasing and decreasing river discharge (Figure 38). The plots reveal that SPM concentration generally increases with river discharge but the scattering of the data points is wide.

For Pin-0 located in close proximity of the river mouth the scattering of points is similar regardless if the river discharge is increasing or decreasing. Very high SPM concentrations seem to be associated with increasing discharge since they also include SPM observations at the peak discharge. On the other hand, for stations located further down the Kitimat Arm the plots are showing similar pattern to the Class III counterclockwise loop relation described by Williams (1989). That indicates that SPM is peaking after the maximum discharge is reached and is lingering in the surface water while discharge had already reached low levels, which results in large range of SPM concentration for the same river flow. The plots for the station further from the mouth are consistent with patterns associated with larger lag between river discharge and SPM plume.

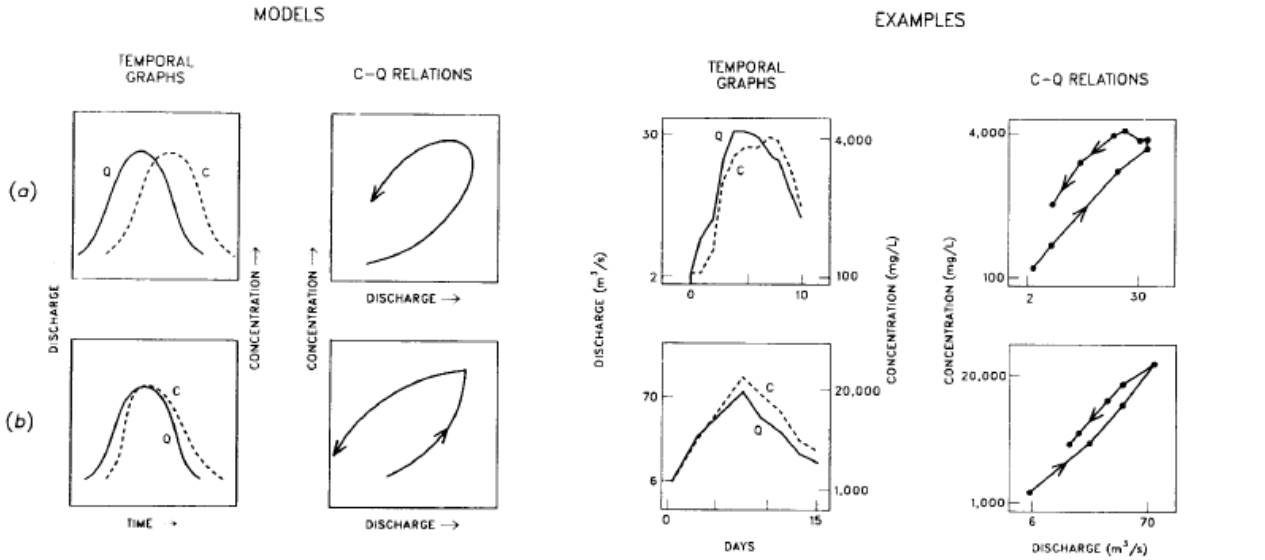

Fig. 5. Counterclockwise-loop *C–Q* relations (Class III): (a) water discharge peaking before sediment concentration, exemplified by Muddy Creek near Vaughn, Mont., March 15–24, 1969; (b) simultaneous peaks of water and sediment, exemplified by Animas River at Farmington, N.M., May 24–31, 1975. Data from U.S. Geological Survey files.

Figure 37: Class III relationship between river discharge Q and sediment concentration C, adopted from Williams (1989).

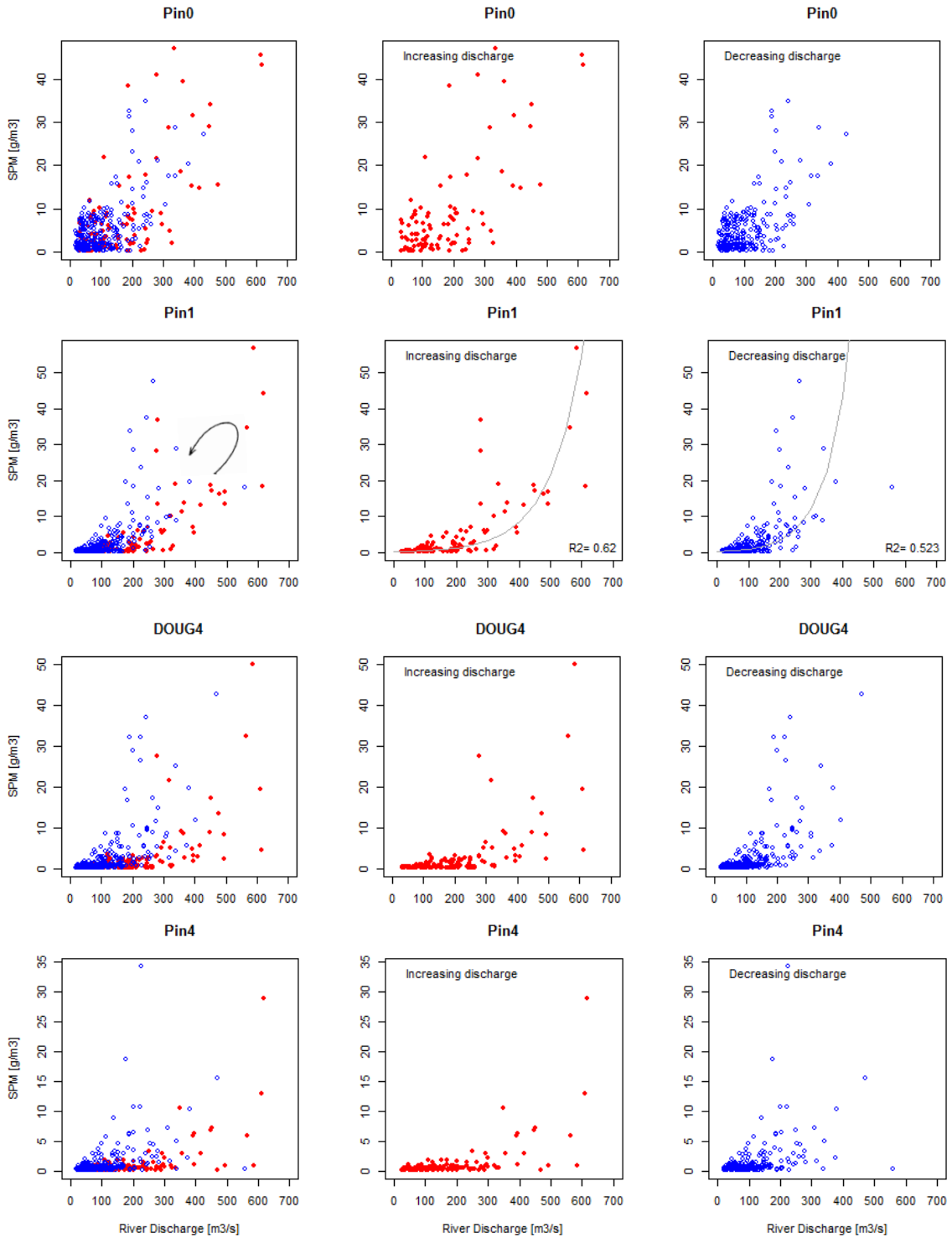

Figure 38: SPM concentration extracted from MERIS images plotted versus Kitimat river discharge. The data corresponding to the decreasing river discharge are shown in red and the data corresponding to increasing river discharge are shown in blue. The plots on the left are showing all data points plotted together. The middle and right plots are showing the data for increasing and decreasing discharge plotted separately for better visibility.

EXTREME EVENTS

Time series of SPM concentrations derived from MERIS data show occasional high SPM concentration values, which prompted further investigation of the daily images in the MERIS dataset and Environment Canada climate archive rainfall data for the Kitimat 2 station (http://climate.weather.gc.ca).

Examination of both datasets showed that the events with extremely high SPM concentration coincide with rainfall events in the preceding days that are reported by Environment Canada.

The maximum value observed for the entire time series is 57.2 g/m^3 at Pin 1 on January 27, 2011, which occurred after a total of 144.5 mm of rain was recorded at Kitimat 2 on January 25th and 26th, 2011. The suite of MERIS SPM images for January 27, 28 and 30 shows a progression of the SPM plumes in the Kitimat region and in the middle of the channel at the mouth of Quaal River (Figure 39). Large concentrations of SPM in the plumes decreased rapidly and were not appearing in the January 30 image.

The second highest SPM concentration peak of 51 g/m^3 was observed on October 12, 2005 at Pin-0, and occurred after four days of rain, from 9th to 12th of October, with a total amount of precipitation of 165 mm. The image from October 12, 2005 is not shown since most of the Douglas Channel was not visible due to the cloud coverage.

Another interesting event was observed on October 17, 2004 when SPM concentration was unusually high (close to 10 g/m^3) along the entire Douglas Channel. This occurred after two consecutive rain events, one from October 4th to 7th delivering 163 mm of rain followed by another period of rain lasting from October 9th to 12th and delivering 130 mm of rain, with a total amount of precipitation of 293 mm of rain in 8 days. The corresponding image of October 17th 2004 shows high SPM concentration in the Channel and the following available image for October 20th, 2004 shows low SPM concentration (Figure 40).

These three events illustrate the dynamic of SPM concentration in the Douglas channel following intense rain events. A larger number of rain events could be analysed to further assess the sediment distributions following the periods of heavy rainfall.

January 27, 2011 Very high SPM concentration in the Kitimat region (about 50 g/m^3), and distinctive Quaal river SPM plume visible in the middle section of the Douglas Channel, following heavy rainfall (144 mm) on January 25th and 26th.	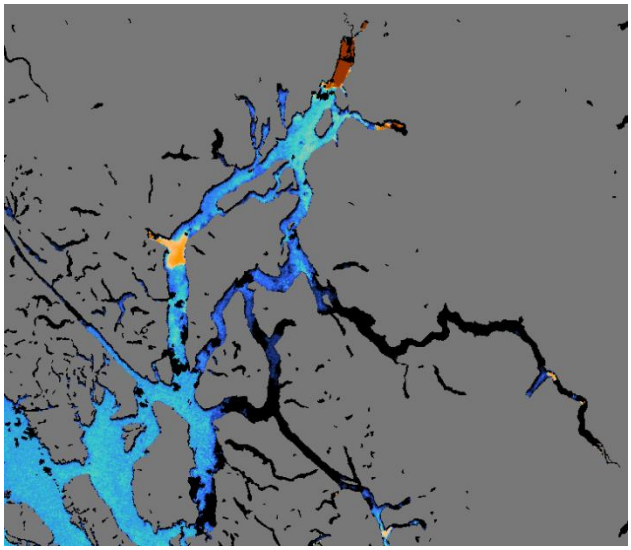
January 28, 2011 SPM settling and migrating down the channel from the Kitimat River combined with the plumes created by the streams on the north-west side of the Kitimat Arm. The SPM concentration decreased to about 10 g/m^3. The Quaal River plume is not visible anymore. Slightly increased SPM concentration down the Channel may be remnants of the Quaal river plume from the day before possibly combined with the additional turbid stream discharges from the sides of the channel.	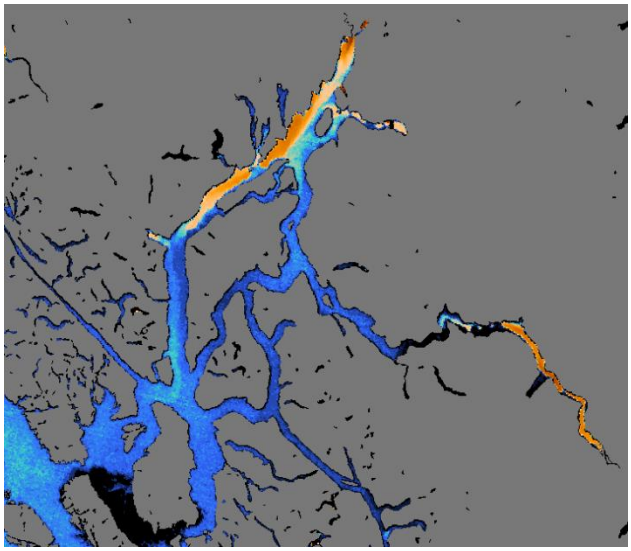
January 30, 2011 SPM plumes had cleared. The SPM concentration in the Kitimat region is down to <1 g/m^3. A section with slightly increased SPM concentration between 1 and 2 g/m^3 is visible in the lower part of the channel, and can be interpreted as the remnants from the plumes that are exiting the channel. 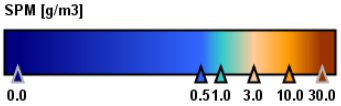	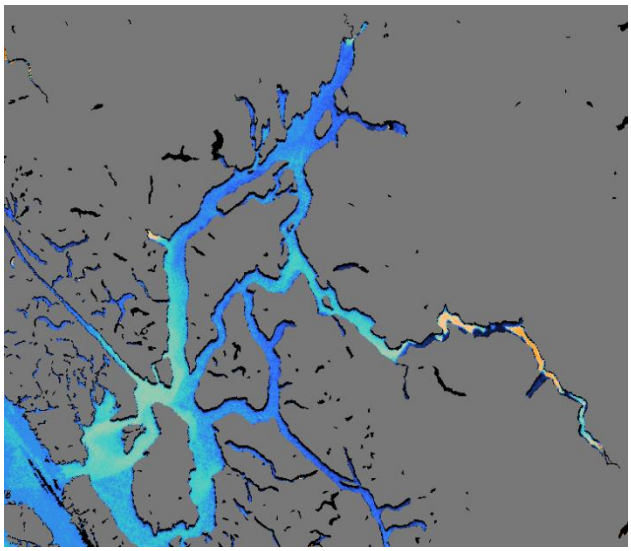

Figure 39: MERIS SPM images following an intense rain event in January 2011.

October 17th, 2004

High SPM concentration throughout the Douglas Channel following two consecutive rain events from October 4th to 7th and October 9th to 12th that delivered in total 293 mm of rain.

Black region on both images represent invalid pixels with no data (possibly under clouds).

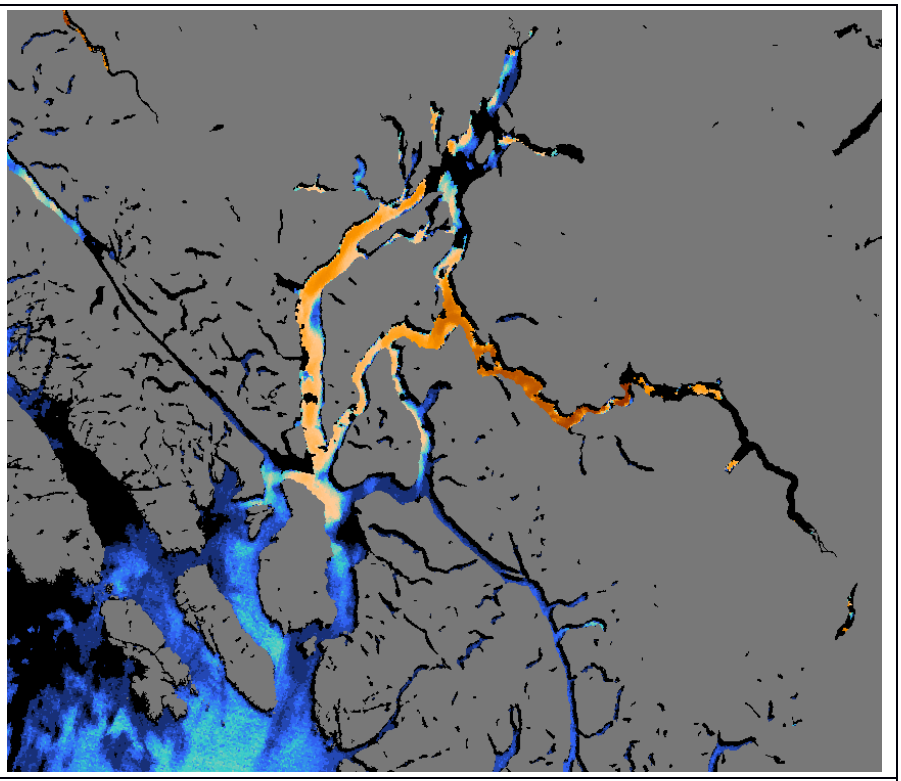

October 20th, 2004

Three days after high SPM concentration was observed on MERIS image the SPM concentration in the channel returned to low values with exception of the region toward the mouth of the Gardner Canal.

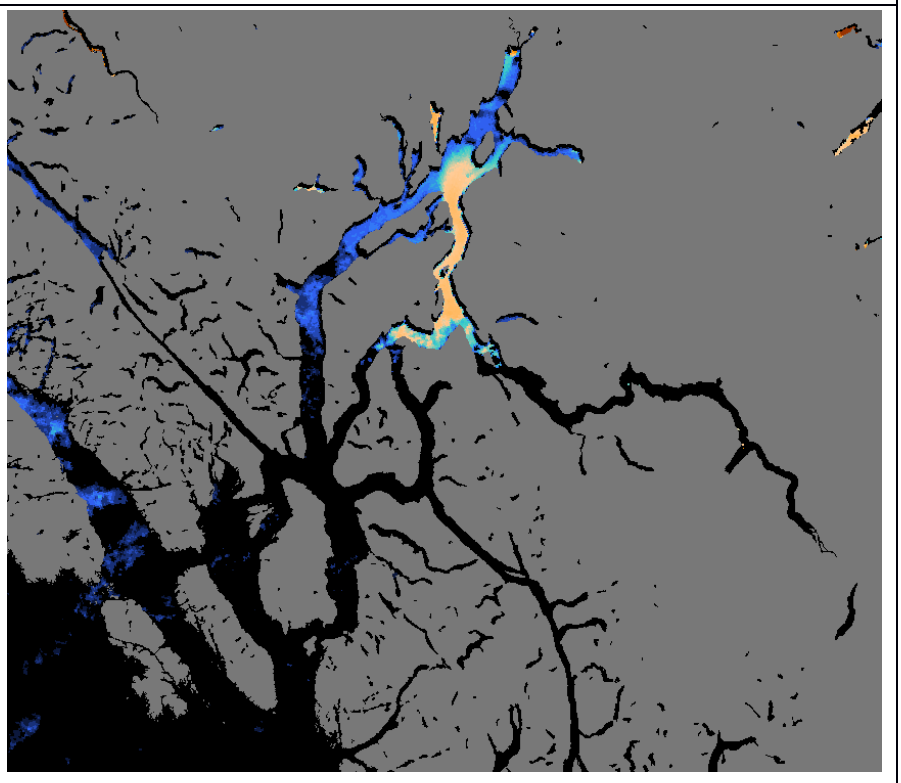

Figure 40: MERIS SPM images following rain event in October 2004.

SPM outliers were further evaluated on the time series plots of rain and river discharge events. For the events with high SPM concentrations the rainfall events are commonly followed day later by a peak in the river discharge. Since SPM data is sparse due to the frequent cloud cover it is difficult to deduce the timing of the SPM plumes. However, SPM concentrations seem to follow expected pattern with higher SPM values observed closer to the peak in river discharge that are declining sharply after the discharge event. Two examples of time series of rainfall at the Kitimat Townsite, the Kitimat River discharge, and SPM concentration for couple of SPM outliers at Pin-1 is shown on Figure 41. The rest of the plots for all major SPM outliers are included in Appendix A.

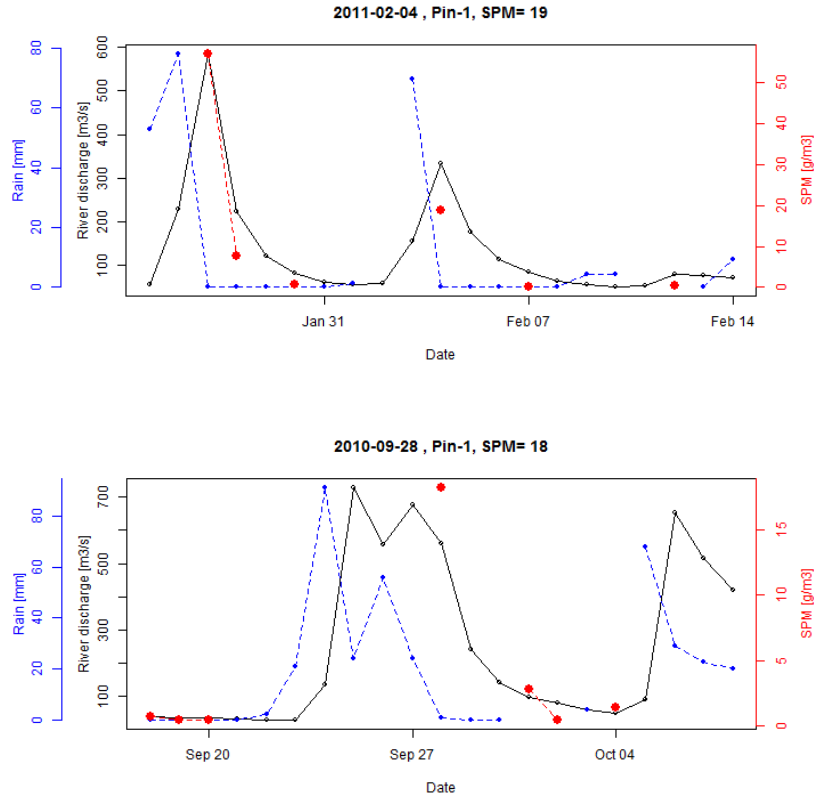

Figure 41: Time series of rainfall at Kitimat Townsite (blue), Kitimat River discharge (black), and SPM concentration (red) for the time period surrounding SPM outliers for two heavy rainfall events.

CONCLUSIONS

MODIS and MERIS ocean-colour satellite data provided valuable insight into spatial and temporal patterns of suspended particulate matter (SPM) in the surface waters of Douglas Channel, despite the area being declared as the cloudiest region in Canada.

Both sensors are showing similar SPM patterns, and comparable values for the areas with low SPM concentrations. The differences become substantial for the regions with high SPM load, like Skeena River and sediment plumes, where MERIS SPM estimates are considerably higher than the MODIS estimates. This divergence was attributed mostly to the different approaches for SPM computation.

Further investigation revealed that MODIS data is greatly affected by the so-called adjacency effect leading to the high SPM values of the pixels close to the coast. This is partially due to the nature of the SPM algorithm that is using red spectral band where the adjacency effect is the strongest. MERIS was seemingly less affected by the proximity of the coast, perhaps as it employs multi-spectral SPM algorithm. To improve quality of MODIS results in the narrow parts of the channel an adjacency effect correction would be required.

Monthly SPM climatology for MODIS and MERIS revealed in general low seasonal SPM concentrations in the channel that is often below 1 g/m^3, but also pointed to the high monthly standard deviations, which indicated large range in SPM concentrations that was particularly high for January and October.

The investigation of MERIS daily SPM time series at stations along the Douglas Channel revealed low median SPM along the channel of about 0.5 g/m^3 with periodic intense events with very high SPM concentrations in the upper part of the channel that can range close to 60 g/m^3. Those events were subsequently related to the periods of heavy rain that increases the fresh water flow and associated transport of sediment from rivers and creeks. The events appear to be short lived with the SPM concentration dropping quickly to the background level in a few days, which indicates that SPM is rapidly removed from the surface layer by sinking. The series of images following extreme events show that SPM plumes appear to be localized to the discharge locations, rarely extending throughout the Channel.

Daily time series data was also used to establish relationship between river discharge and SPM concentration from MERIS for station in the Kitimat Arm, which seem to be consistent with counter-clockwise C-Q relationship, indicating that SPM plumes follow river discharge peaks. This exercise demonstrated potential of using MERIS SPM products for hydrological studies.

Monthly spatial and seasonal SPM patterns correspond to the seasonal rainfall and river discharge patterns and are characterized by low annual SPM background values along the Douglas Channel with station close to Kitimat and Kemano river mouths showing seasonal variability that are consistent with hydrology. At those locations SPM concentration and river discharge are both peaking in June when the discharge is the largest due to the snow melt. Two smaller SPM peaks are detected in October and April and are consistent with the peaks observed in the rainfall. Larger number of images with high SPM that are observed in January can be due to the rain-on-snow events that result in amplified runoff.

Even though the absolute values of SPM concentrations were not validated due to the lack of ground truth data, the observed spatial and temporal SPM patterns were confirmed by the environmental patterns in rain and river discharge. Furthermore, SPM concentrations measured at station DOUG-4 in 2015 ranged from 6.3 mg/m3 in July to 47.8 mg/m3 in October (Johannessen et al. 2015) are in agreement with the ranges of the satellite-derived SPM. A validation exercise performed in the Bay of Fundy, Nova Scotia, showed that MERIS SPM estimates are within 30% of the ground truth SPM (Lazin and Bugden, unpublished).

This study demonstrated the value of including ocean colour data in environmental studies to assess spatial and temporal patterns that could not be measured otherwise. Given the excellent performance of MERIS sensor European Space Agency launched Ocean Land Color Instrument (OLCI) on board Sentinel-3 satellite in February 2016 that will provide continuity of MERIS class observations well into the future.

REFERENCES

Conway, K.W., Kung, R.B., Barrie, J.V., Hill, P.R., and Lintern, D.G. 2013. A preliminary assessment of the occurrence of submarine slope failures in coastal British Columbia by analysis of swath multibeam bathymetric data collected 2001-2011. Geological Survey of Canada Open File Report 734, Natural Resources Canada, Sidney, 38 pp.

Doerffer, R. and Schiller, H.: ATBD 2.12. 1997. Pigment index, sediment and gelbstoff retrieval from directional water leaving reflectances using inverse modelling technique, Doc. No. PO-TN-MEL-GS-0005, Algorithm Theoretical Basis Document (ATBD) 4, GKSS Forschungszentrum Geesthacht, Institute of Hydrophysics, 21502 Geesthacht Germany

Doerffer, R. and Schiller, H. 2008. MERIS Regional Coastal and Lake Case 2 Water Project Atmospheric Correction ATBD. Doc. No. GKSS-KOF-MERIS-ATBD01, Algorithm Theoretical Basis Document (ATBD), GKSS Forschungszentrum Geesthacht, Institute of Hydrophysics, 21502 Geesthacht Germany

Doxaran D., Devred E. and Babin M. 2015. A 50% increase in the mass of terrestrial particles delivered by the Mackenzie River into the Beaufort Sea (Canadian Arctic Ocean) over the last 10 years, *Biogeosciences*, bg-2014-574

Frouin R., Deschamps, P.Y. and Steinmetz, F. 2009. Environmental Effects in Ocean Color Remote Sensing, in Ocean Remote Sensing: Methods and Applications, edited by Robert J. Frouin, Proc. of SPIE Vol. 7459, 745906 · © 2009 SPIE · CCC code: 0277-786X/09/$18 · doi: 10.1117/12.829871

Henri Laur, 2013. 1st IOCS meeting, From MERIS to OLCI – Ocean Colour at ESA

Johannessen, S.C., Wright, C.A., and Spear, D.J. 2015. Seasonality and physical control of water properties and sinking and suspended particles in Douglas Channel, British Columbia. Can. Tech. Report. Hydrog. Ocean. Sci. 308: iv + 26 p.

Karanka, E.J. 1993. Cumulative effects of forest harvesting on the Kitimat River, British Columbia. Can. Man. Rep. Fish. Aquat. Sci. 2218:67 p.

Macdonald, R.W. 1983a and 1983b. Proceedings of a Workshop on the Kitimat Marine Environment. Can. Tech. Rep. Hydrogr. Ocean Sci. 18, 1-218. http://www.dfo-mpo.gc.ca/Library/52404-1.pdf, http://www.dfo-mpo.gc.ca/Library/52404-2.pdf

Nechad B., Ruddick K. & Park Y. 2010. Calibration and validation of a generic multisensor algorithm for mapping of total suspended matter in turbid waters**.** *Remote Sensing of Environment*, Vol. 114, pp. 854–866.

Wan, D., C. G. Hannah, M. G.G. Foreman, and S. Dosso. 2017. Sub-tidal circulation in a deep-silled fjord: Douglas Channel, British Columbia. *Journal of Geophysical Research Oceans*. doi:10.1002/2016JC012022

Wang, M. and Shi, W. 2007. The NIR-SWIR combined atmospheric correction approach for MODIS ocean color data processing, Opt. Express, 15, 15722–15733

Williams, G. P. 1989. Sediment concentration versus water discharge during single hydrologic events in rivers. *Journal of Hydrology*, *111*(1), 89-106.

Wright, C.A., Johannessen, S.C., Hannah, C., and Vagle, S. 2015. Physical, Chemical and Biological Oceanographic Data Collected in Douglas Channel and the Approaches to Kitimat, July 2013 - June 2014. Canadian Data Report of Hydrography and Ocean Sciences 196, Fisheries and Oceans Canada, Sidney, viii+66.

Wu, Y., C.G. Hannah, B. Law, T. King, and B. Robinson 2016. An Estimate of the Sinking Rate of Spilled Diluted Bitumen in Sediment Laden Coastal Waters, Proceedings of the Thirty-ninth AMOP Technical Seminar, Environment and Climate Change Canada, Ottawa, ON, pp. 331-347

ACKNOWLEDGMENTS

This work was performed at the DFO Remote Sensing Unit at the Bedford Institute of Oceanography, Dartmouth, NS. We would like to thank Carla Caverhill and George White for providing computing resources, space and support during project setup and execution.

APPENDIX A: MODIS MONTHLY SPM CLIMATOLOGY IMAGES

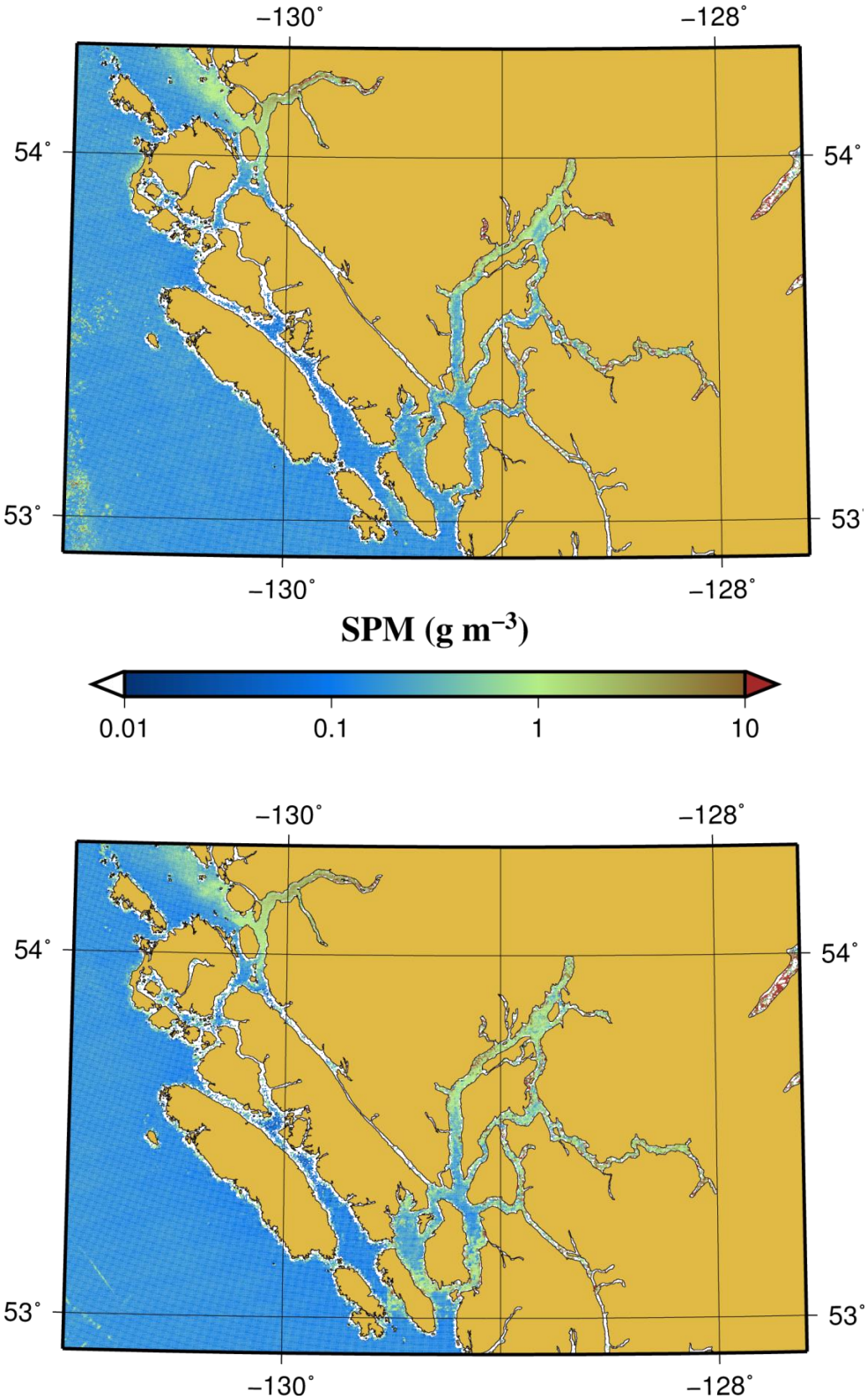

Figure 42: MODIS SPM climatology (2003-2014) for January (top) and February (bottom).

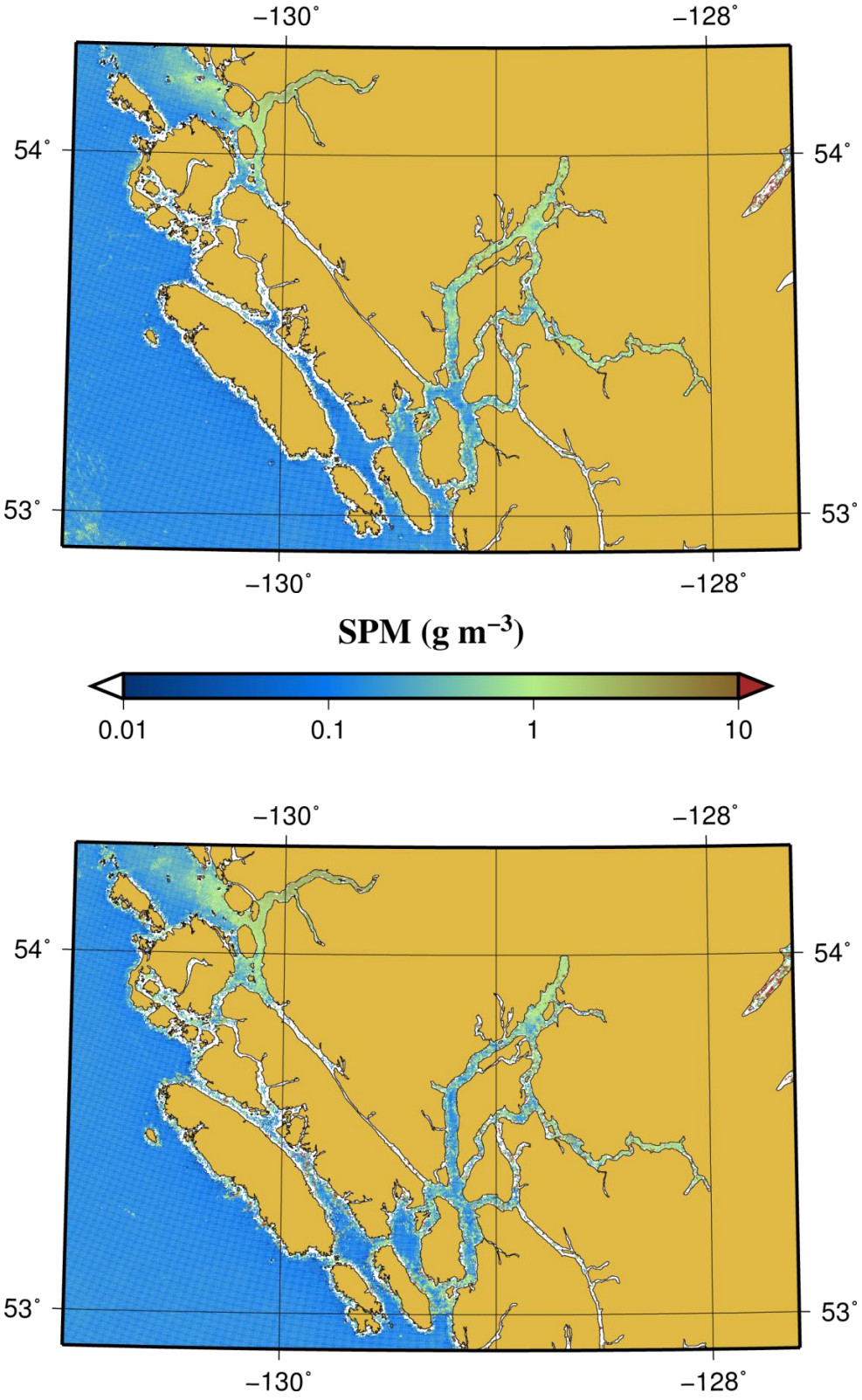

Figure 43: MODIS SPM climatology (2003-2014) for March (top) and April (bottom).

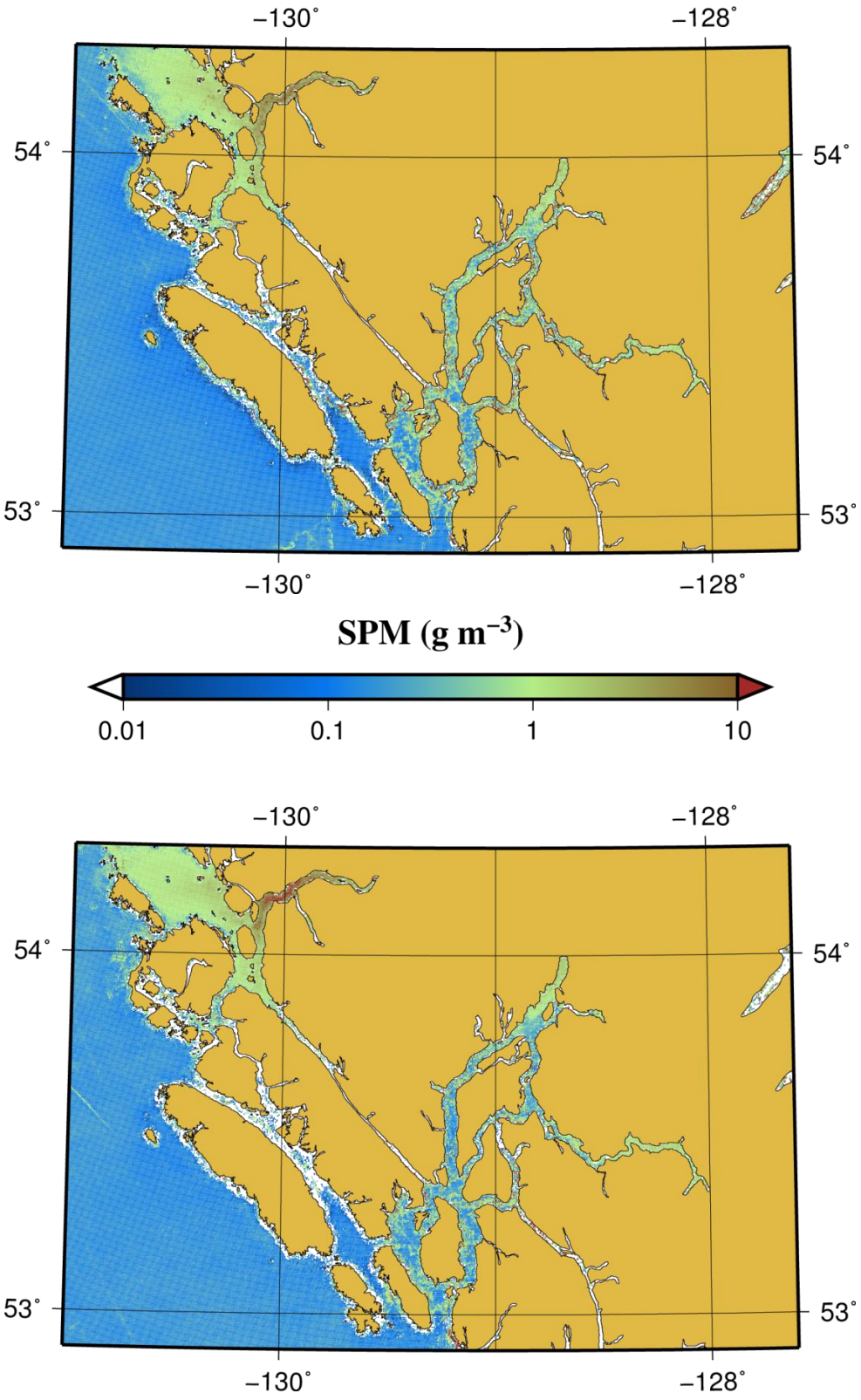

Figure 44: MODIS SPM climatology (2003-2014) for May (top) and June (bottom).

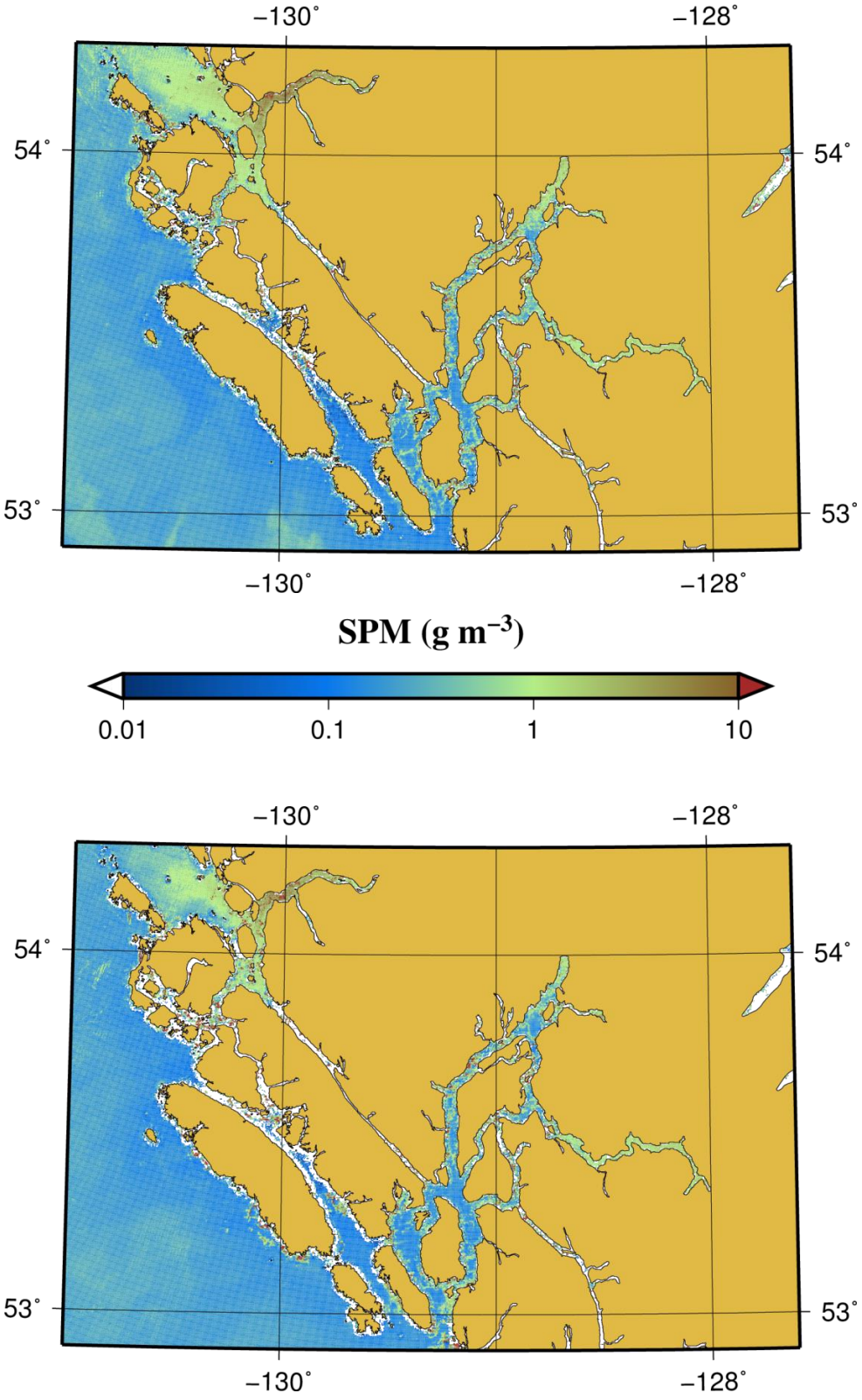

Figure 45: MODIS SPM climatology (2003-2014) for July (top) and August (bottom).

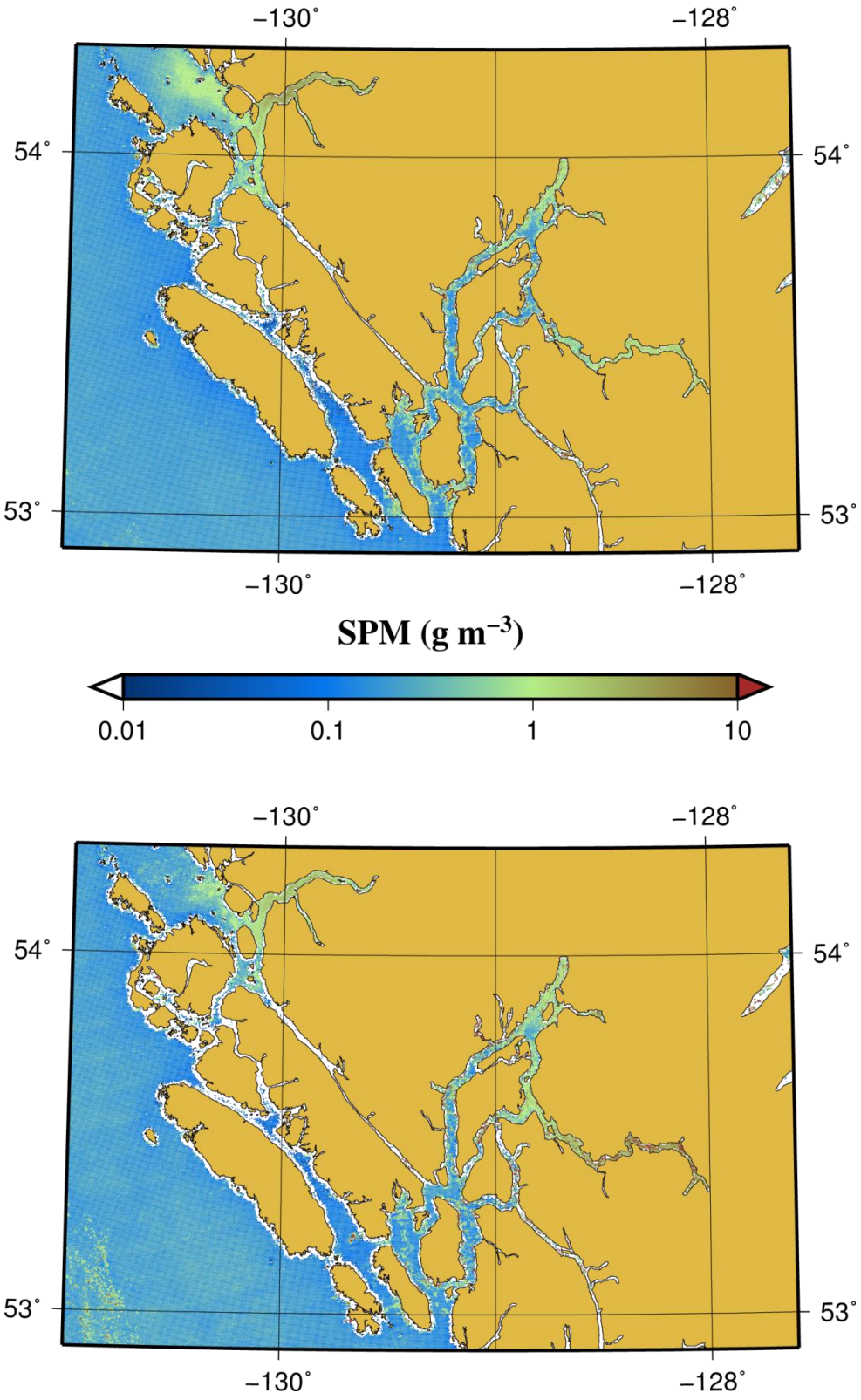

Figure 46: MODIS SPM climatology (2003-2014) for September (top) and October (bottom).

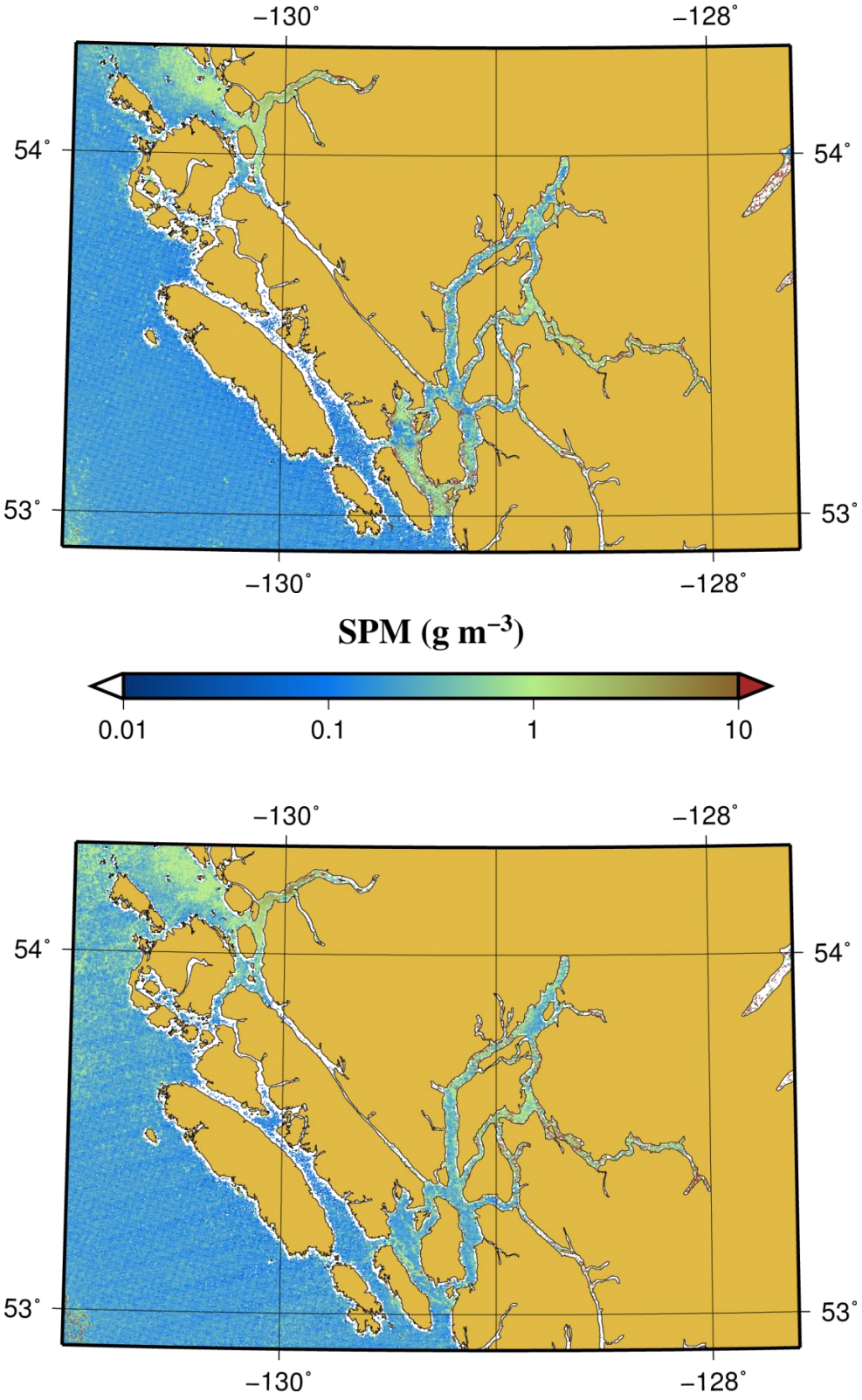

Figure 47: MODIS SPM climatology (2003-2014) for November (top) and December (bottom).

APPENDIX B: MERIS MONTHLY SPM CLIMATOLOGY IMAGES

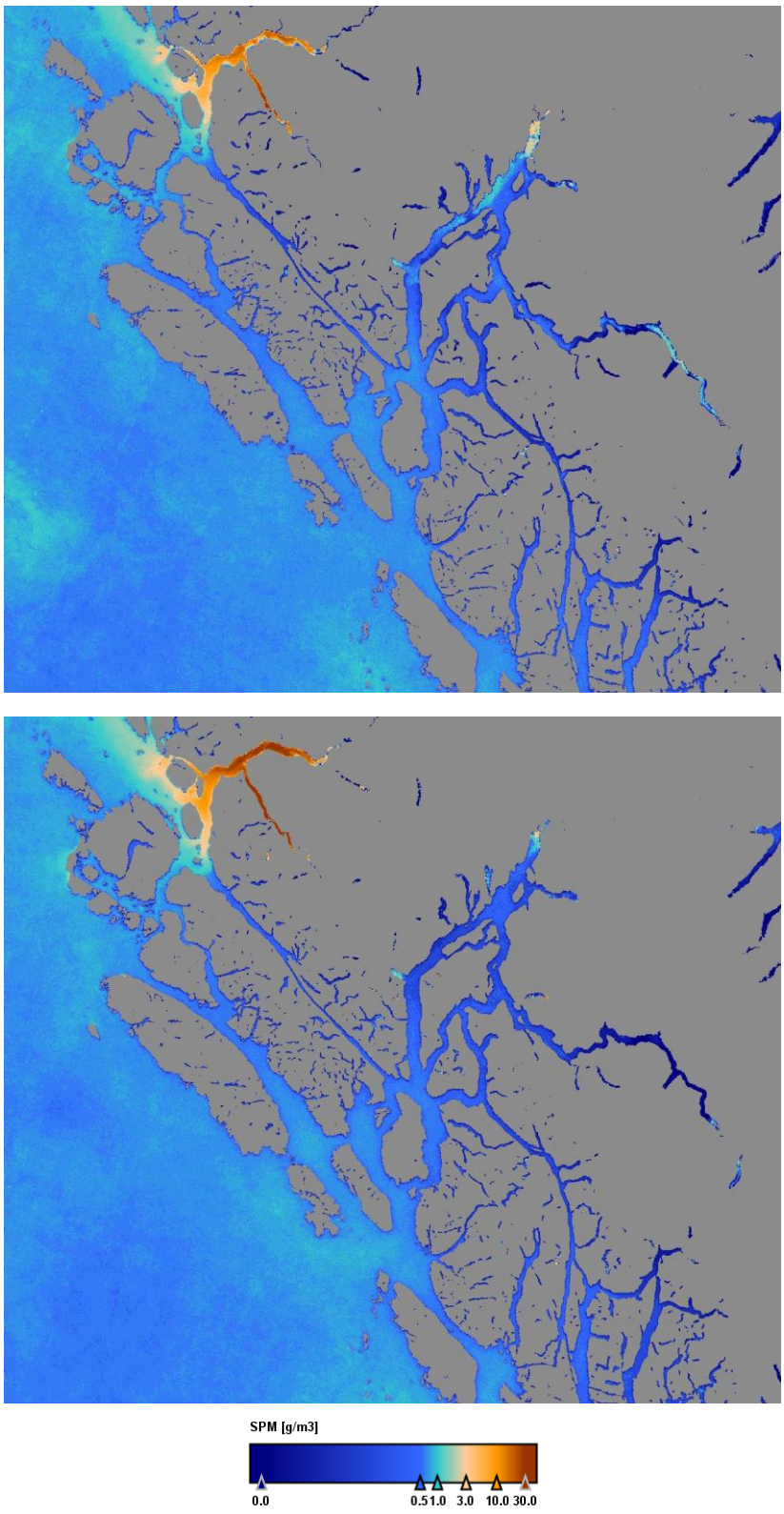

Figure 48 : MERIS SPM climatology (2003-2012) for January (top) and February (bottom).

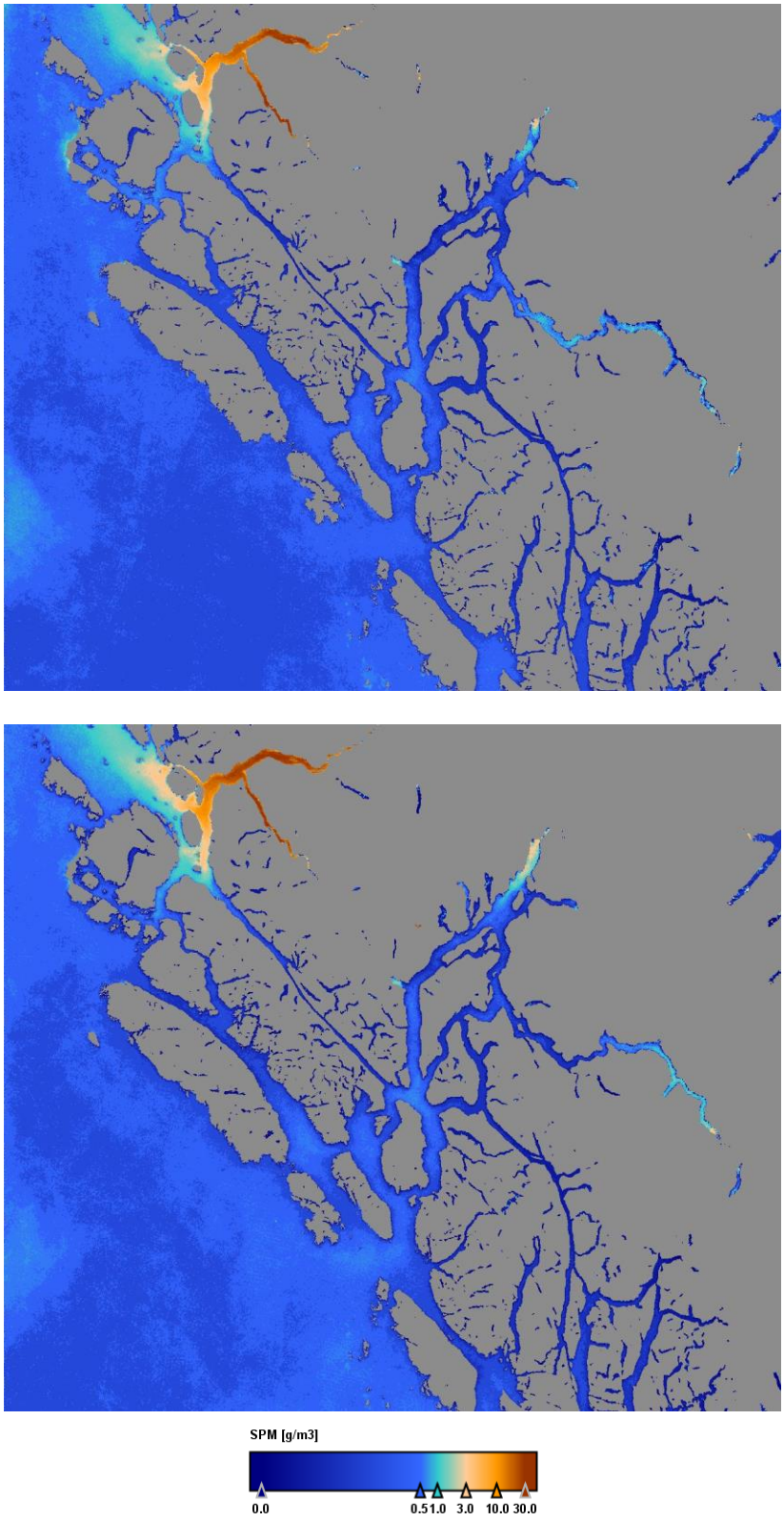

Figure 49 : MERIS SPM climatology (2003-2012) for March (top) and April (bottom).

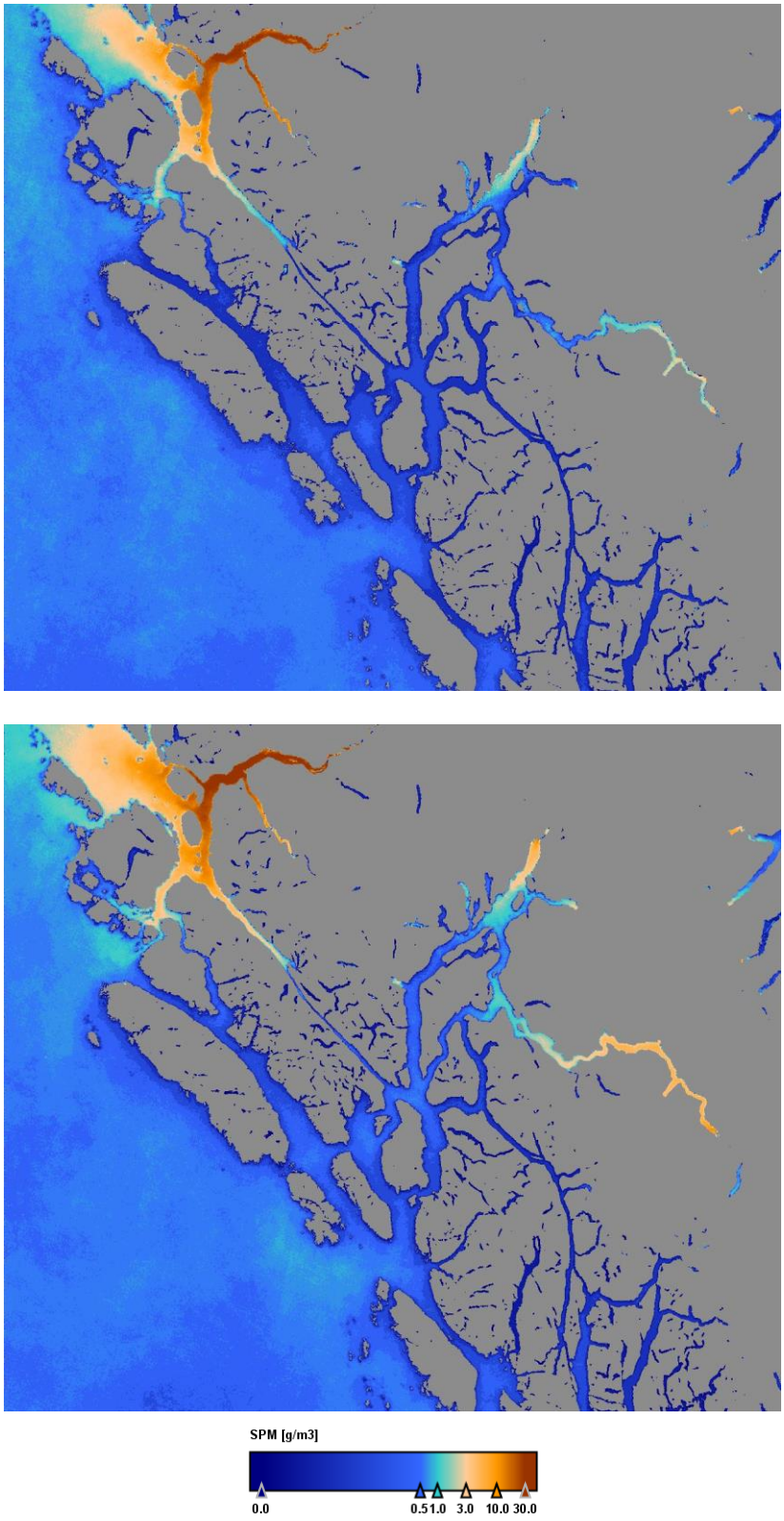

Figure 50 : MERIS SPM climatology (2003-2012) for May (top) and June (bottom).

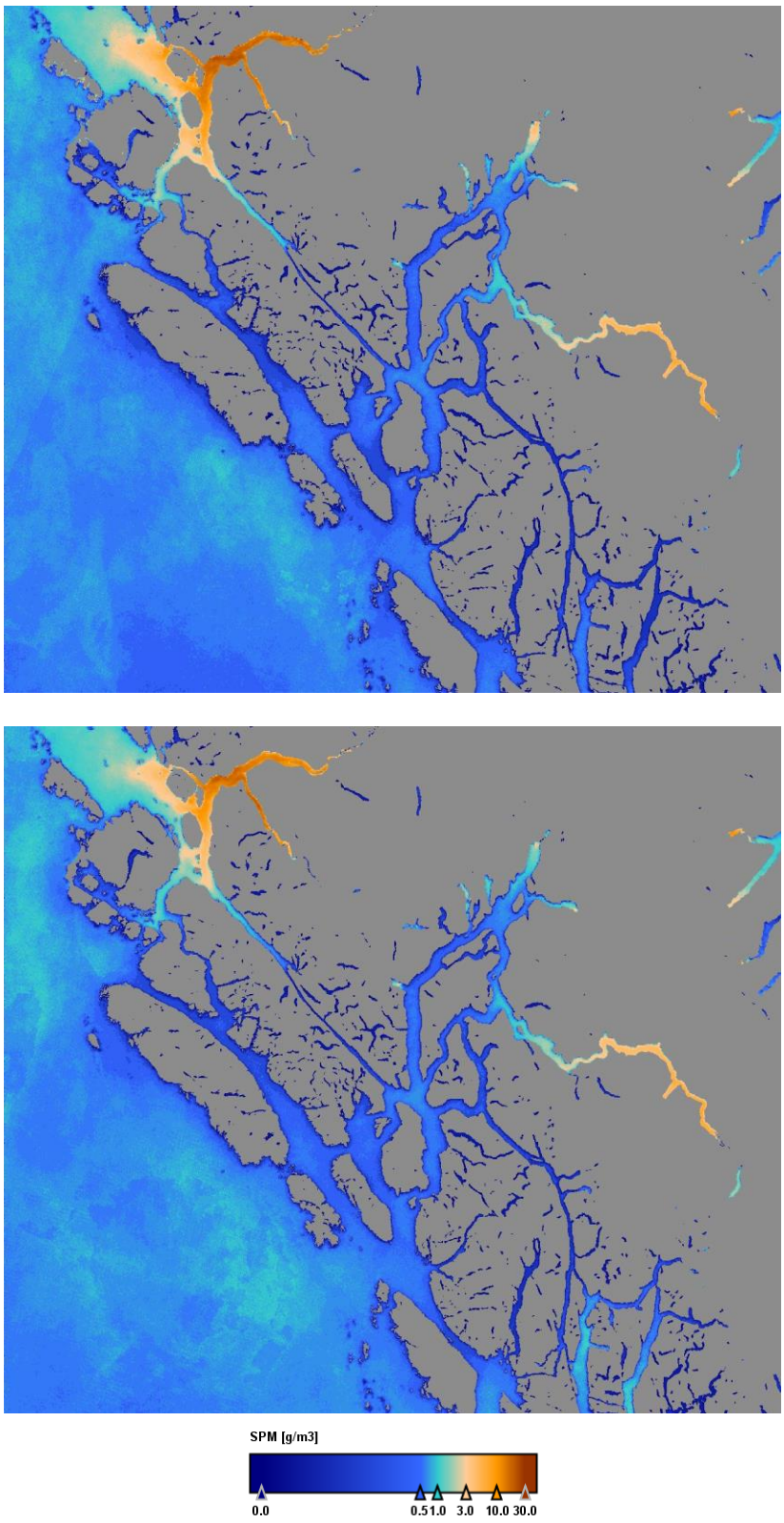

Figure 51 : MERIS SPM climatology (2003-2012) for July (top) and August (bottom).

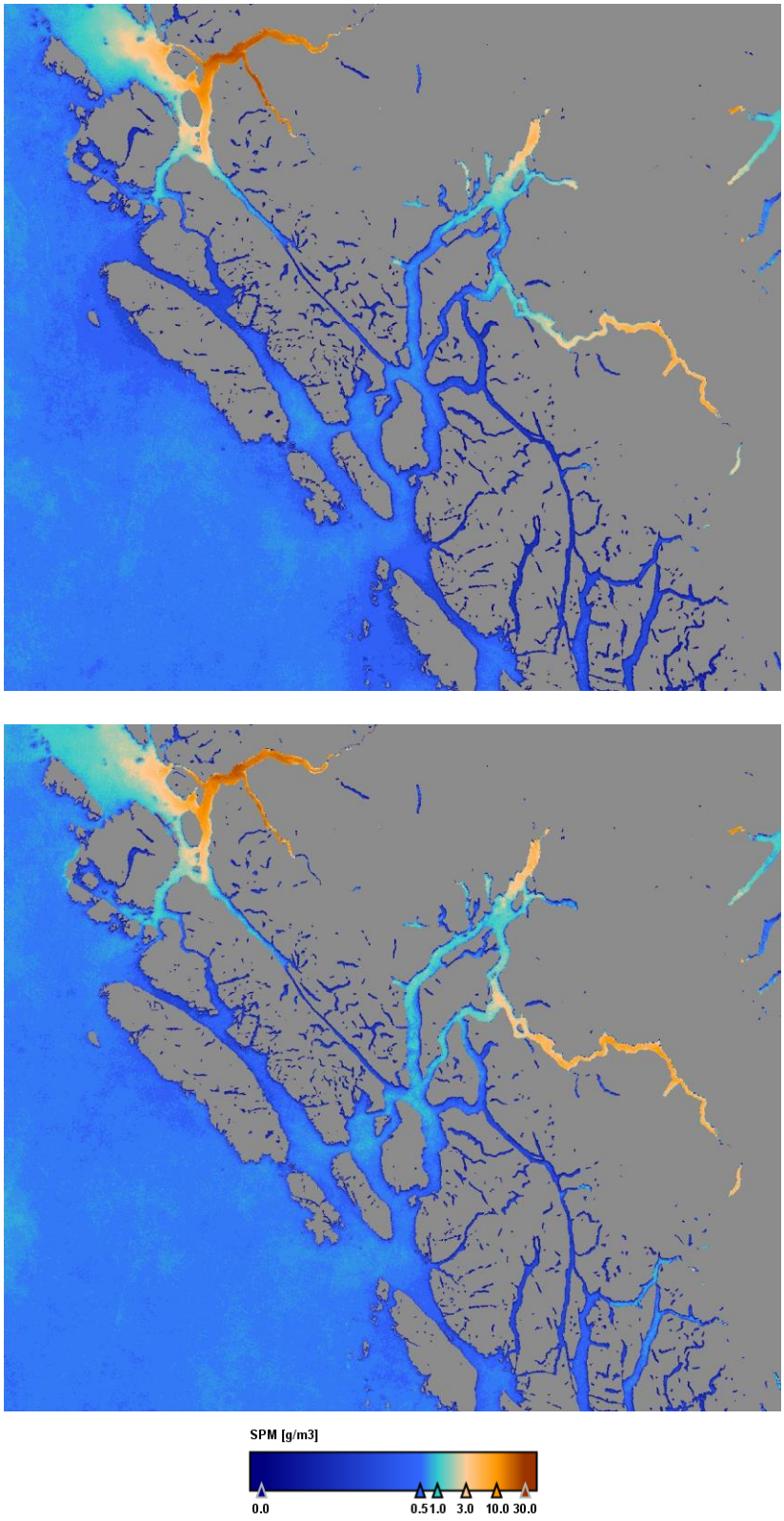

Figure 52 : MERIS SPM climatology (2003-2012) for September (top) and October (bottom).

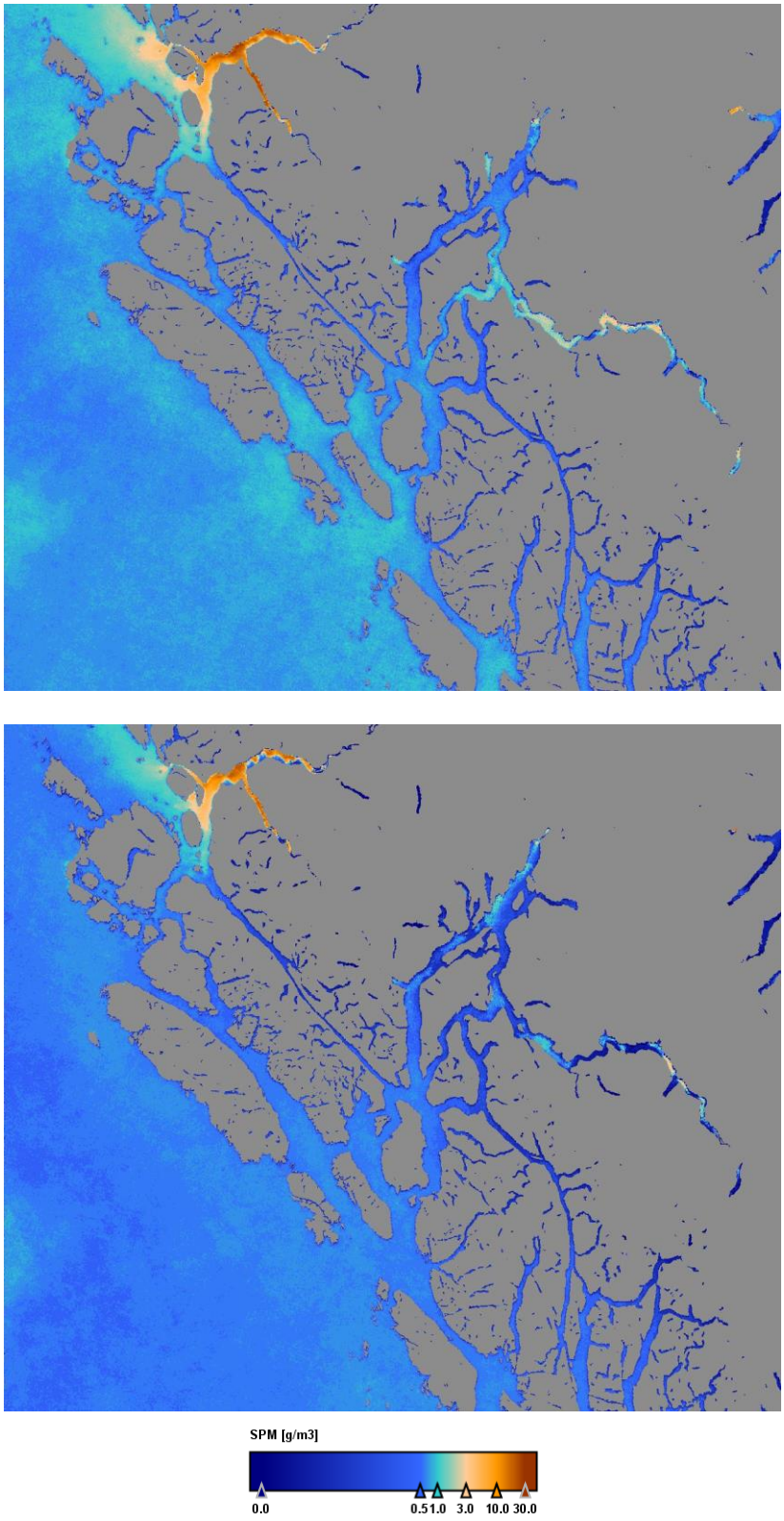

Figure 53: MERIS SPM climatology (2003-2012) for November (top) and December (bottom).

APPENDIX C: MERIS MONTHLY SPM CLIMATOLOGY AT STATIONS

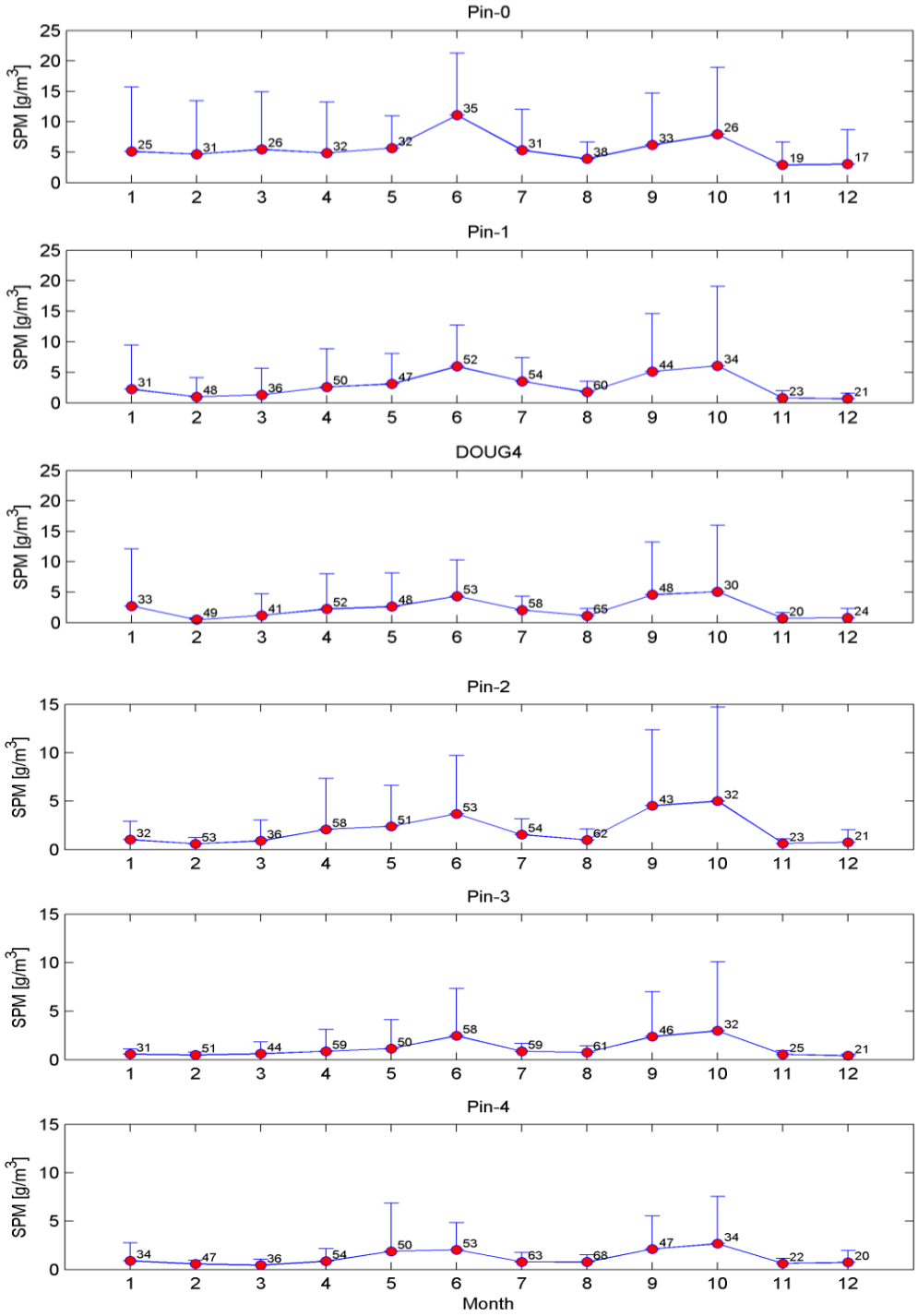

Figure 54: Monthly SPM climatology derived from MERIS ocean colour data (2003-2012) for the 3x3 pixel box centered at the stations in the Kitimat area. The labels beside the symbols represent number of images used for computing climatology, with error bars showing one standard deviation derived for each station and month.

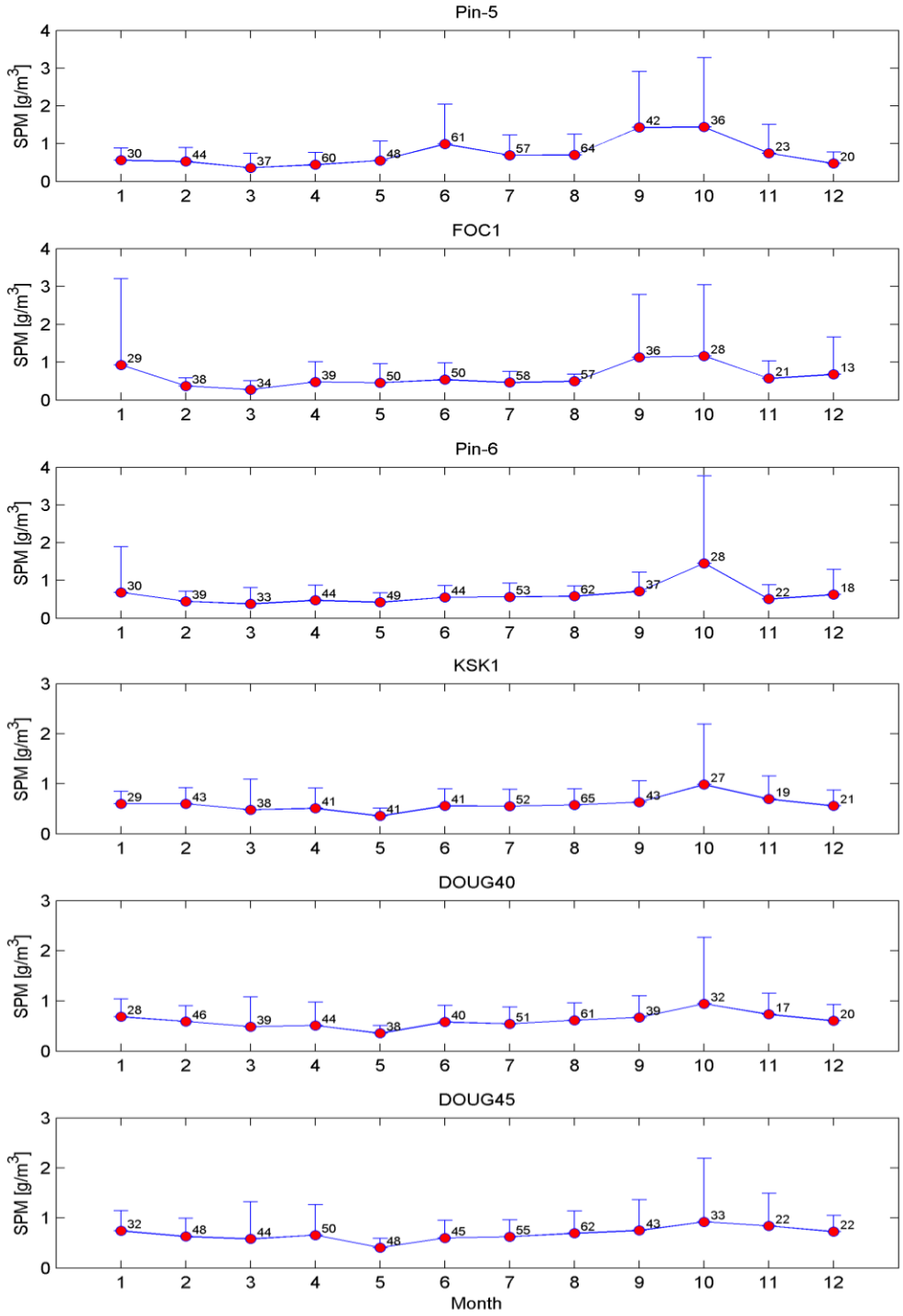

Figure 55 : Monthly SPM climatology for the 3x3 pixel box centered at the stations in Douglas Channel derived from MERIS ocean colour data (2003-2012). The labels beside the symbols represent number of images used for computing climatology with error bars showing one standard deviation derived for each station and month.

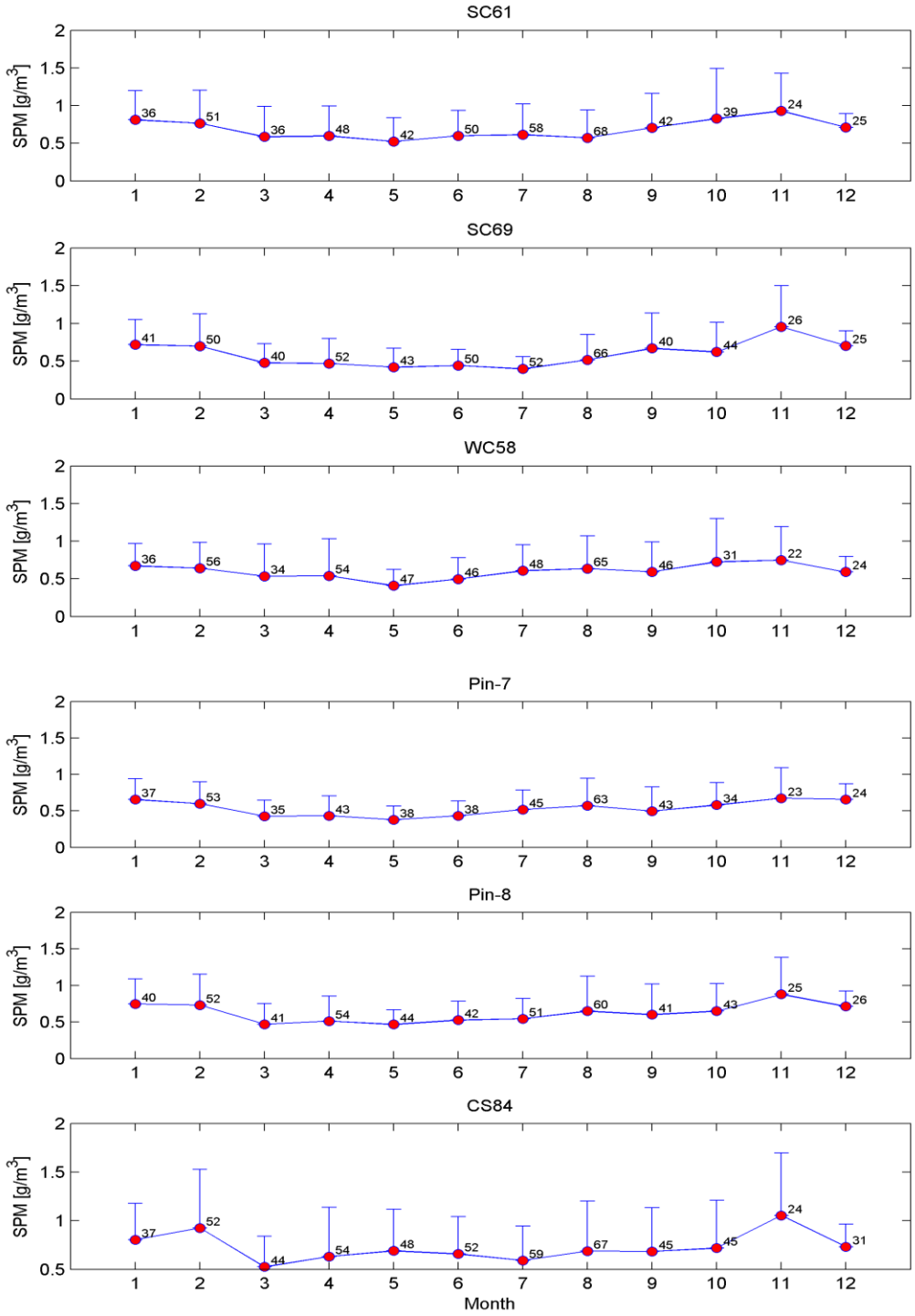

Figure 56: Monthly SPM climatology for the 3x3 pixel box centered at the stations in Douglas Channel derived from MERIS ocean colour data (2003-2012). The labels beside the symbols represent number of images used for computing climatology with error bars showing one standard deviation derived for each station and month.

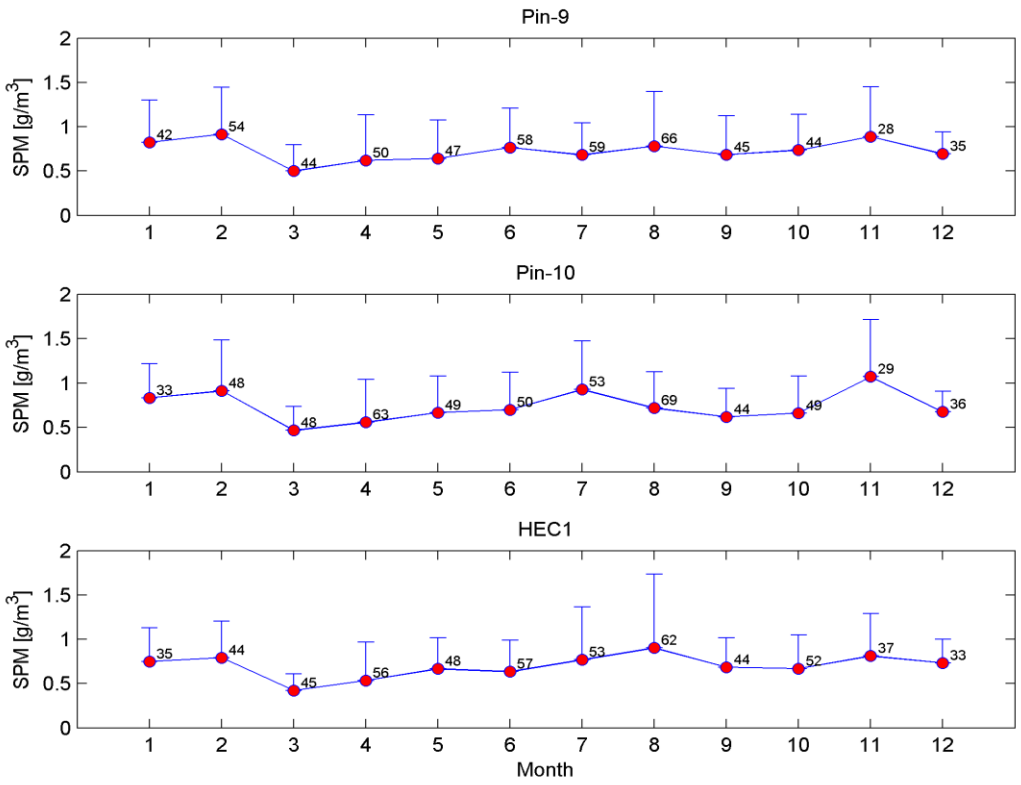

Figure 57 : Monthly SPM climatology for the 3x3 pixel box centered at the stations outside of Douglas Channel derived from MERIS ocean colour data (2003-2012). The labels beside the symbols represent number of images used for computing climatology with error bars showing one standard deviation derived for each station and month.

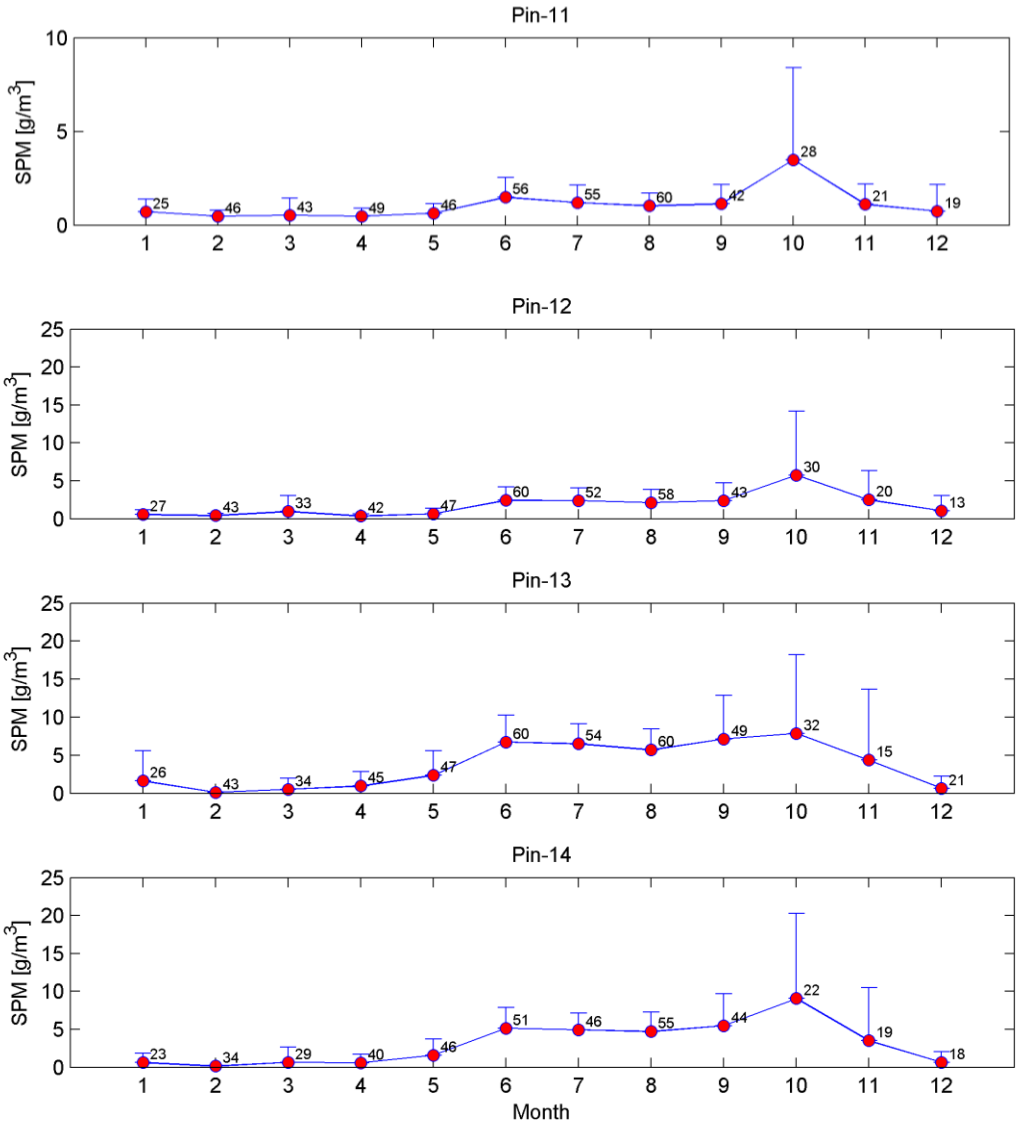

Figure 58 : Monthly SPM climatology for the 3x3 pixel box centered at the stations in the Gardner Canal derived from MERIS ocean colour data (2003-2012). The labels beside the symbols represent number of images used for computing climatology with error bars showing one standard deviation derived for each station and month.

APPENDIX D: RAIN, KITIMAT RIVER DISCHARGE, AND SPM OUTLIERS

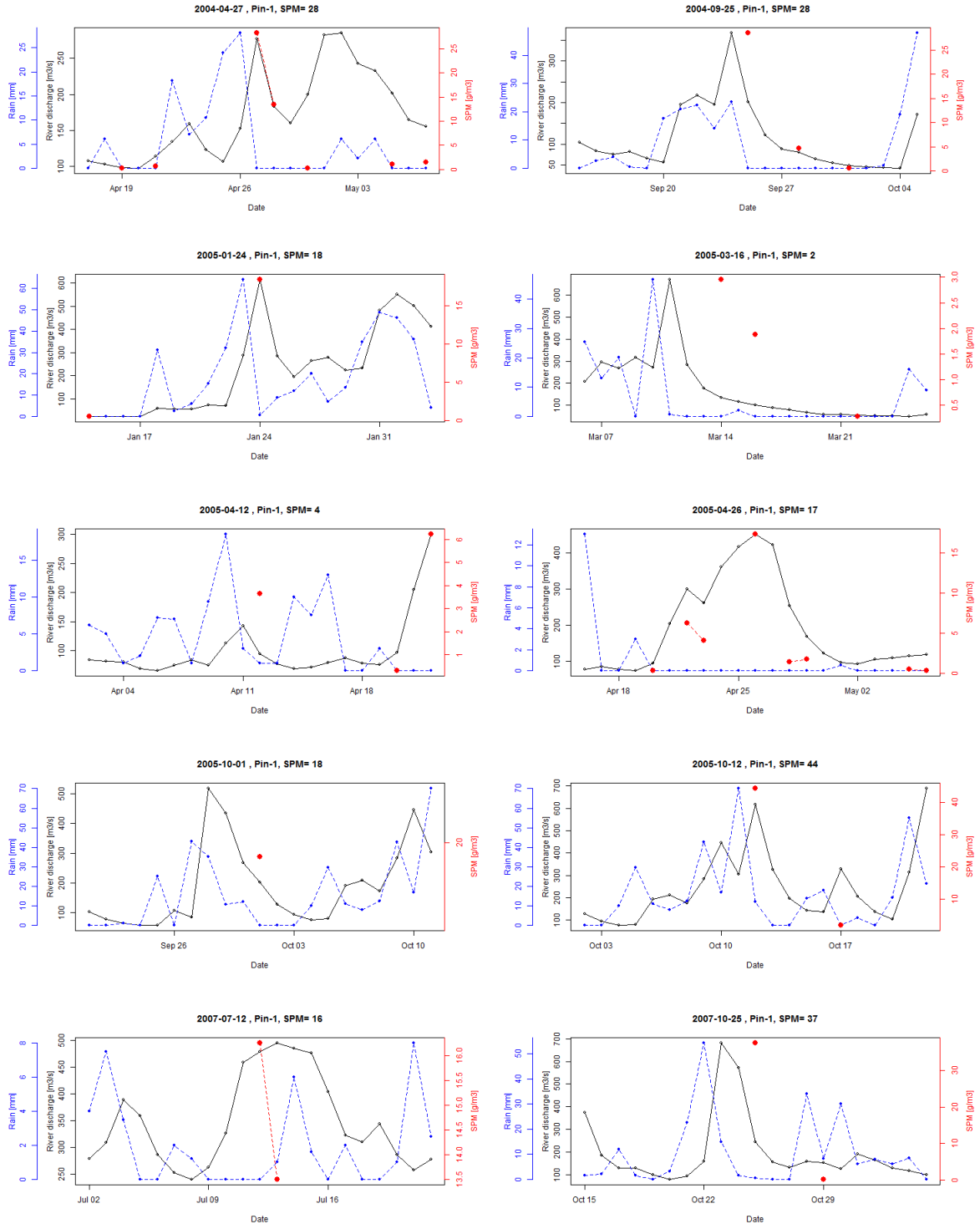

Figure 59: Time series of rainfall at the Kitimat Townsite station (blue), Kitimat River discharge (black), and SPM concentration (red) for the time period surrounding SPM outliers identified at Pin-1 location.

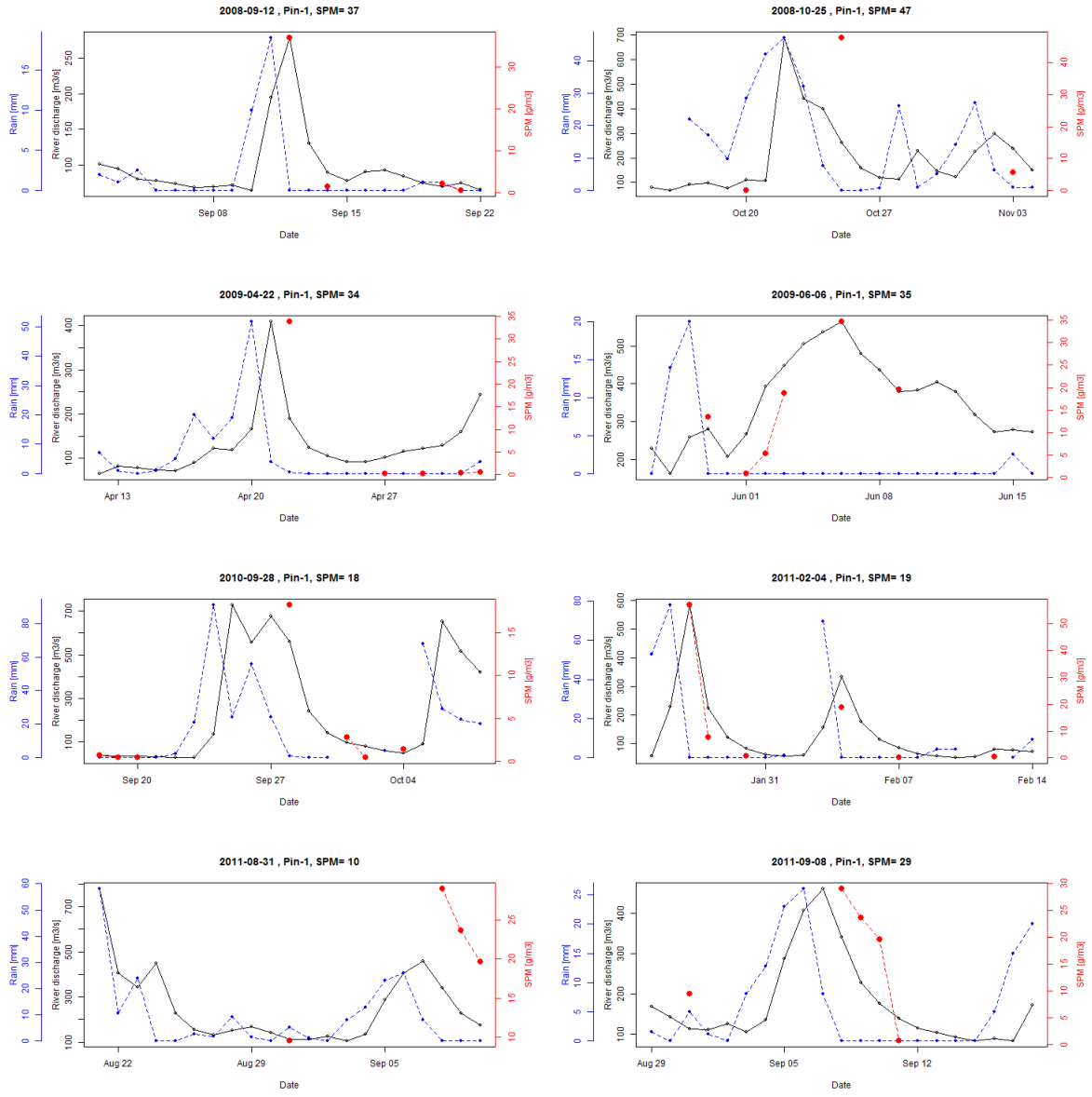

Figure 60: Time series of rainfall at the Kitimat Townsite station (blue), Kitimat River discharge (black), and SPM concentration (red) for the time period surrounding SPM outliers identified at Pin-1 location.